AD-A072 567 PENNSYLVANIA STATE UNIV UNIVERSITY PARK APPLIED RESE--ETC F/G 13/10
DEVELOPMENTAL EFFORTS ON A DIFFUSER AND PUMP INLET FOR A WATER --ETC(U)
APR 79 A M YOCUM N00024-79-C-6043
UNCLASSIFIED ARL/PSU/TM-79-51 NL

| OF |
AD
A072567

END
DATE
FILMED
9-79
DDC

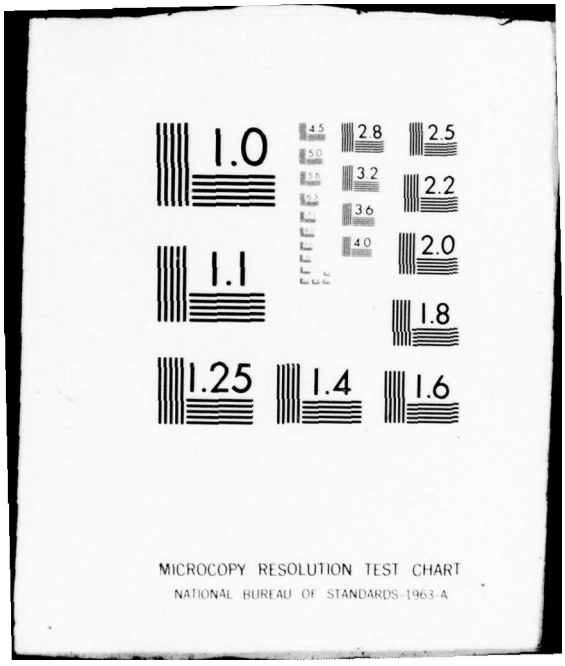
1.0
1.1
1.25
1.4
1.6
1.8
2.0
2.2
2.5
2.8
3.2
3.6
4.0
4.5
5.0
5.6
MICROCOPY RESOLUTION TEST CHART
NATIONAL BUREAU OF STANDARDS-1963-A

LEVEL II

B.S.

AD A072567

DEVELOPMENTAL EFFORTS ON A DIFFUSER AND PUMP INLET FOR A WATER JET PROPULSION SYSTEM

A. M. Yocum

Technical Memorandum
File No. TM 79-51
April 4, 1979
Contract No. N00024-79-C-6043

Copy No. 23

DDC FILE COPY

The Pennsylvania State University
Institute for Science and Engineering
APPLIED RESEARCH LABORATORY
Post Office Box 30
State College, PA 16801

NAVY DEPARTMENT
NAVAL SEA SYSTEMS COMMAND

JOB

391 007

UNCLASSIFIED

SECURITY CLASSIFICATION OF THIS PAGE (When Data Entered)

(14) ARL/PSU/TM-79-51

REPORT DOCUMENTATION PAGE

READ INSTRUCTIONS BEFORE COMPLETING FORM

1. REPORT NUMBER: 79-51	2. GOVT ACCESSION NO.
3. RECIPIENT'S CATALOG NUMBER	
4. TITLE (and Subtitle): (6) Developmental Efforts on a Diffuser and Pump Inlet for a Water Jet Propulsion System	5. TYPE OF REPORT & PERIOD COVERED: (9) Technical Memorandum
6. PERFORMING ORG. REPORT NUMBER	
7. AUTHOR(s): (10) A. M. Yocum	8. CONTRACT OR GRANT NUMBER(s): (15) N00024-79-C-6043
9. PERFORMING ORGANIZATION NAME AND ADDRESS: Applied Research Laboratory, P.O. Box 30, State College, PA 16801	10. PROGRAM ELEMENT, PROJECT, TASK AREA & WORK UNIT NUMBERS: (11) 4 Apr 79
11. CONTROLLING OFFICE NAME AND ADDRESS: Naval Sea Systems Command, Washington, DC 20362	12. REPORT DATE: April 4, 1979
	13. NUMBER OF PAGES: 83
14. MONITORING AGENCY NAME & ADDRESS (if different from Controlling Office): (12) 88p.	15. SECURITY CLASS. (of this report): UNCLASSIFIED
	15a. DECLASSIFICATION/DOWNGRADING SCHEDULE

16. DISTRIBUTION STATEMENT (of this Report)

Approved for Public Release. Distribution Unlimited.
Per NAVSEA - July 31, 1979.

17. DISTRIBUTION STATEMENT (of the abstract entered in Block 20, if different from Report)

18. SUPPLEMENTARY NOTES

19. KEY WORDS (Continue on reverse side if necessary and identify by block number)

water jet
diffuser
pump
inlet

20. ABSTRACT (Continue on reverse side if necessary and identify by block number)

Results from three studies relating to the development of a water jet propulsion system for a high speed planing craft are presented. More specifically, these studies apply to the development of the diffuser and pump inlet of the system and represent a continuation of previous work done at ARL/PSU in this area. The first study investigates the possible interaction of the flow between the diffuser and a vaned-volute type pump inlet. No interaction was revealed. The second study determined the feasibility of an improved vaned-volute type

Over

DD FORM 1 JAN 73 EDITION OF 1 NOV 65 IS OBSOLETE

UNCLASSIFIED

SECURITY CLASSIFICATION OF THIS PAGE (When Data Entered)

20. inlet using conventional pump design techniques to lay out the vanes. With the restrictions placed on the design by the propulsion system, flow separation from the vanes is likely and, thus, this type of inlet was found to be infeasible. The third study consisted of the design and model testing of a new diffuser and a conventional double suction pump inlet. The design and test results are documented in this report. Test results showed that the diffuser efficiency was improved slightly and the losses through the pump inlet were reduced by more than a factor of two from the losses in the vaned-volute inlet.

Subject: Developmental Efforts on a Diffuser and Pump Inlet for a Water Jet Propulsion System

References: See page 26

Abstract: Results from three studies relating to the development of a water jet propulsion system for a high speed planing craft are presented. More specifically, these studies apply to the development of the diffuser and pump inlet of the system and represent a continuation of previous work done at ARL/PSU in this area. The first study investigates the possible interaction of the flow between the diffuser and a vaned-volute type pump inlet. No interaction was revealed. The second study determined the feasibility of an improved vaned-volute type inlet using conventional pump design techniques to lay out the vanes. With the restrictions placed on the design by the propulsion system, flow separation from the vanes is likely and, thus, this type of inlet was found to be infeasible. The third study consisted of the design and model testing of a new diffuser and a conventional double suction pump inlet. The design and test results are documented in this report. Test results showed that the diffuser efficiency was improved slightly and the losses through the pump inlet were reduced by more than a factor of two from the losses in the vaned-volute inlet.

Acknowledgment: This work was sponsored by DTNSRDC, Annapolis, MD.

Table of Contents

List of Figures

List of Figures (continued)

Nomenclature

A	area
α	divergence angle of diffuser sides
B	width
C_L	lift coefficient
C_{pr}	pressure recovery coefficient defined in Equation 1
C_{P_S}	static pressure coefficient = $(P_s - P_{atm})/\frac{1}{2}\rho V_\infty^2$
C_{P_T}	total pressure coefficient = $(P_T - P_{atm})/\frac{1}{2}\rho V_\infty^2$
ΔC_{P_T}	total pressure loss coefficient through a component
η_p	pressure recovery efficiency defined in Equation 2
g	acceleration of gravity
H	diffuser height
h_L	head loss
K	vortex strength
K_L	loss coefficient defined in Equation 17
L	diffuser length
n	number of vanes
P_{atm}	atmospheric pressure
P_S	static pressure
P_T	total pressure
Q	flow rate
r	radius
r_{v_0}	outer radius of the volute at $\theta = 0$ (see Figure 3)
ρ	mass density
t_3	spacing between vanes at location 3

Nomenclature (continued)

V	velocity, when used with a number subscript it is the average velocity at that location
V_∞	reference velocity measured at the ninth tube of the total pressure rake in the throat
W_∞	vectorial mean velocity through the vanes, approximated as the arithmetic mean
x, y, z	coordinates, see figures for orientation

Subscripts

1	refers to station 1 at the inlet to the diffuser
2	refers to station 2 at the exit of the diffuser
3	refers to station 3 at the inlet to the vane channel in the volute-vane inlet design
4	refers to station 4 at the exit of the vane channel in the volute-vane inlet design
R	refers to the radial coordinate
θ	refers to the circumferential coordinate
m	refers to the meridional component
avg	average value
x, y, z	refer to the x, y & z coordinates

INTRODUCTION

This report presents the results from studies done for DTNSRDC as a continuation of their development of a waterjet propulsion system for a high speed planing craft. The proposed system consists of a wide slot inlet on the bottom of the craft and a series of diffusing ducts leading to several double suction pumps mounted across the rear of the craft. The Fluids Engineering Department of ARL/PSU has been involved with several aspects of this system. Work has been performed on the design and testing of an air model of the inlet diffuser and the double suction pump inlet. The inlet tested was a volute type inlet with vanes near the hub to remove the swirl in the flow. This type of inlet was designed and tested as an attempt to avoid some of the common problems inherent with conventional inlets. The results from the studies of this inlet are presented in Reference [1].

The Fluids Engineering Department of ARL/PSU has also carried out the design of a double suction pump intended to meet the specifications required by the propulsion system. In this design, a one-dimensional approach is used to size the pump, an axisymmetric solution of the flow through the impeller is obtained with a streamline curvature type of analysis, and the three-dimensional vanes for the impeller are laid out using a graphical transformation. In a joint program between ARL and DTNSRDC the graphical method of vane design has also been computerized by M. C. Brophy [2].

This report focuses on the characteristics of the diffuser and the inlet to the double suction pump, with the purpose being to present the results from studies conducted to answer several questions raised during the initial tests [1]. In the original tests, the diffuser was found to perform reasonably well and no flow separation in the diffuser was detected. In addition, the nonuniform velocity profile, created to simulate the real fluid removed from the boundary layer on the bottom of the craft, was found to decrease through the diffuser. Although this is a favorable response since it lessens the chance for flow separation, the decrease in the velocity gradient was not expected and the question of a possible flow interaction between the diffuser and inlet was raised. To investigate the possible interaction, the volute was replaced by a straight section and flow surveys were conducted at the exit of the diffuser. The results from these tests are presented in this report.

The tests conducted with the vaned volute revealed that the flow leaving the volute was not uniform and the total pressure losses through the volute were also very high. The cause of these problems was suspected to be flow separation from the vanes. To avoid flow separation from the vanes it was suggested that the flow passages and vanes could be designed using conventional pump design techniques. A preliminary design analysis using this approach is presented in this report. It was found that, with the geometric restrictions for this particular application, flow separation from the vanes would be hard to avoid.

The final topic presented in this report is the design and testing of a conventional double suction pump inlet. Even if the vaned volute had been successful, data for a conventional inlet would be useful for comparing performance and enabling the selection of the best inlet. However, with the problems encountered with the vaned volute, a conventional inlet was the most suitable alternative. The design of the inlet is documented in this report and results from model tests similar to the tests for the vaned volute are also presented.

INFLUENCE OF THE VOLUTE ON THE DIFFUSER PERFORMANCE

To investigate the possible flow interaction between the diffuser and volute, the volute was replaced by a straight section and flow measurements were made at the inlet and exit of the diffuser. A photograph of this experimental setup is shown in Figure 1. Not visible in the photograph is a section of 1/8 inch honeycomb located in the straight section directly upstream of the elbow. This honeycomb is provided to reduce the effect the elbow will have on the flow in the straight section. Besides these modifications, the remainder of the facility is the same as for the tests with the volute. The same type of instrumentation was also used as it is documented in Reference [1]. In addition to the instrumentation, it was possible to observe a tuft on a probe through the transparent section shown in the photograph.

The results from the tests with the straight section downstream of the diffuser must be interpreted with care. For an unknown reason, during these tests the flow rate was reduced by approximately 17% from the previous tests, and the flow was also found to be unsteady. For two similar tests, vertical flow surveys at the diffuser exit were found to yield significantly different velocity and total pressure profiles. One survey showed a profile similar to the one measured with the volute, while the other test results indicated a nearly uniform flow. Measurements at the diffuser inlet also showed variations from test to test, indicating the entire flow field was changing and not just the flow through the diffuser.

The primary purpose of the tests was to determine if the volute effected the occurance of separation in the diffuser. Therefore, the tests conducted are still of value, despite the problems encountered in the measurements. Observations of a tuft on a probe revealed no separation at the exit of the diffuser. The absence of any flow separation is also supported by the diffuser performance parameters, which demonstrate no decrease in pressure recovery when the volute is replaced by the straight section. The performance parameters were defined in Reference [1], but will be repeated here for convenience.

$$\text{Pressure recovery coefficient, } C_{pr} = \frac{P_{S_2} - P_{S_1}}{\frac{1}{2}\rho V_1^2} \qquad (1)$$

$$\text{Pressure recovery efficiency, } \eta_p = \frac{C_{pr}}{1 - \left(\frac{A_1}{A_2}\right)^2}$$

$$= \frac{\text{actual pressure recovery}}{\text{ideal pressure recovery}} \qquad (2)$$

For the two tests conducted with the straight section, the values of η_p were found to be .82 and .88. The previously determined value of efficiency as reported in Reference [1] is .81, thus, the performance of the diffuser is approximately the same or slightly better without the volute downstream. These recently obtained values of efficiency should be used with caution, since errors may be present due to the unsteadiness of the flow. However, the efficiency does indicate that no separation has occurred, and it can be concluded that the volute did not strongly influence the flow in the diffuser. It can also be concluded, since the diffuser performance was not reduced, that the reduction in mean velocity was not due to an interaction, but was probably caused by increased losses somewhere else in the system.

To investigate the source of the unsteadiness, liners were installed in the diffuser to eliminate the adverse pressure gradient which might cause an unsteady phenomenon to occur in the diffuser. The unsteadiness, however, was found to be unchanged by the liners and, therefore, it is speculated that the unsteadiness was caused by either a characteristic of the fan or flow separation in one of the other ducts. The unsteadiness in not suspected of influencing the interaction between the diffuser and downstream section, thus, the conclusion of no strong interaction should be valid.

PRELIMINARY DESIGN OF AN INLET VOLUTE AND VANES

Data from the initial tests with the vanes volute suggested that the high losses and nonuniform flow were caused by flow separation from the vanes and vortices formed in each vane channel. It was considered that these problems could be avoided if conventional pump or turbine practice was employed to determine the geometry of the meridional flow passage and also to design the vanes. In the original vaned volute, the geometry of the flow passage in the meridional plane was not given sufficient consideration, because the volute was designed from primarily a two-dimensional standpoint. Consequently, the flow had to negotiate a fairly sharp 90° bend. To improve the flow, the radius of the bend should be increased to the maximum allowed within the spacial restrictions. In addition, the vanes, which in the original inlet were also two-dimensional, should be designed giving three-dimensional consideration to the flow. The flow is obviously three-dimensional, since the flow in the volute must

be turned 90° into a direction perpendicular to the approximately two-dimension volute. Once the meridional passage is defined, the vanes can be designed by transforming the three-dimensional vane geometry to a two-dimensional surface employing the Prasil transformation.

A preliminary design of a volute type inlet with vanes was conducted to investigate the feasibility of an inlet designed using the new approach. A sketch of a meridional plane of the pump revealing the inlet, pump impeller, and exit is shown in Figure 2. This figure and Figure 3, which is a sketch of the volute contour, define the parameters which are involved in a design. Beginning with the geometry of the flow channel in which the vanes are located, this section is designed primarily on an intuitive basis with the objective of turning the flow into the axial direction as smoothly as possible. However, there are several parameters which effect the geometry that are determined from other considerations. The inlet radius (r_3) is selected on the basis of spacial restrictions and also vane performance considerations. The amount of flow acceleration in the meridional plane also effects the geometry of this passage. Accelerating the flow in the meridional plane is desirable because it reduces the amount of flow retardation in the vane channel and, thus, lessens the likelihood of flow separation from the vanes. A tradeoff must be made, however, since an acceleration requires the flow to be diffused more in the inlet duct resulting in larger losses and larger duct sizes. Once the inlet radius (r_3) and the meridional flow acceleration (A_3/A_4) are selected, the width of the vane channel inlet (B_3) is determined from conservation of mass. The inlet and exit of the channel are now specified and the remainder of the design is based on good engineering judgement. One practice, which is traditionally followed to improve the quality of the flow, is to increase the radius of the outer contour near the eye of the pump.

The design of the meridional flow passage has been described, and it was found that some of the variables are determined from the vane design. The design of the vanes and volute are also interrelated, since the purpose of the vanes is to remove the swirl created by the volute. With the different components of the inlet related, one approach for the design of the total inlet is to conduct a parametric study investigating the effect of the different variables. The primary design objectives for the inlet are that there is no swirl at the exit of the vanes and no flow separation from the vanes.

The variables under the control of the designer are the number of vanes (n), the inlet radius (r_3), the width of the inlet duct (B_2), and the amount of flow acceleration in the meridional plane of the vane channel (A_3/A_4). However, all of these variables have restrictions. The inlet radius and width are restricted by spacial limitations, the flow acceleration is restricted by the required amount of diffusion in the inlet duct, and the number of vanes is restricted by blockage and possible fouling if there are two many vanes. To determine whether separation is likely to occur, the lift coefficient of the vanes (C_L) and the flow retardation (V_4/V_3) are calculated and compared to the separation data presented in Reference [3].

The velocity at the inlet to the vanes must be known in order to evaluate the lift coefficient and the amount of flow retardation. This velocity can be calculated by knowing the flow rate through the pump and by assuming a free vortex distribution of V_θ in the volute. The circumferential velocity component is thus expressed as:

$$V_\theta = \frac{K}{r} \quad , \tag{3}$$

where K is a constant describing the strength of the vortex. To evaluate the constant K, the flow rate at $\theta = 0$ is first expressed in terms of V_θ.

$$Q = B_2 \int_{r_3}^{r_{V0}} V_\theta \, dr \tag{4}$$

where B_2 = width of the volute, assumed constant. Substituting Equation (3) into Equation (4) yields:

$$Q = B_2 \int_{r_3}^{r_{V0}} \frac{K}{r} \, dr = B_2 K \int_{r_3}^{r_{V0}} \frac{dr}{r} \tag{5}$$

Integrating and rearranging Equation (5) one gets the necessary relationship for K.

$$K = \frac{Q}{B_2 \ln\left(\frac{r_{V0}}{r_3}\right)} \quad . \tag{6}$$

In Equation (6), Q is known and B_2 and r_3 are varied in the parametric study. The value of r_{V0} is unknown at this point, but it is related to the average velocity at the diffuser exit. Since the inlet is designed such that V_r at the vane channel inlet is equal to the average velocity at the volute inlet, it is found that $A_2 = A_3$. The amount of flow acceleration in the meridional plane of the vane channel is also initially specified in the parametric study, thus, A_3 is known. An expression for r_{V0} can now be written as:

$$r_{V0} = r_3 + A_3/B_2 \tag{7}$$

The meridional velocity in the eye of the pump (V_{m_e}) is known and the velocity ratio for the flow through the vanes can be determined assuming no swirl remains downstream of the vanes.

$$\frac{V_4}{V_3} = \frac{V_{m_e}}{\sqrt{V_{r_3}^2 + V_{\theta_3}^2}} \tag{8}$$

where $V_{\theta_3} = \frac{K}{r_3}$

and $V_{r_3} = V_{m_e} \frac{A_4}{A_3}$

The lift coefficient (C_L) is also needed to determine the likelihood of flow separation. For a radial flow vane system, C_L can be expressed as:

$$C_L = (V_{\theta_3} r_3 - V_{\theta_4} r_4) \frac{4\pi}{n\ell W_\infty} \tag{9}$$

Average values of V_{θ_4} and r_4 should be used in Equation (9) if swirl remains at station 4. However, if the swirl is zero in the eye, Equation (9) reduces to:

$$C_L = \frac{2 V_{\theta_3} t_3}{\ell W_\infty} \tag{10}$$

where t_3 is the spacing between the vanes at location 3 and W_∞ is the vectorial mean velocity which can be approximated by the arithmetic mean

$$W_\infty = \frac{V_3 + V_4}{2} \tag{11}$$

For the inlet shown in Figure (2), where $r_3 = 8.75$, a complete design of the vane geometry was carried out using the Prasil transformation. It was found in this design that the length, ℓ, of the vanes was 5.5 inches. In the parametric study when r_3 is varied, the length of the vanes were assumed to be proportional to r_3 with the above design used to determine the constant of proportionality.

The results from the parametric study are presented in Figures 4 and 5. These figures show the variation of C_L and V_4/V_3 as a function of the duct width B_2. The effects of r_3 and A_3/A_4 are also demonstrated in Figures 4 and 5, respectively, by the different lines. Throughout the study, the lift coefficient was calculated assuming there were 10 vanes.

The criterion for evaluating the likelihood of flow separation is found in Figure 261 of Reference [3]. Although there is a lot of variation in the data, in general it is found that the lift coefficient should not be much greater than 1, and the value of V_4/V_3 should not be less that .6. As the value of V_4/V_3 increases, however, the safe limit for C_L also increases. Referring first to Figure 4, it is seen that regardless of the duct width (B_2) and the vane inlet radius (r_3) the value of V_4/V_3 is always less than .6. The lift coefficient is also found to be quite high, with the value usually greater than 2.0. As shown in Figure 4, increasing B_2 or r_3 both have faborable effects on C_L and V_4/V_3, i.e. C_L decreases and V_4/V_3 increases; however, only modest gains are obtained by increasing these variables. In addition, relatively large values of B_2 and r_3 are around 6.5 inches and 8.25 inches, respectively, and a significant increase in these values would not be possible within the spacial restrictions of the pump design.

Figure 5 presents data similar to Figure 4, with the various lines representing different values of flow acceleration in the meridional plane. From the figure it is seen that A_3/A_4 has little effect on C_L, but increasing A_3/A_4 has a significant effect on the flow retardation (V_4/V_3). For a duct width around 6.5 to 7.0 a value of A_3/A_4 of 1.2 will increase the velocity ratio to approximately .6. The lift coefficient, however, will still be around 2.0. It appears that the only way to significantly reduce the lift coefficient will be to increase the number of vanes. Doubling the number of vanes to 20 will cut the lift coefficient in half. This large number of vanes, however, may not be practical. It should also be pointed out that with $A_3/A_4 = 1.2$, the required diffusion ratio in the inlet duct will be 1.98, since the overall diffusion ratio from the inlet of the duct to the eye of the pump is specified to be 1.65. An area ratio of 1.98 will require a long duct with increased losses and greater onboard water weight. With this configuration, the volute will also be quite large ($r_{v_0} = 22$ inches), which may create additional complications.

To conclude this section on the feasibility of a volute and vane type pump inlet, it does appear that this type of inlet could be built without having the flow separate from the vanes. However, the large number of required vanes, the amount of diffusion in the inlet duct, and the size of the volute does not make this type of inlet an attractive choice.

DIFFUSER AND CONVENTIONAL PUMP INLET DESIGN AND MODEL TESTS

4.1 Prototype Design

Due to the unattractive features of the volute and vane type inlet, a conventional inlet was designed for the pumps of the planing craft. In a conventional inlet, the fluid is distributed around the circumference of the pump by passages which curve around both sides of the pump axis. This configuration, thus, eliminates most of the swirl in the flow, since the swirl from the two streams cancel out. Swirl can be put into the flow

by designing the inlet with the inlet flange offset from the axis of the pump.

To match the geometry of the pump inlet and to provide the required amount of diffusion, a new diffusing transition section was also designed. Both the diffuser and pump inlet were initially designed for the prototype system, and then a model of the inlet was designed and fabricated to evaluate its performance. A sketch of the general layout of the diffuser and a pump inlet is shown in Figure 6. This figure shows a few key dimensions and also identifies the various stations and parameters referred to in the discussion of the design.

The inlet and exit geometry of the diffuser are specified by the design of the inlet slot and the pump inlet, respectively. To avoid too great a transition in geometry, the pump inlet was made as wide as possible within the spacial restrictions imposed by the size of the craft. The width (B_2) was chosen to be 5.7 inches and the height (H_2) was then determined to be 16.4 inches. Since $A_2 = A_3$, these dimensions provide a 15% acceleration in the meridional plane from Station 3 to Station 4. With the overall diffusion ratio between Station 1 and Station 4 specified as 1.65, the area ratio for the diffuser can be calculated as follows:

$$\frac{A_2}{A_1} = \frac{A_4}{A_1}\frac{A_3}{A_4}\frac{A_2}{A_3} = (1.65)\ (1.15)\ (1) = 1.9 \qquad (12)$$

The aspect ratio of the inlet slot was chosen to be the same as the original model, so that this part of the model would not have to be rebuilt. The aspect ratio (H_1/B_1) for the original model was .267. With H_1/B_1 and A_1 known, the dimensions of the inlet slot can be calculated. These values are shown in Figure 6.

The remainder of the diffuser design consists of determining a smooth transition between the known inlet and exit geometries that will yield a high efficiency in pressure recovery. It is stated in Reference [4] that the total expansion angle for maximum efficiency for a duct with two parallel and two diverging walls is about 7 to 12 degrees. Since in the present case two walls are converging and, therefore, the pressure gradient is diminished, the maximum divergence angle of 12 degrees was selected. For the shortest possible diffuser with a 12 degree maximum divergence, the diverging walls must also be straight. Under these conditions, the total length of the diffuser can be calculated from the following equation:

$$L = (H_2 - H_1)/(2 \tan 6^\circ) = 60.75 \text{ in.} \qquad (13)$$

The width of the diffuser was varied so that the change in area with respect to distance would be constant. Equation (14) expresses the variation of the half width (B) which will yield the desired area variation.

$$B = \frac{.7289\ z + 49.20}{3.63 + .2102\ z} \qquad (14)$$

where B and z are in inches.

To demonstrate the rate of diffusion in the present duct as compared to other diffuser geometries, Figure 7 is a plot of the cross sectional area as a function of distance. Included in the figure are the area variations for a conical and square diffuser with the same inlet and exit areas and also for a diffuser with the same inlet and exit geometries as the present diffuser but with four straight sides. It is seen from Figure 7 that the area changes for conventional conical and square diffusers are much steeper than the change in the present diffuser. The reason for this being that the present diffuser must also serve as a transition section and thus is much longer than normally necessary.

The fourth curve in Figure 7, which demonstrates the area change the present diffuser would have if it had four straight sides, shows that the initial increase in area is similar to a conventional diffuser but with the flow over-diffused and then accelerated in the latter portion of the duct. This extra diffusion would increase the chance of flow separation, thus, this geometry does not appear to be an optimum configuration. The data shown in Figure 7, however, does suggest it may be possible to shorten the diffuser by having a more rapid increase in area until A_2 is reached, and then making a sharper transition to the required exit geometry while keeping the area constant. Caution must be taken, however, to assure the divergence angle in the transition is not too large to cause separation, since the pressure normally will continue to rise after the duct area is constant. The diffuser geometry shown in Figure 6 represents a conservative design and was selected as the final design for the present study.

The design of the prototype pump inlet was not carried out in as much detail as the diffuser, since the final design will depend on the information gained during the design of the model and its performance tests. However, some of the basic design parameters were selected and a general layout of the prototype inlet was drawn from which a detailed design of a model inlet could be made. The geometry of the meridional flow passage from Station 3 to Station 4 is shown in the preliminary detailed drawings of the pump designed for the planing craft. A sketch of this geometry is shown in Figure 6. Two of the other parameters which must be specified in the beginning of a design are the location of the splitter and the offset of the pump center from the center of the diffuser. The splitter is located 45° from the centerline of the inlet duct to comply with conventional practice. The amount of offset is calculated on the basis of conservation of angular momentum from the known desired amount of swirl in the eye of the pump. With 25% preswirl for the present pump, the required offset was found to be 1.39 inches as is indicated in Figure 6.

The flange geometry at the exit of the diffuser has a strong influence on the shape of the pump inlet. It is recalled that the dimensions of the flange were specified at the onset of the diffuser design on the basis of minimizing the transition in geometry in the diffuser and on spatial restrictions of the pump. The pump inlet also had some bearing on the selection of the flange dimensions, since large outward curvature of the inlet casing should be avoided. As shown in Figure 6, the diffuser exit geometry selected provides smooth entry into the pump with only a small amount of outward curvature.

The remaining details of the inlet design consist of specifying the geometry of the outer flow passage as a function of circumferential location. Since the passage geometry near the exit of the diffuser is for the most part fixed, a section in this region can be used as a reference and the cross-sectional area of the flow passage can be varied linearly from the reference section to a zero area at the splitter. This part of the design was not carried out in detail for the prototype inlet, but will be presented in more detail for the model inlet.

4.2 Model Design

A model of the diffuser and pump inlet shown in Figure 6 was designed and constructed to experimentally evaluate the performance of the system. As shown in Figure 6, the real diffuser feeds the inlets of two neighboring pumps; thus, a model with one pump inlet requires a diffuser which represents half of the prototype diffuser. For this reason, the model diffuser is asymmetrical with a straight solid wall representing the line of symmetry indicated in Figure 6.

The design parameters for the model diffuser are the same as for the real system. These parameters are listed below for completeness:

$$\frac{H_1}{B_1} = .267$$

$$\frac{H_2}{B_2} = 2.877$$

$$\frac{A_2}{A_1} = 1.90$$

$$\alpha = 12°$$

In addition to modeling the prototype diffuser, the new diffuser was also designed to be compatible with the facility of Reference [1].

The diffuser inlet dimensions are, therefore, specified by the section of the facility which is provided to create a velocity profile similar to the boundary layer on the planing craft. Near the entrance of the diffuser, the walls of the inlet section curve outward slightly to provide smooth entry into the diffuser. Therefore, the diffusion process actually begins upstream of the diffuser channel. The dimensions at the throat are:

$$H_1 = 2.50 \text{ in.}$$

and

$$B_1 = 9.375 \text{ in.}$$

while the dimensions where the diffuser channel begins are

$$H_1' = 2.83 \text{ in.}$$

and

$$B_1 = 9.375 \text{ in.}$$

Starting at location 1' the diffuser is designed similar to the prototype diffuser. The length of the duct is determined to be 40.39 in. Three sides are straight, two sides diverge at a 12° total divergence angle, and the width is varied to yield a linear area change as expressed by Equation (15).

$$B = \frac{.4459\ z + 26.53}{2.83 + .2102\ z} \tag{15}$$

A photograph of test facility revealing the geometry of the diffuser is shown in Figure 8.

To construct a model of the pump inlet, detailed three-dimensional specifications of the flow passages are required. First, a preliminary sketch of the outer contour of the inlet was made by following conventional practice and by meeting the specific geometric requirements of the present system. The diffuser exit geometry was known, the offset was determined to be 0.75 in. for 25% swirl in the eye, and the splitter was located 45° from the centerline. Secondly, the contour of the passage in a meridional plane leading into Section 3 was designed to provide a smooth transition from the width of the passage at Station 2 to the width at Station 3. With this much of the inlet design completed, the remainder of the design consisted of determining the variation of the flow passage around the circumference.

Reference sections were selected at $\theta = 45°$ and 150° as identified in Figure 9. The area of these sections were determined and the area of the remaining sections were calculated with a linear variation between the reference sections and zero area at the splitter. Each section located as shown in Figure 9 could then be designed to yield the required area. The

resulting sections are shown in Figure 10. It should be noticed in Figure 10, that in order to maintain a reasonable geometry as the splitter is approached, the side as well as the outer wall dimensions must approach the dimensions of Station 3.

The model inlet was constructed by producing numerous 1/8 inch sections which were stacked together to yield rough contours of the flow passages. To produce these sections, a computer program was written which took the sections of Figure 10 and through a spline curve fitting procedure would produce the section geometry at any axial location. Figure 9 is an example of one of these sections, located at the center of the inlet. After stacking the sections, the contours were smoothed by using a plaster type filler material and the final flow passage shapes were checked using templates of the sections shown in Figure 10. Figure 11 is a photograph of the two halves of the inlet revealing the inner contours of the inlet. Photographs of the inlet installed in the test loop are shown in Figures 8 and 12.

4.3 Test Program

Apparatus and Experimental Procedures

The test program conducted with the new diffuser and conventional type pump inlet was similar to the test program with the vaned volute. Except for the diffuser and pump inlet, the remainder of the experimental apparatus was also the same as the previous program [1]. A photograph of the facility is shown in Figure 8, and a schematic of the facility and the instrumentation is shown in Figure 13.

From the schematic, it may be noticed that control valves on the 1200 CFM exhauster are not present, as they were in the previous program. This was due to the 1200 CFM exhauster being the limiting component in the system with regard to maximizing the flow velocity. It is desirable to have as high a velocity as possible in order to improve the flow measurements. The maximum velocity in the throat of the present setup was approximately 120 ft/sec, which is the same as it was for the previous tests [1].

The instrumentation and the experimental procedures were also similar to the previous tests except for a few minor modifications. The flow was once again aligned with the diffuser using wedge probes located just upstream of the dividers to sense the flow direction. These wedge probes were connected to two U-tube manometers. The flow conditions at the throat of the facility were determined using a nine tube total pressure rake and static pressure wall taps on the top and bottom of the duct.

Near the exit of the diffuser, vertical surveys were conducted with both a three-hole prism probe and a five-hole prism probe. The five-hole probe, which was used for most of the tests, was not long enough to reach all the way across the diffuser; thus, the three-hole probe was used to ob-

tain a complete survey. The three-hole probe was used in the nulling mode, while the five-hole probe was always used in the non-nulling mode. Comparisons of the data from the two probes served to verify that the instrumentation and data reduction programs were working properly.

As shown on the schematic of Figure 13, the diffuser flow surveys were not conducted right at the exit of the diffuser, but a short distance upstream. This was necessitated by the diffuser extending into the casing of the model pump inlet and also by the space required by the traversing device. Therefore, the location of the traverses was approximately 5.9 inches upstream of the diffuser exit. These surveys were conducted in 0.25 inch increments. The device used for positioning the probes and nulling the three-hole probe can be seen in the photograph of Figure 12.

Circumferential surveys were conducted in the test section of the model, 4.69 inches downstream of the lip of the inlet. Three surveys were conducted at radial locations 1/4, 1/2 and 3/4 of the distance across the annulus using 6 degree increments for the full 360 degrees. After examining the initial data from these surveys, a modification was made to the inlet hoping to improve one area where the total pressure losses were large. The three circumferential surveys in the test section were then repeated with the modified inlet installed.

The major change in the experimental procedures was that all pressure measurements made through the scanivalve and pressure transducer were made five times, with the raw data averaged before the data was reduced. This was done to eliminate some of the scatter in the data. To facilitate the data acquisition, an automated system was used which made a pressure reading, punched the data on paper tape, and then indexed the scanivalve. Only the positioning of the probe was done manually.

Results and Discussion

The results from the various tests are presented in this section. The velocity and pressure measurements for each test are first presented and briefly discussed. Overall results which describe the performance of the diffuser and the pump inlet are then given near the end of the section.

Measurements were made at the throat of the facility at the beginning of each test because these data are needed as a reference. As in the previous study [1], the velocity (V_∞) measured at the ninth tube of the total pressure rake is used to nondimensionalize the velocities and pressures throughout the study. When all the throat data from the various tests were plotted, there was found to be a significant amount of scatter from test to test. Rather than presenting all of this data, lines representing the mean of the data are plotted in Figure 14. The scatter in the original data is attributed to an unsteadyness in the flow rather than experimental error. Therefore, it is felt that the lines in Figure 14 represent fairly accurately

the time mean flow in the throat. This conclusion will be further supported by the data from the other stations, which show that the measured mass flow at the various stations agree within 4%.

The velocity and pressure profiles from the current study are compared with the corresponding data from the previous study in Figure 14. These comparisons show that the velocity and total pressure profiles are not as steep as in the previous tests. One possible explanation for this is that the unsteadyness observed in the flow may have induced additional mixing downstream of the wires, thus smoothing out the profiles. Although the inlet profiles have changed slightly, the performance of the components in the two studies can still be compared, since the performance parameters are based on changes through the component rather than absolute values. The effects of the changes in the inlet profiles on the component performances are not considered to be significant.

The next set of data presented are the velocity and pressure measurements made just upstream of the diffuser exit. Figures 15 and 16 show the velocity profiles measured with the three-hole probe and five-hole probe, respectively. Figures 17 and 18 similarly present the pressure profiles measured by the two probes. Comparisons of the data indicate that the two probes yield almost identical results. The data from the five-hole probe exhibited slightly more scatter than the three-hole probe data, but this was not unexpected because the type of five-hole probe used is extremely sensitive to velocity fluctuations parallel to its axis. The good agreement between the two probes indicate the data acquisition and the data reduction programs were operating properly.

The data in Figures 15 through 17 can be compared to the corresponding data in Figure 8 and 9 of Reference [1] to see if the flow through the two diffusers responds similarly. Although there are found to be some differences, for the most part the velocity and total pressure profiles are quite similar. The major difference between the flows in the two diffusers is in the static pressure. For the previous diffuser P_s decreased with increasing x/H, while for the present diffuser P_s increases slightly with increasing x/H.

The final sets of data obtained from measurements made in the test section are presented in Appendices A and B. The data in Appendix A were obtained with the pump inlet model in its original form as shown in the photograph of Figure 11. Appendix B contains data taken after the model was modified. In both Appendices, there are five figures for each of the three circumferential surveys. The five figures present the three velocity components, total pressure and the static pressure as a function of the circumferential location. Initially the discussion will be concerned with the data of Appendix A, and, thus, the observations leading to the modification of the inlet can be made. It will be noted now, however, that the modification was unsuccessful in improving the performance of the inlet.

To help visualize the nature of the flow in the test section, the velocity components plotted in the figures of Appendix A are presented in pictorial form in Figures 19 and 20. Figure 19 shows the distribution of the vectorial combination of V_θ and V_R in the measurement plane of the test section. The arrows indicate the direction of the velocity vector at each measurement location and the length of the arrows are proportional to the magnitude of the velocity. Figure 20 similarly gives the pictorial representation of the axial velocity component.

One of the performance criterion of the pump inlet is the uniformity of the flow going into the eye of the pump. Figures 19 and 20 can be readily used to examine the uniformity of the flow and to locate problem areas. The velocity vectors, $\vec{V} = \vec{V}_\theta + \vec{V}_R$, shown in Figure 19 are quite uniform except in the sector between 90° and 200° where there appears to be some distortion. The significant improvement in this aspect of the flow is apparent when Figure 19 is compared to the corresponding figure for the volute type inlet. The $\vec{V}_\theta + \vec{V}_R$ distribution for the vaned-volute was highly irregular and was found to be composed of vortices created in each vane channel. No such flow irregularities are observed for the present inlet.

One other aspect of the flow which is apparent from Figure 19 is the large amount of swirl present. It is recalled that the inlet was designed to have 25% swirl in the eye of the pump. However, for the three circumferential surveys with r = 1.93, 2.54 and 3.14, the arithmetic averages of V_θ/V_m are .773, .712 and .563, respectively. This is estimated to be an excessive amount of swirl which would create problems in obtaining the required amount of head rise through the pump. Therefore, this aspect of the flow must be improved.

Comparing Figure 20 with Figure 11 of Reference [1], it does not appear that the uniformity of the axial velocity component was improved as significantly as the $\vec{V}_\theta + \vec{V}_R$ component. Although Figure 20 shows there are many small velocity fluctuations, the data in the appendix more clearly show there are fewer large velocity defects with the present inlet than with the vaned-volute inlet. As with $\vec{V}_\theta + \vec{V}_R$, the sector with the large velocity defect is between 90° and 200°.

To gain further insight into the cause of the velocity irregularities in the sector between 90° and 200°, the total pressure profiles in Appendix A can be examined. In Figures A.9 and A.14, an abvious total pressure defect is observed centered around 160°. Therefore, the velocity distortions observed in Figure 19 and 20 seem to be caused by a wake or separated region in the inlet. To trace the origin of the total pressure deficit, it must be remembered that the swirl in the flow has circumferentially displaced the deficit. On the basis of the average swirl in the flow, the mean axial velocity, and the distance between the lip of the inlet and the probe, it was found that the total pressure deficit was displaced approximately 70°. Thus, the problem appears to originate in the region around 90°.

The desire to eliminate the velocity and total pressure defects was the motivation for making a modification to the inlet. As shown in the schematic of Figure 13, the 90° location is in the section of the inlet facing the diffuser. With this in mind, the photograph of Figure 11 shows that in this region the lip of the inlet poses an abrupt obstacle to the flow. Therefore, it was felt that the flow was separating from the lip causing the observed velocity and total pressure defects.

The lip is necessary to prevent the flow from going directly into the eye without distributing itself around the circumference. Reference [5] gives an example of an inlet which was built without the lip and for which test results showed that the flow rate was reduced by 10% from design due to the pump being unevenly supplied. However, for the present inlet, it was felt that the lip was not properly dividing the flow into the streams which should go directly into the eye and those which should be directed around the circumference. In Figure 21, three sketches of the flow in the region of the lip show the desired flow pattern, the suspected flow pattern with flow separation, and the modification made to the lip to achieve the desired flow. The modification consists of a splitter to divide the two flow regions and an extension below the splitter which reduces the bluntness of the lip. The extension below the splitter was centered on the centerline of the diffuser rather than on the axis of the pump. This was done to direct more flow to the top of the inlet and, thus, reduce the amount of swirl in the flow. The photograph of the inlet in Figure 22 clearly shows the modification which was made.

The test data for the modified inlet are presented in Appendix B; and similar to before, Figures 23 and 24 give the pictorial representation of the velocity field. It is clear from the data that the modification was unsuccessful in eliminating the velocity and total pressure defects. In fact, the defects have become larger. On the more positive side, Figure 24 does show that the flow outside the distorted area has become more uniform. Therefore, the concept of dividing the flow does appear to improve the quality of the flow around most of the circumference, although the problem in the region around 90° must still be solved. Shown in Figure 22 are tufts which were used to observe the nature of the flow in the inlet. Despite the large total pressure wake found in the data, a separated region was not apparent from the behavior of the tufts. Therefore, understanding the cause of the total pressure defect will require detailed flow surveys in the inlet.

Before leaving the discussion of the modified inlet, one more point can be brought out. The extension below the splitter did reduce the swirl in the flow as planned. For the modified inlet, the average values of V_θ/V_m are .457, .408, and .296 for the three surveys at radii of 1.93, 2.54, and 3.14 inches, respectively. Therefore, the problem of the excessive amount of swirl in the flow can be solved by changing the shape of the extension as well as using the obvious solution of changing the offset of the pump with respect to the diffuser.

With all of the flow measurements described, the performances of the diffuser and pump inlet with respect to losses can be discussed. In Table 1, the average dimensionless velocity, the mass average total pressure coefficient and the dimensionless average flow rate are given for the three measurement stations. The dimensionless flow rates are given only for a check on the accuracy of the measurements and show that the measured flow rates differ by less than 4%. The most important parameters in Table 1 are the total pressure coefficients which are used to calculate the losses through the components. The manner in which the total pressure coefficients were mass averaged is the same as described in Reference [1].

For the diffuser, the pressure recovery coefficient, C_{pr}, defined in Equation (1), can be calculated from the total pressure loss through the diffuser using the following equation:

$$C_{pr} = 1 - \left(\frac{A_1}{A_2}\right)^2 - \Delta C_{P_T}{}_{1-2} \left(\frac{V_\infty}{V_1}\right)^2 \quad . \tag{16}$$

C_{pr} can in turn be used to calculate the pressure recovery efficiency, η_p, defined in Equation (2). C_{pr} is found to be .591 and η_p is .846. For the previous diffuser, η_p was equal to .812.

It is recalled that the second measurement station was not exactly at the exit of the diffuser, but a short distance upstream. Thus, the efficiency for the total diffuser may be less than reported above. However, up to the measurement location, the performance of the diffuser is found to be better than the previous diffuser. This improvement may be the result of designing the diffuser with a constant rate of area change, since this reduces the pressure gradient at the entrance of the diffuser. The performance gain may also be due to the velocity profile entering the diffuser being more uniform than in the previous tests. For this reason, the comparison of the two diffusers should be interpreted with care. Regardless of the cause of the improvement, the performance of the diffuser is quite satisfactory.

The losses through the pump inlet will be expressed in terms of a head loss coefficient, K_L, as was done in Reference [1]. K_L is defined below:

$$K_L = \text{loss coefficient} = \frac{h_L \, 2g}{V^2} = \Delta C_{P_T} \frac{V_\infty{}^2}{V^2} \tag{17}$$

where

h_L = head loss

V = average axial velocity in the test section

g = acceleration of gravity

ΔCp_T = change in the total pressure coefficient through the pump inlet = $P_{T\ loss}/\frac{1}{2}\rho V_\infty^2$

The value of K_L calculated for the present inlet before the modification was .635. After the inlet was modified, the value of K_L became .852. As previously concluded and again apparent from the values of K_L, the modification made to the inlet was detrimental to its performance. However, both values of K_L for the present inlet are far below the value of K_L = 1.44 which was determined for the vaned-volute. Before the inlet was modified, the losses were reduced by more than a factor of two.

A better understanding of the inlet performance can be gained by comparing the values of K_L with published data for 90° turns. For commercial pipe fittings, a 90° elbow has a loss coefficient of .90. For smooth pipe bends of 90°, the loss coefficient reaches a minimum value of approximately .19 at a value of R/d = 3 (R = radius of the bend, d = diameter of the pipe). On the other end of the scale, the loss coefficient for a mitered bend is 1.1. Turning vanes added to a mitered bend can reduce the loss coefficient to .2.

With the values of K_L ranging from approximately .2 to 1.1, the present inlet falls right in the middle of this range. If the total pressure defect could be eliminated the value of K_L could be reduced to approximately .5. Beyond this value, a further reduction in the losses does not appear feasible. When comparing the pump inlet performance to pipe turns, it must be remembered that the hub portion of the inlet, not present in a pipe, represents addition surface area to cause friction losses and could also induce additional secondary flow losses. It should also be noted that the present inlet turns the flow in a shorter distance than possible with a mitered pipe bend; i.e., the width of the inlet is less than the diameter of the pump eye. Under these observations, the performance of the present inlet is quite good.

SUMMARY AND CONCLUSIONS

Results from several different analytical and experimental studies relating to various aspects of a water jet propulsion system have been given. The first study investigated the possible interaction of the flow between the diffuser and vaned-volute reported in Reference [1]. This was done by replacing the volute with a straight duct and making flow measurements in the diffuser. The results showed no significant change and, thus, demonstrated that the volute had not altered the flow in the diffuser. This is an important conclusion because it eliminates one variable when trying to select the best inlet.

The second study was an analytical investigation of the feasibility of an improved vaned-volute type inlet designed using conventional pump practice. This study showed that for the propulsion system under consideration, the likelihood of avoiding flow separation from the vanes

was not good. The restrictions which the application placed on the design were the number of vanes, the maximum width of the inlet and the amount of meridional flow acceleration through the vanes. For applications where these restrictions are not present, a vaned-volute may still be an attractive choice for a pump inlet.

The third study consisted of designing and testing a conventional type double suction pump inlet which met the specific requirements of the propulsion system. A new diffuser was also designed to match this inlet. Flow surveys at the inlet and exit of the diffuser and pump inlet were conducted in an air model. The efficiency of the diffuser, which had a larger diffusion ratio than the diffuser of Reference [1], was improved slightly. Also, the loss coefficient for the pump inlet was reduced by more than a factor of two from the value obtained for the vaned-volute inlet. However, the flow surveys did reveal a significant total pressure defect in one sector of the flow coming from the inlet, suggesting flow separation had occurred. Elimination of this source of loss would further improve the performance of the inlet. Future studies should be concerned with determining the cause and eliminating the observed total pressure defect.

References

1. Yocum, A. M., "Test Results From a Program Determining the Performance of a Vaned Volute to be Used as a Double Suction Pump Inlet," ARL TM 77-34, February 1977.

2. Brophy, M. C., "Computer-Assisted Design of Pump Impellers," Master of Science Report, Mechanical Engineering Department, The Pennsylvania State University, March 1978.

3. Wislicenus, G. F., Fluid Mechanics of Turbomachinery, Dover Publications, Inc., New York, NY, 1965.

4. Norris, R. Hasmer, Florence F. Buckland, Nancy D. Fitzroy, "Fluid Flow Data Book," Schnectady, NY, General Electric Co. Corporate Research and Development, 1970.

5. Lazarkiewicz, S. and Troskolanski, A. Impeller Pumps, 1st Edition, Pergamon Press, New York, 1965, pp. 261-262.

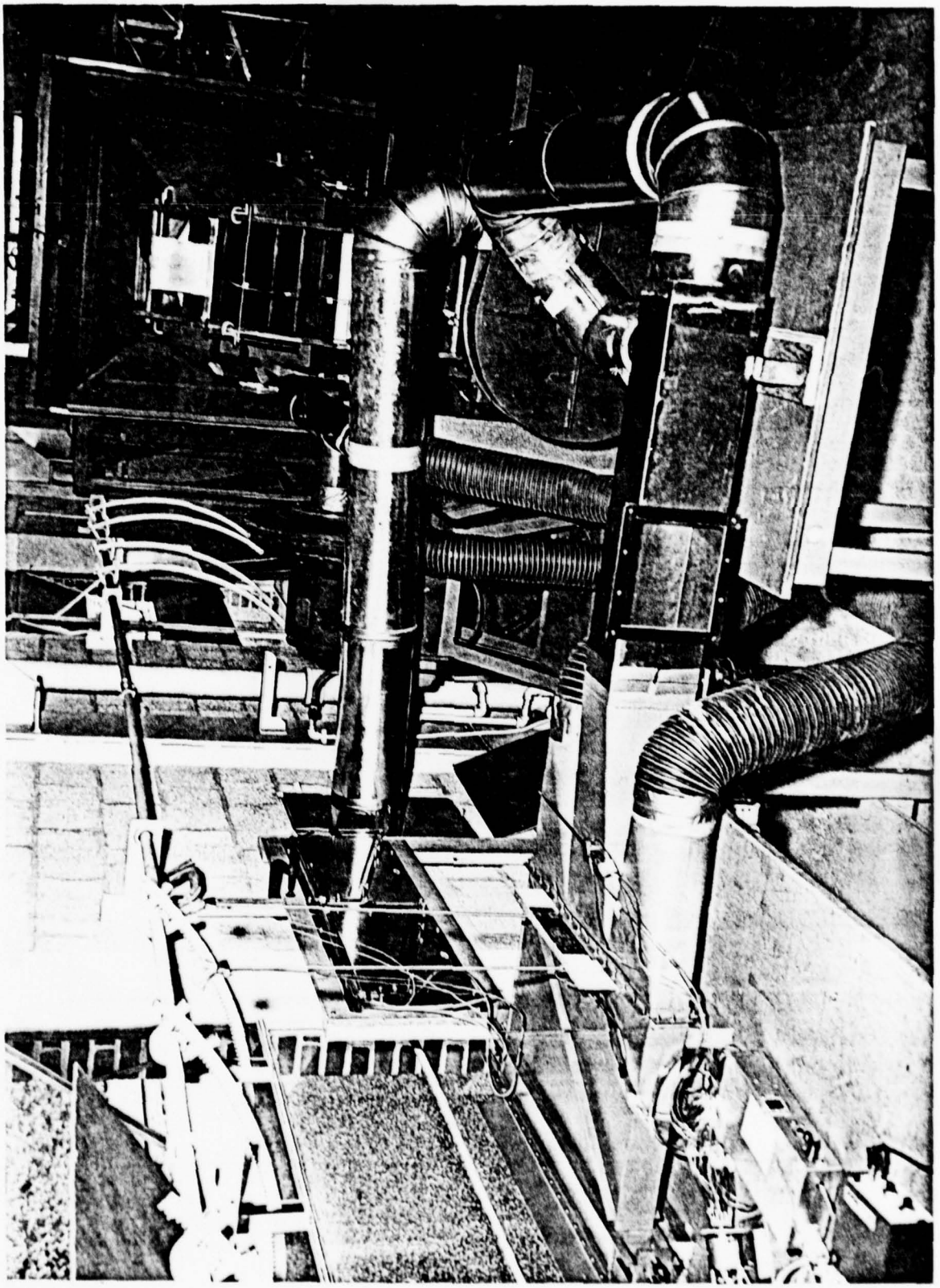

Figure 1 - Photograph of the Test Facility With a Straight Section of Duct Downstream of the Diffuser.

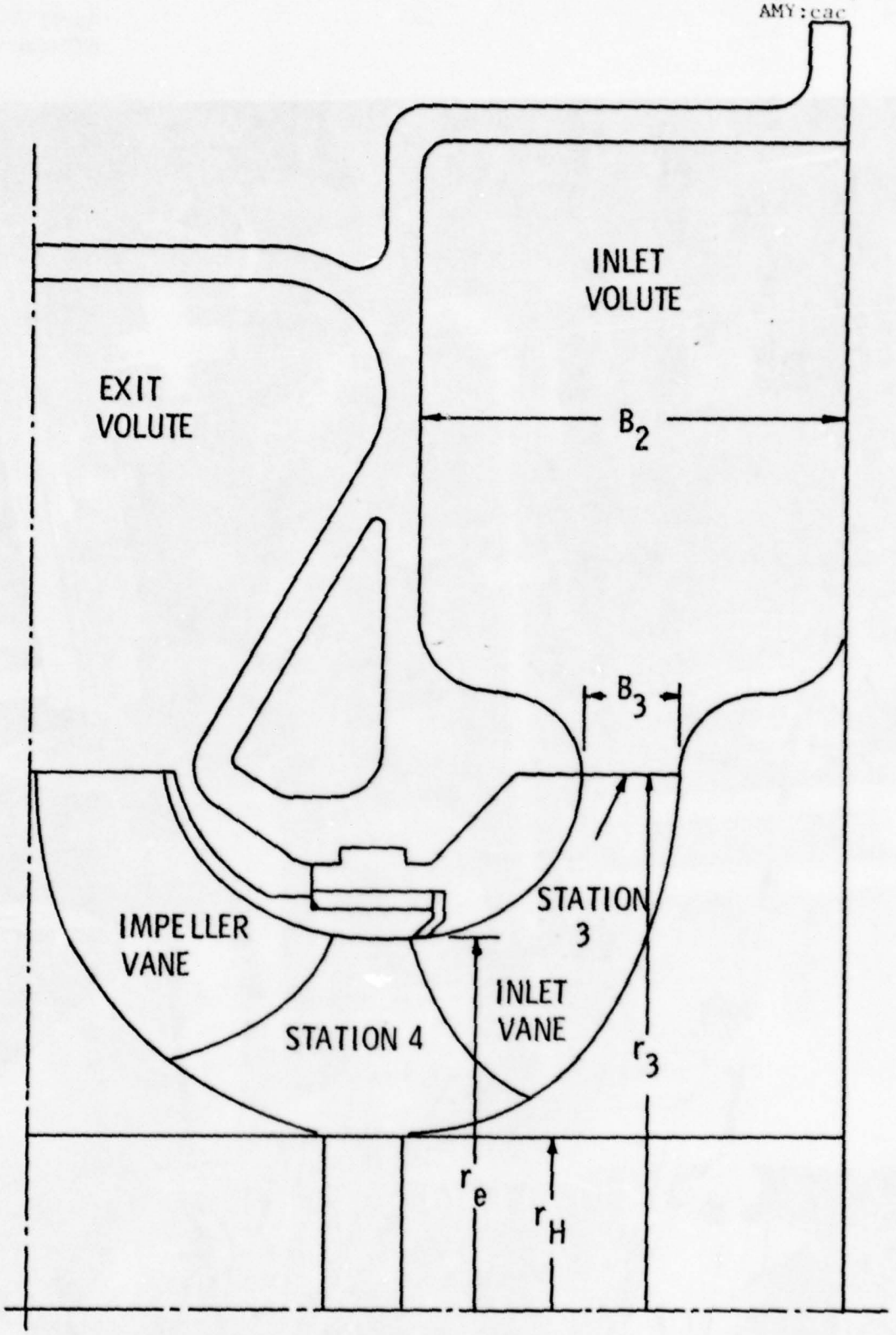

Figure 2 - Sketch of the Meridional Plane of a Pump Revealing the Impeller and the Inlet and Exit Flow Passages.

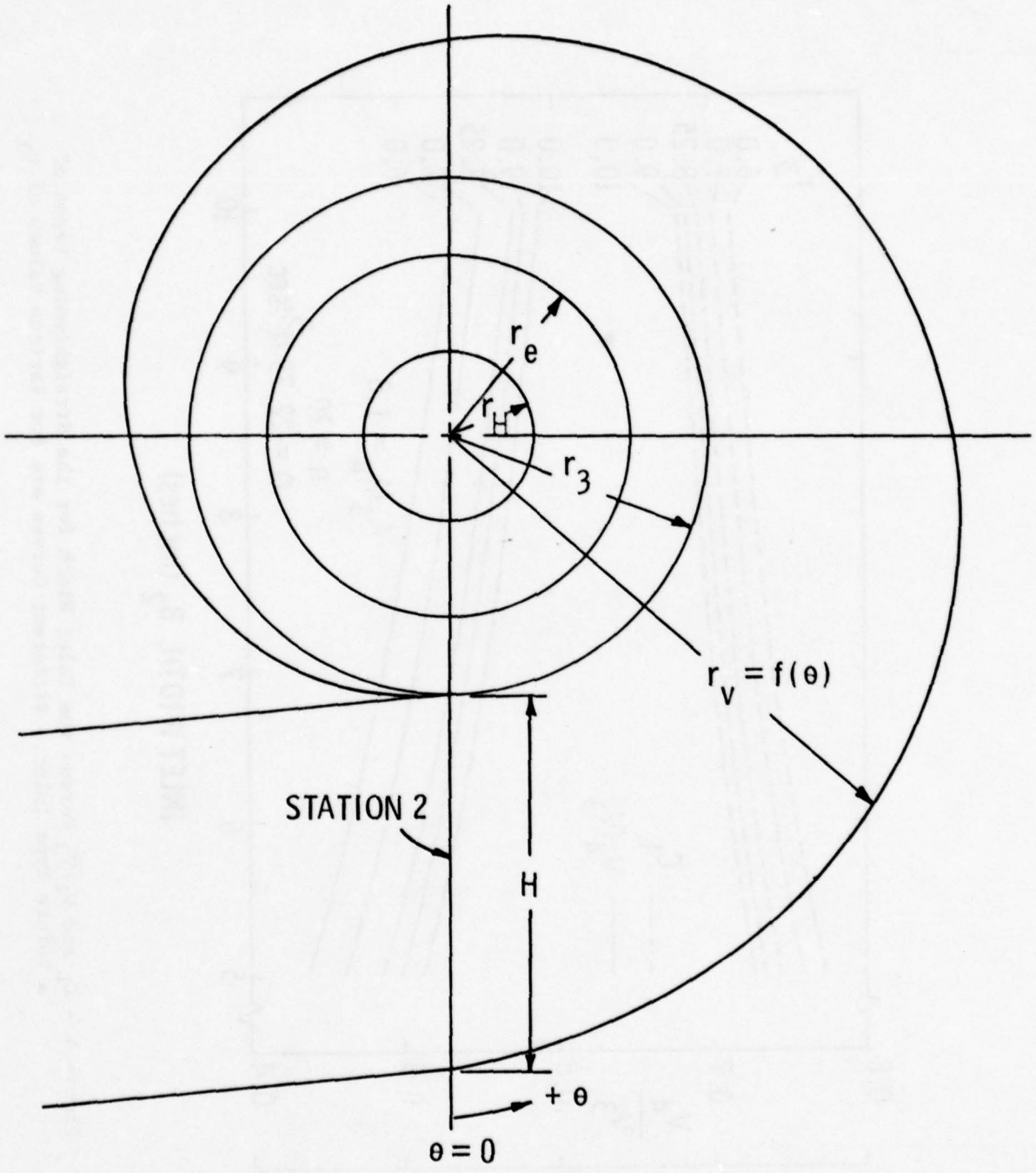

Figure 3 - Sketch of an Inlet Volute Defining Some of the Design Variables Involved.

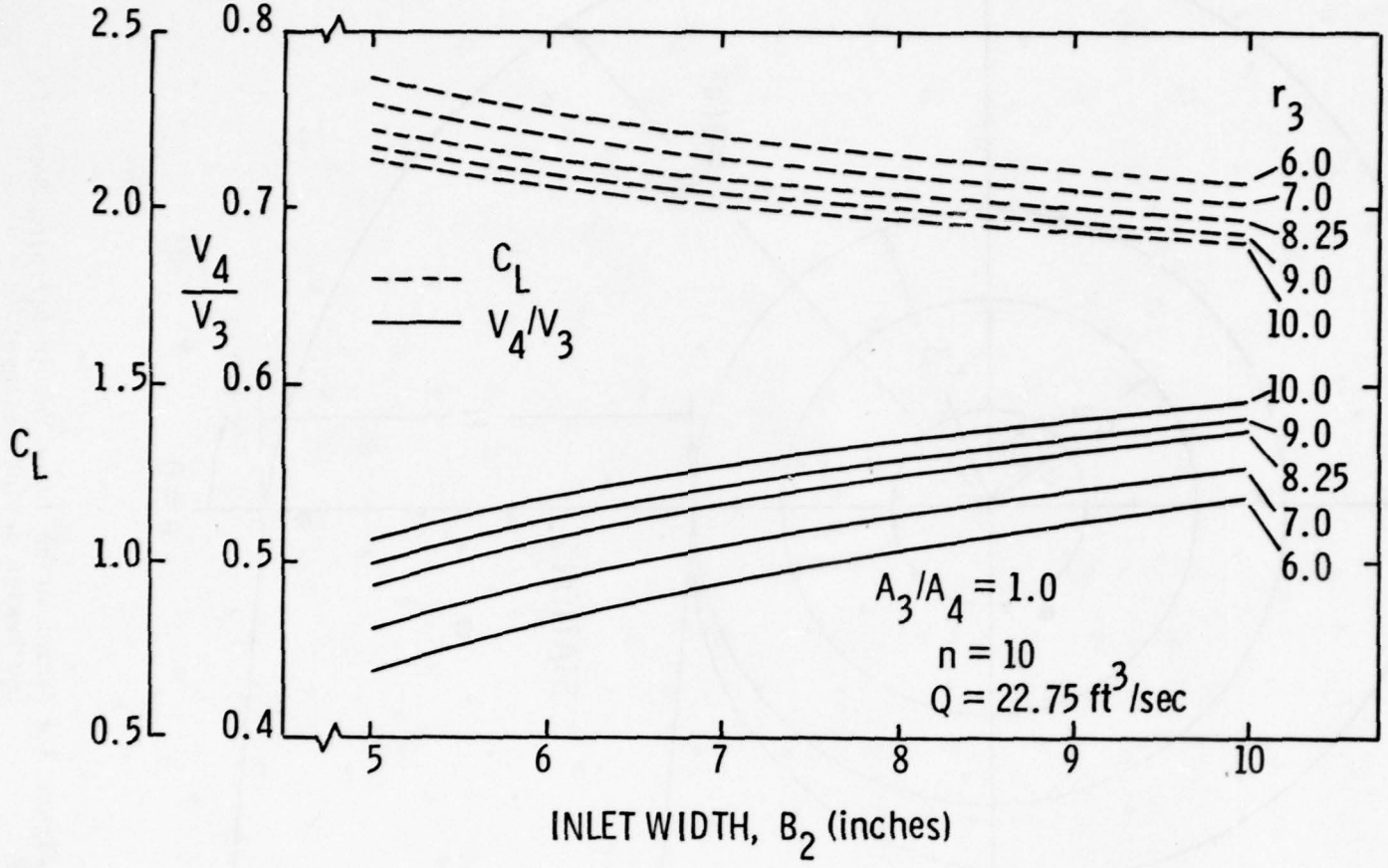

Figure 4 - C_L and V_4/V_3 Versus the Inlet Width for the Straightening Vanes of a Volute Type Inlet. Different Curves are for Various Values of r_3.

April 4, 1979
AMY:cac

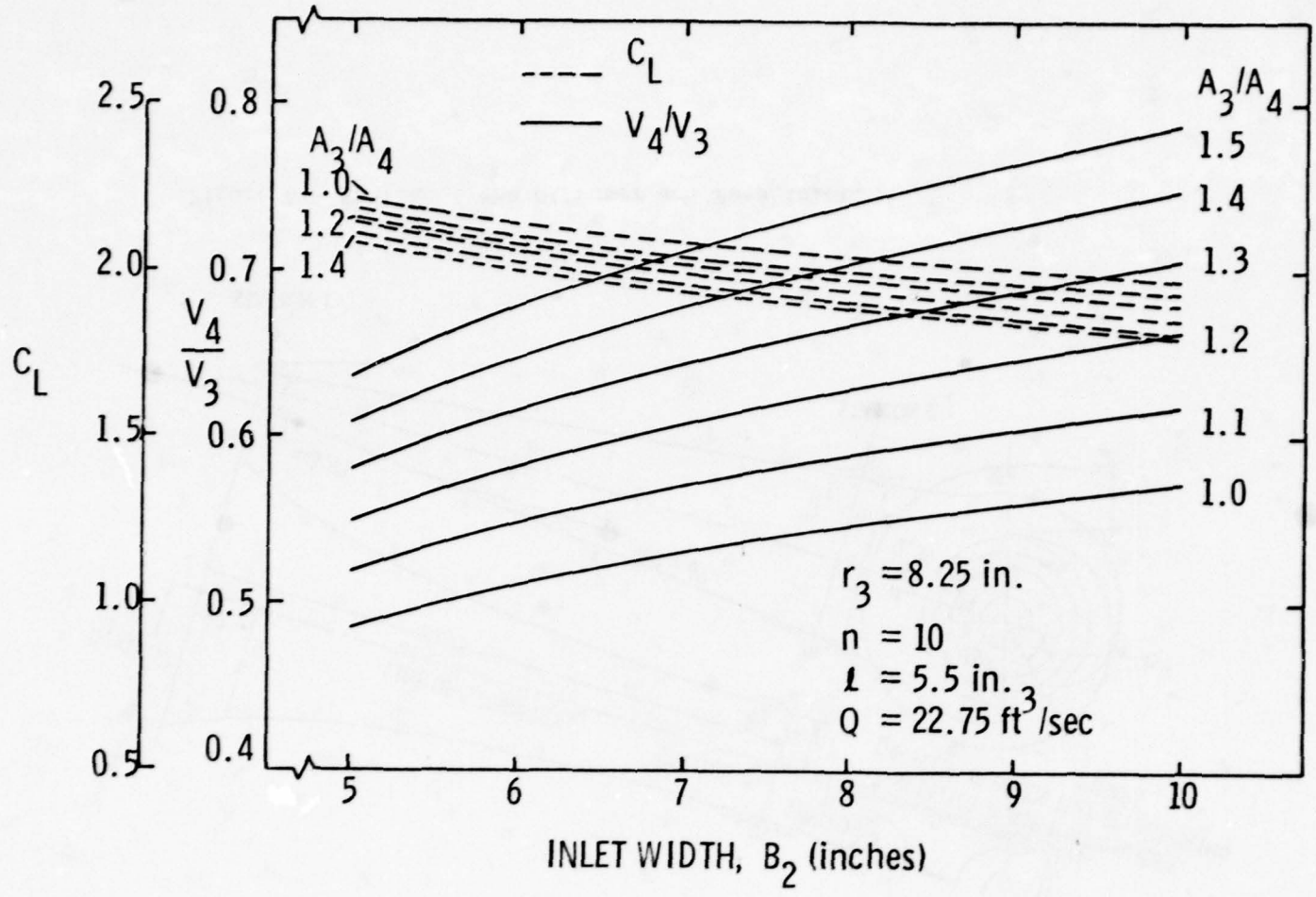

Figure 5 - C_L and V_4/V_3 Versus the Inlet Width for the Straightening Vanes of a Volute Type Inlet. Demonstrated by the Various Curves.

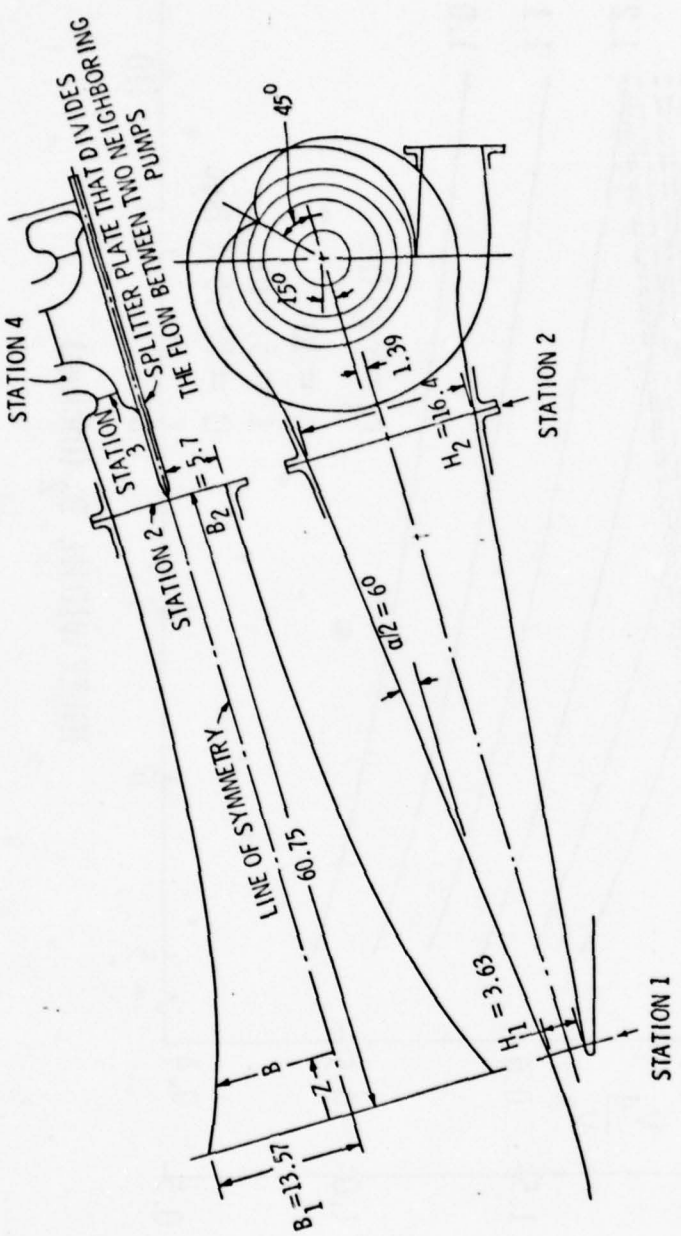

Figure 6 - Sketch of the Diffuser and Pump Inlet.

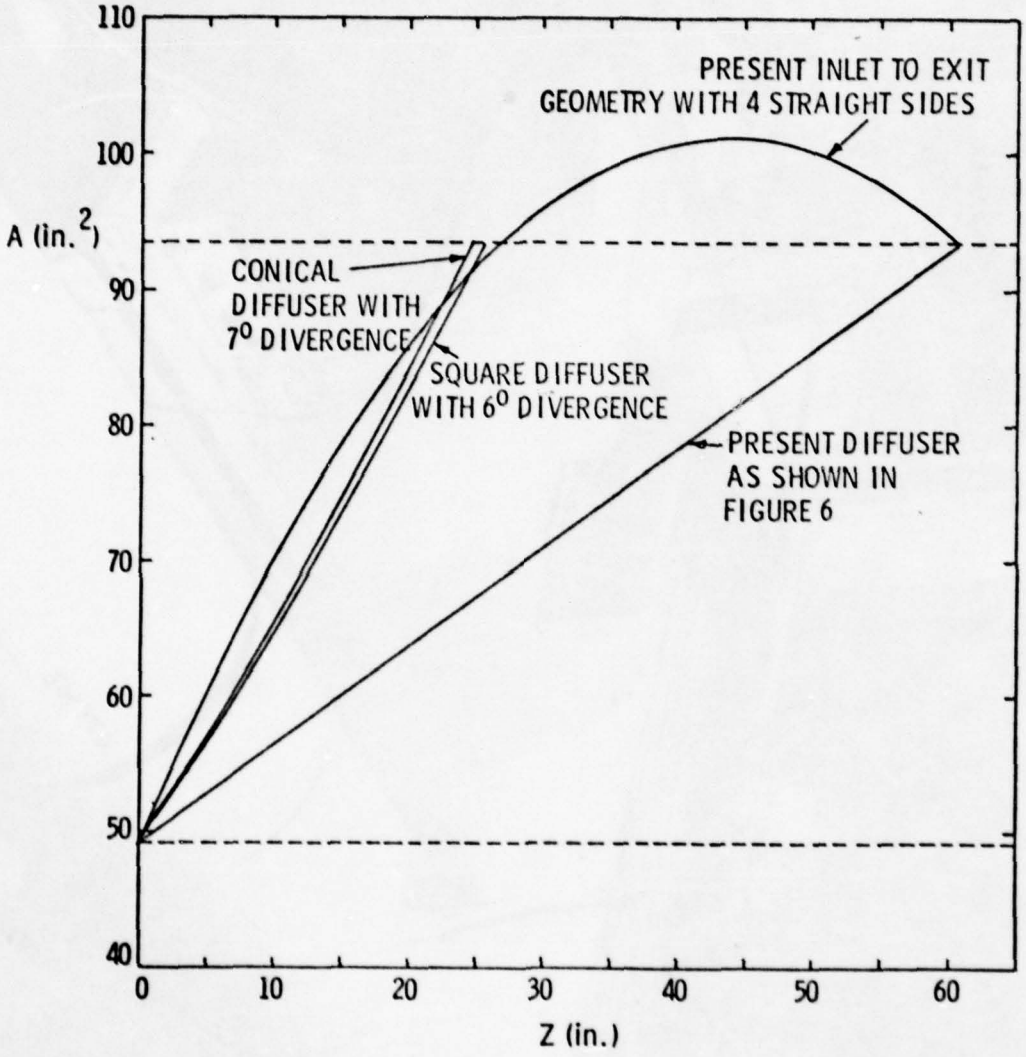

Figure 7 - Duct Area Versus Distance for Several Different Diffuser Geometries.

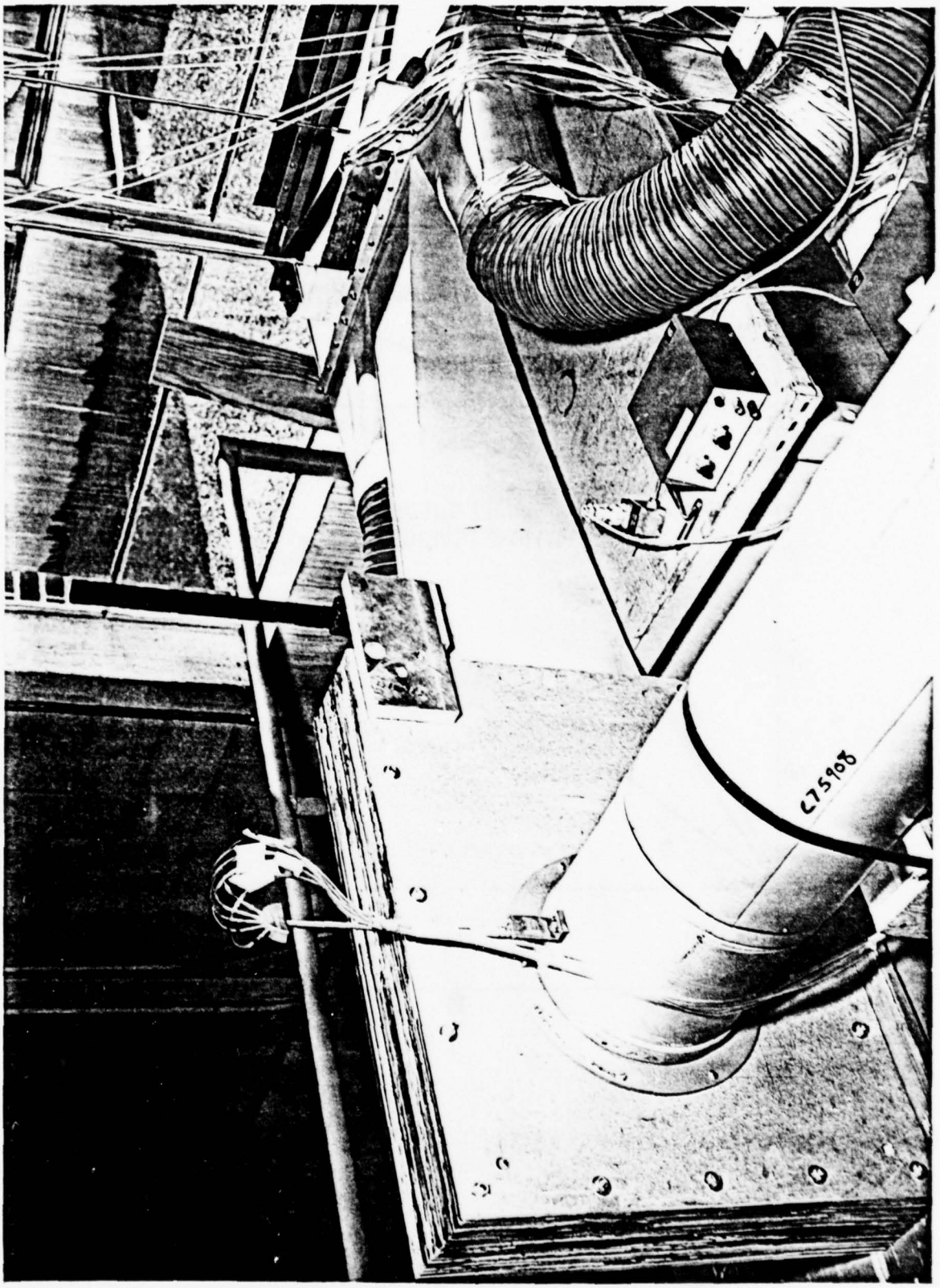

Figure 8 - Photograph of the Test Facility Revealing the Major Components of the System.

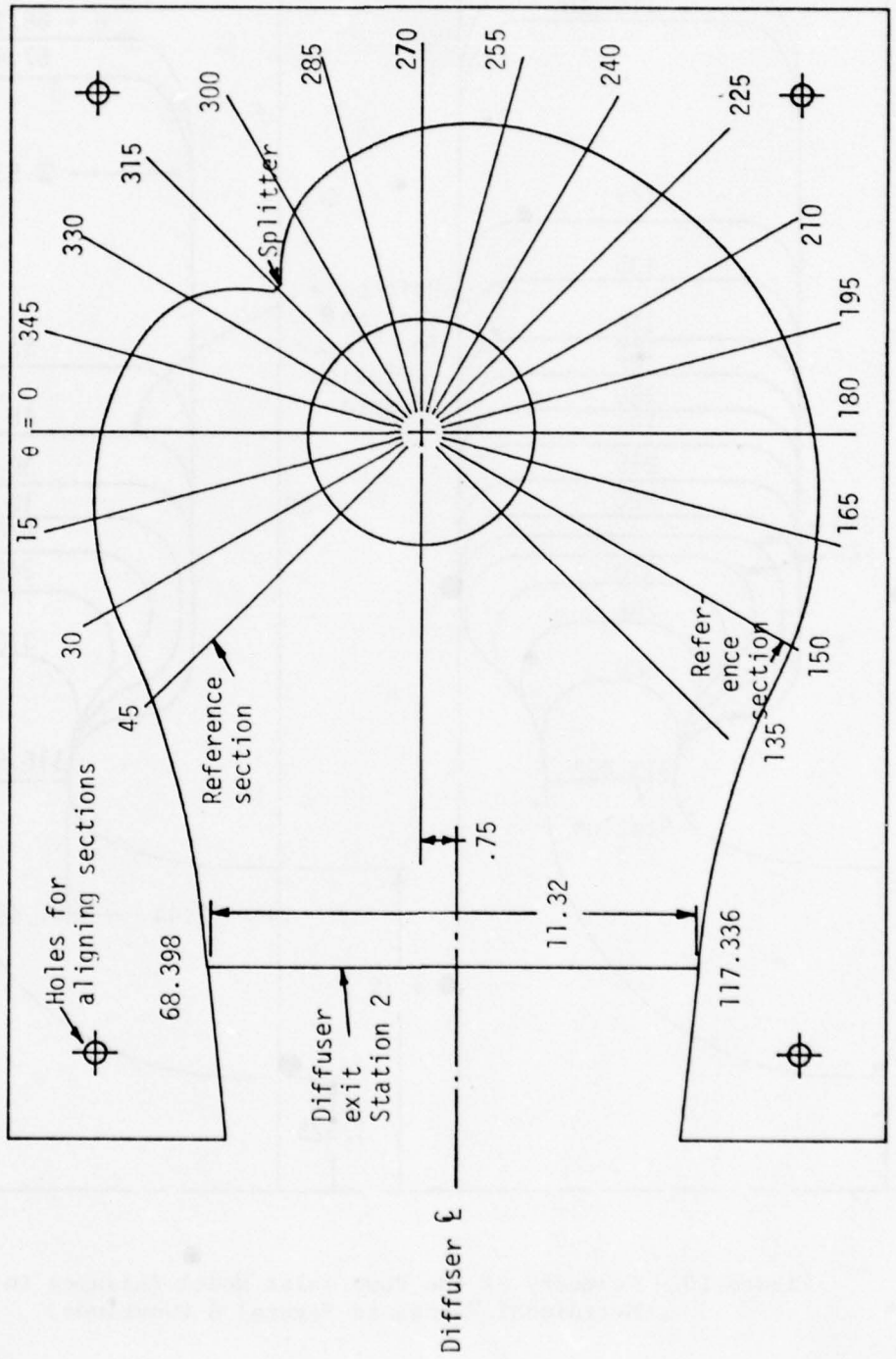

Figure 9 - A Cross Section of the Pump Inlet Model Perpendicular to the Pump Axis.

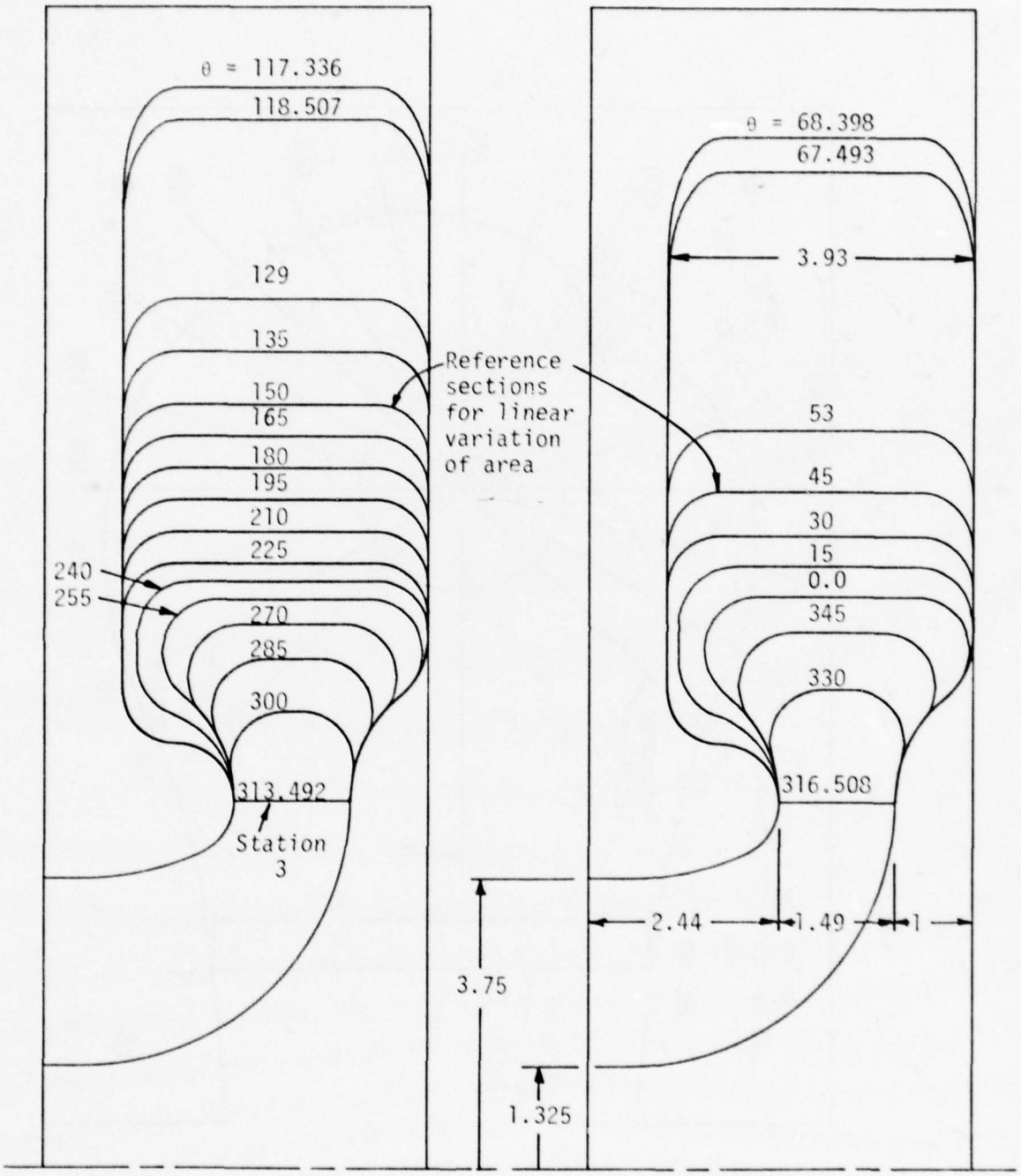

Figure 10 - Geometry of the Pump Inlet Model Passages in Meridional Planes at Several θ Locations.

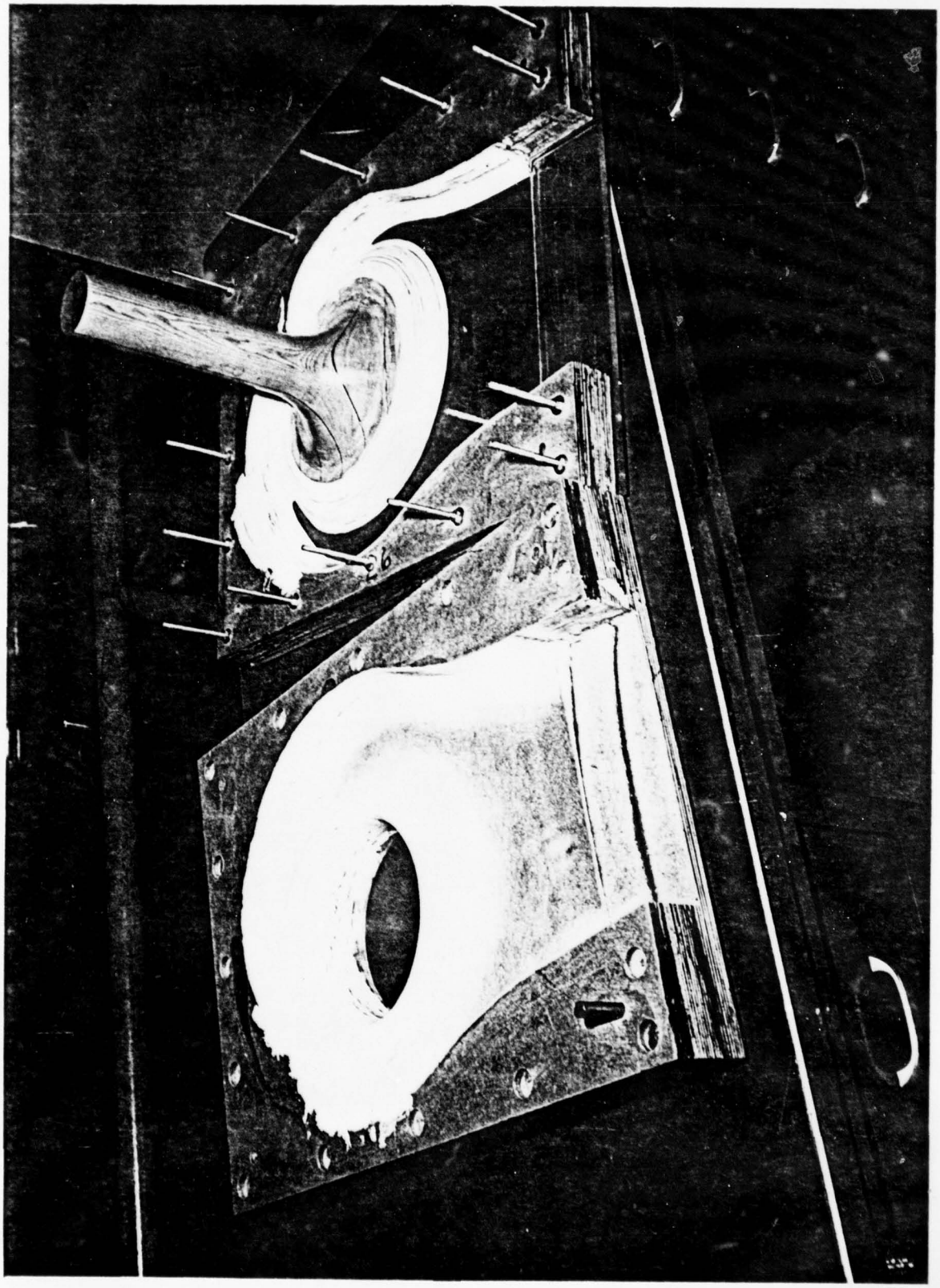

Figure 11 - Photograph of the Two Halves of the Pump Inlet Model Revealing the Shape of the Flow Passages.

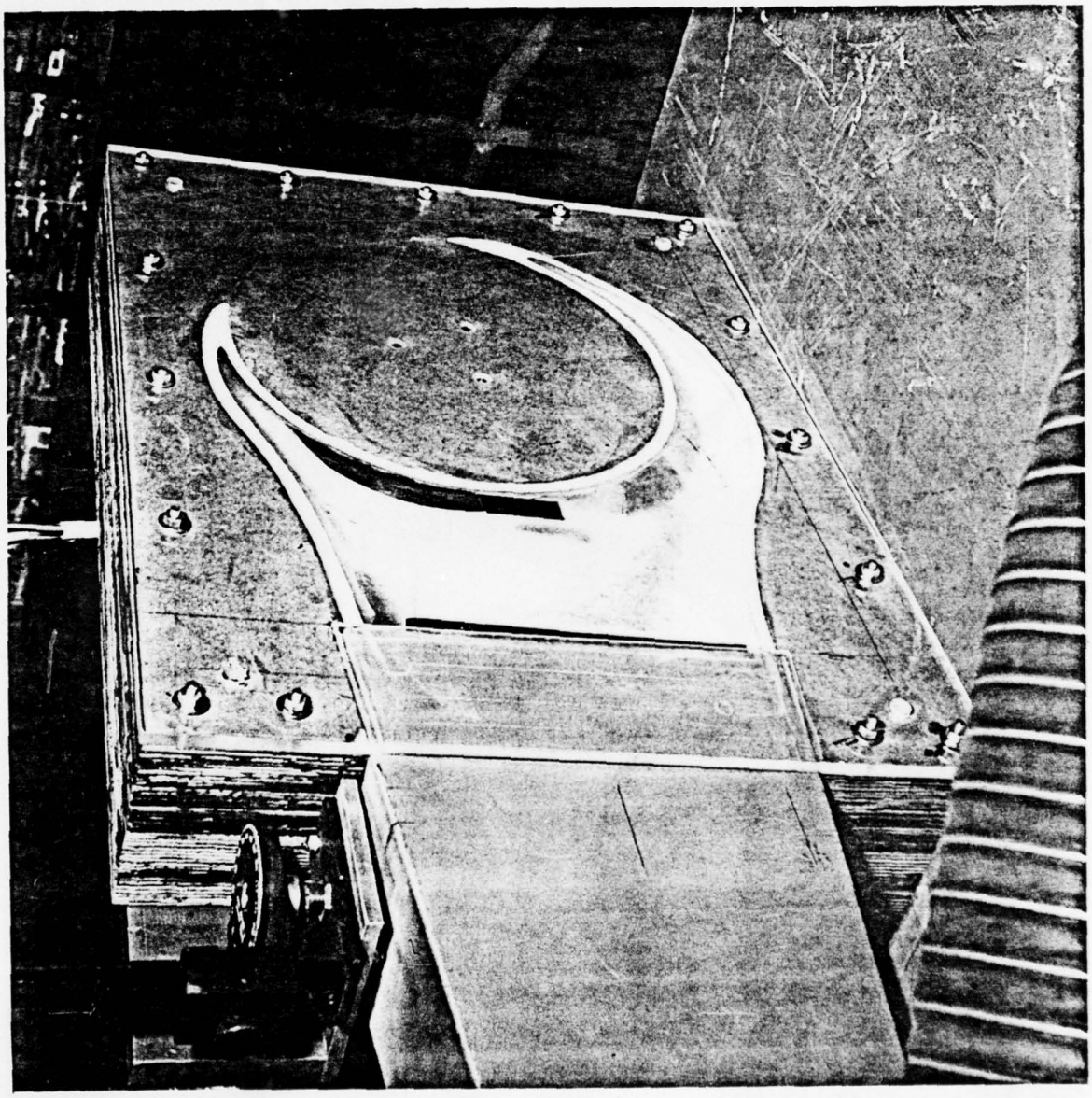

Figure 12 - Photograph of the Pump Inlet Model Installed in the Test Loop.

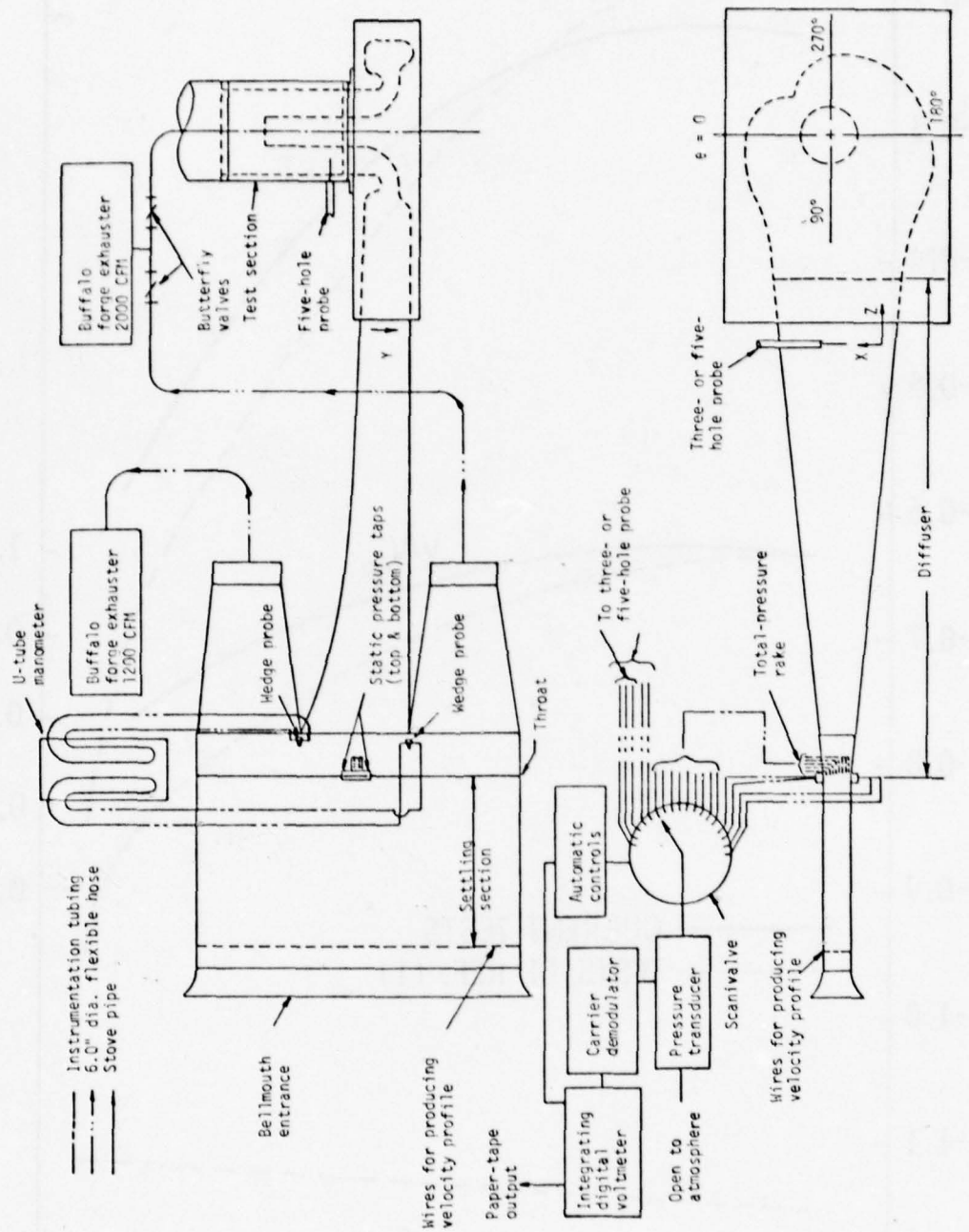

Figure 13 - Schematic of the Test Facility and the Instrumentation.

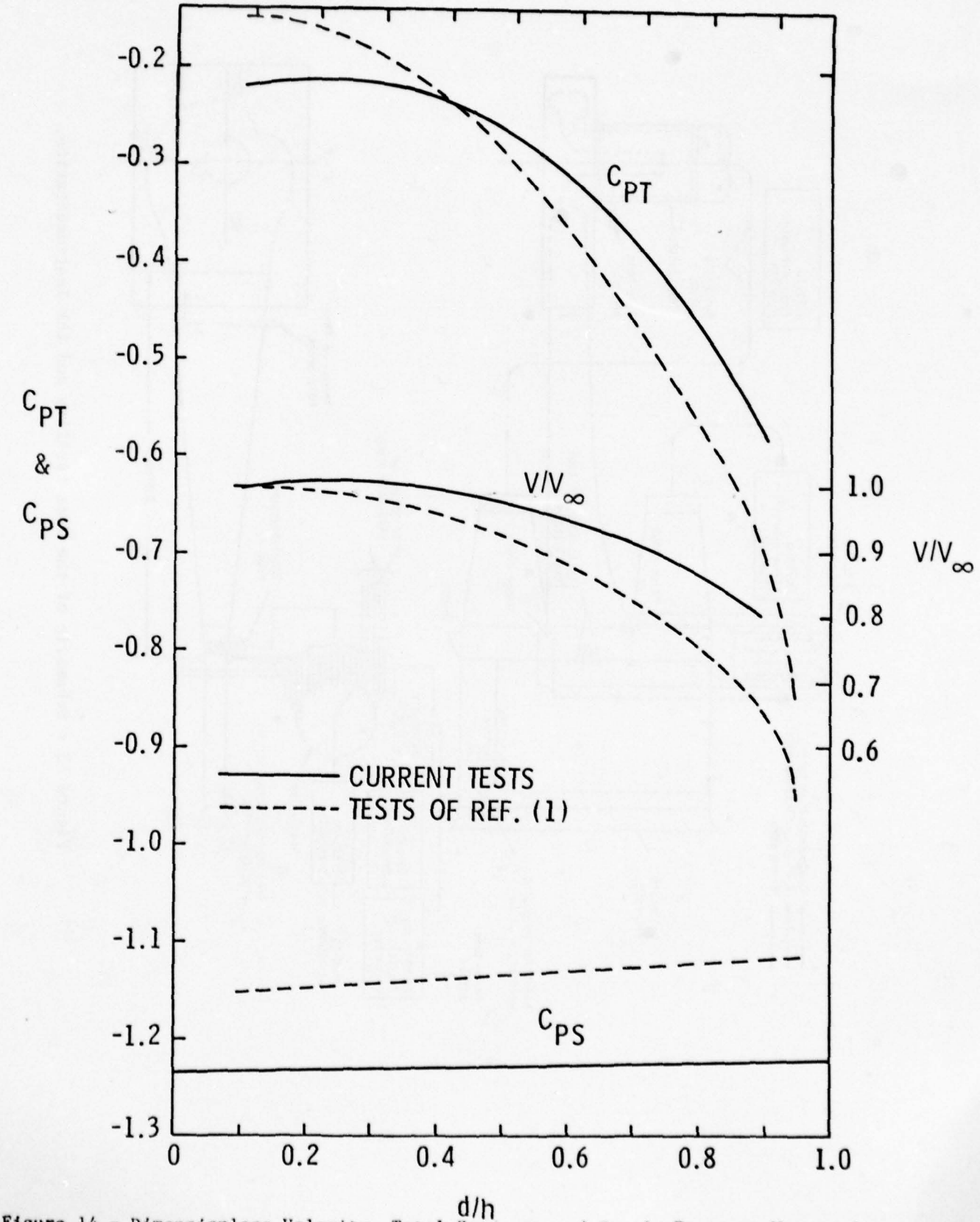

Figure 14 - Dimensionless Velocity, Total Pressure and Static Pressure Measured at the Throat (Diffuser Inlet) for the Current Tests and the Tests of Ref. [1].

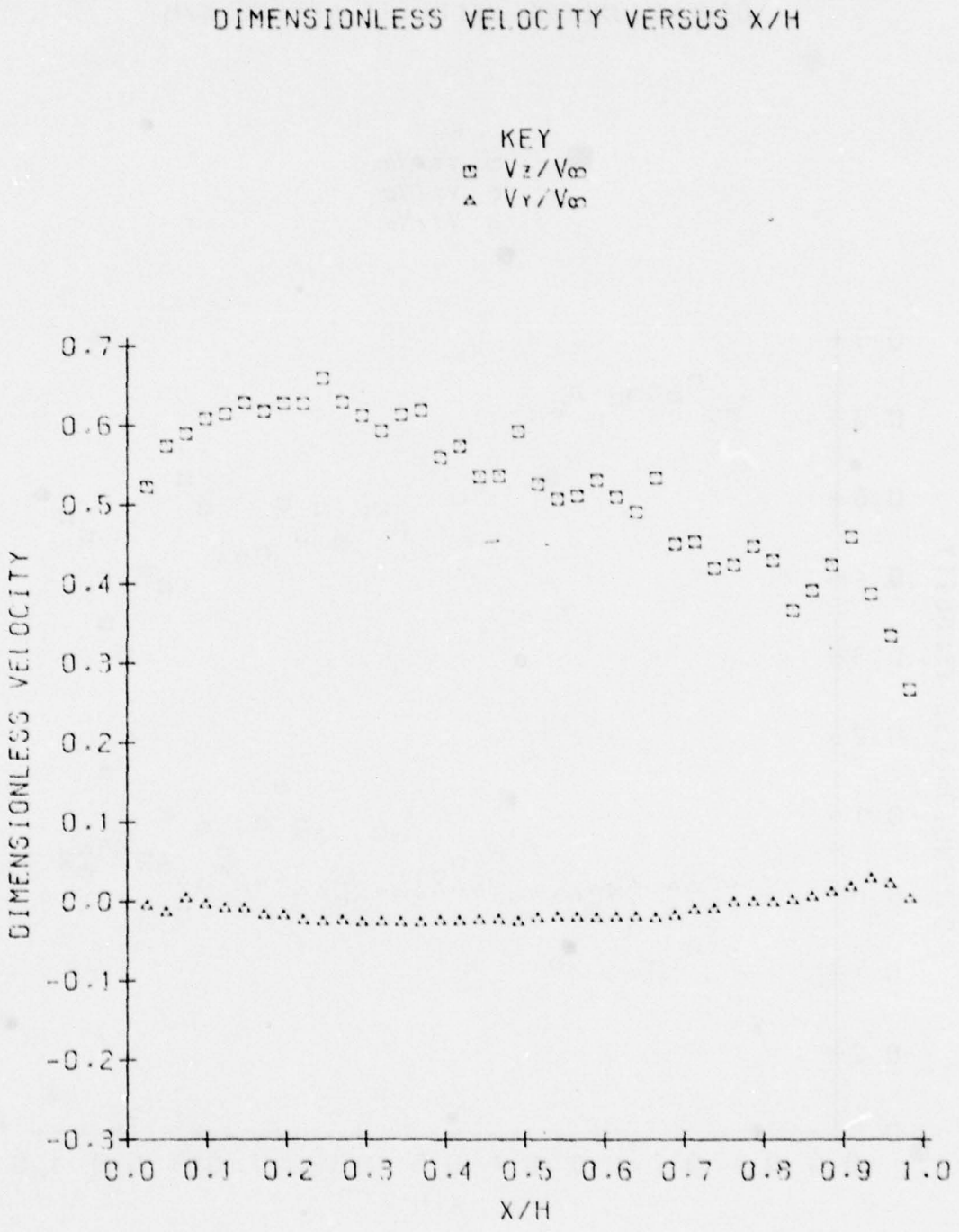

Figure 15 - Velocity Profiles Measured Near the Diffuser Exit With a Three-Hole Probe.

April 4, 1979
AMY:cac

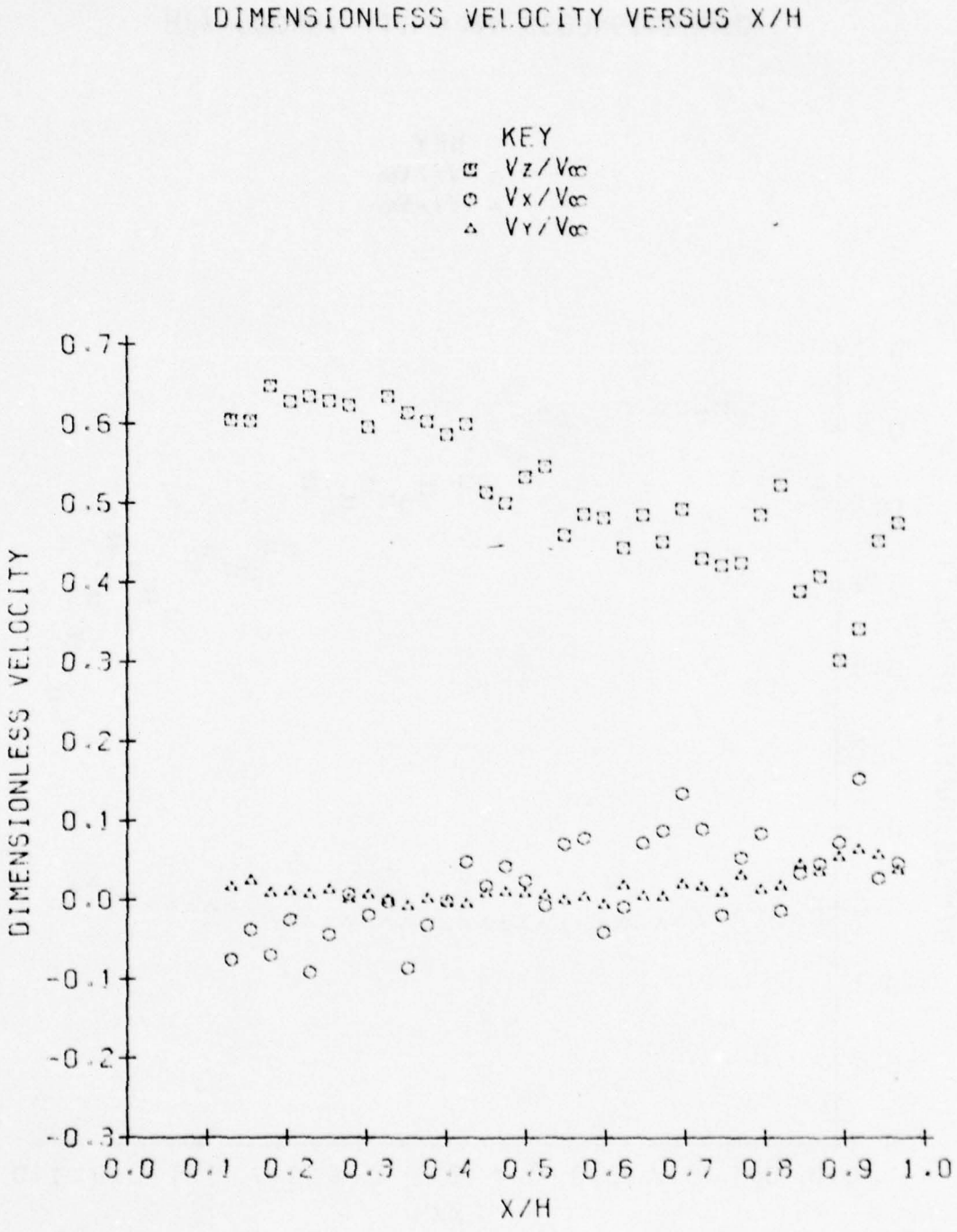

Figure 16 - Velocity Profiles Measured Near the Diffuser Exit With a Five-Hole Probe.

April 4, 1979
AMY:cac

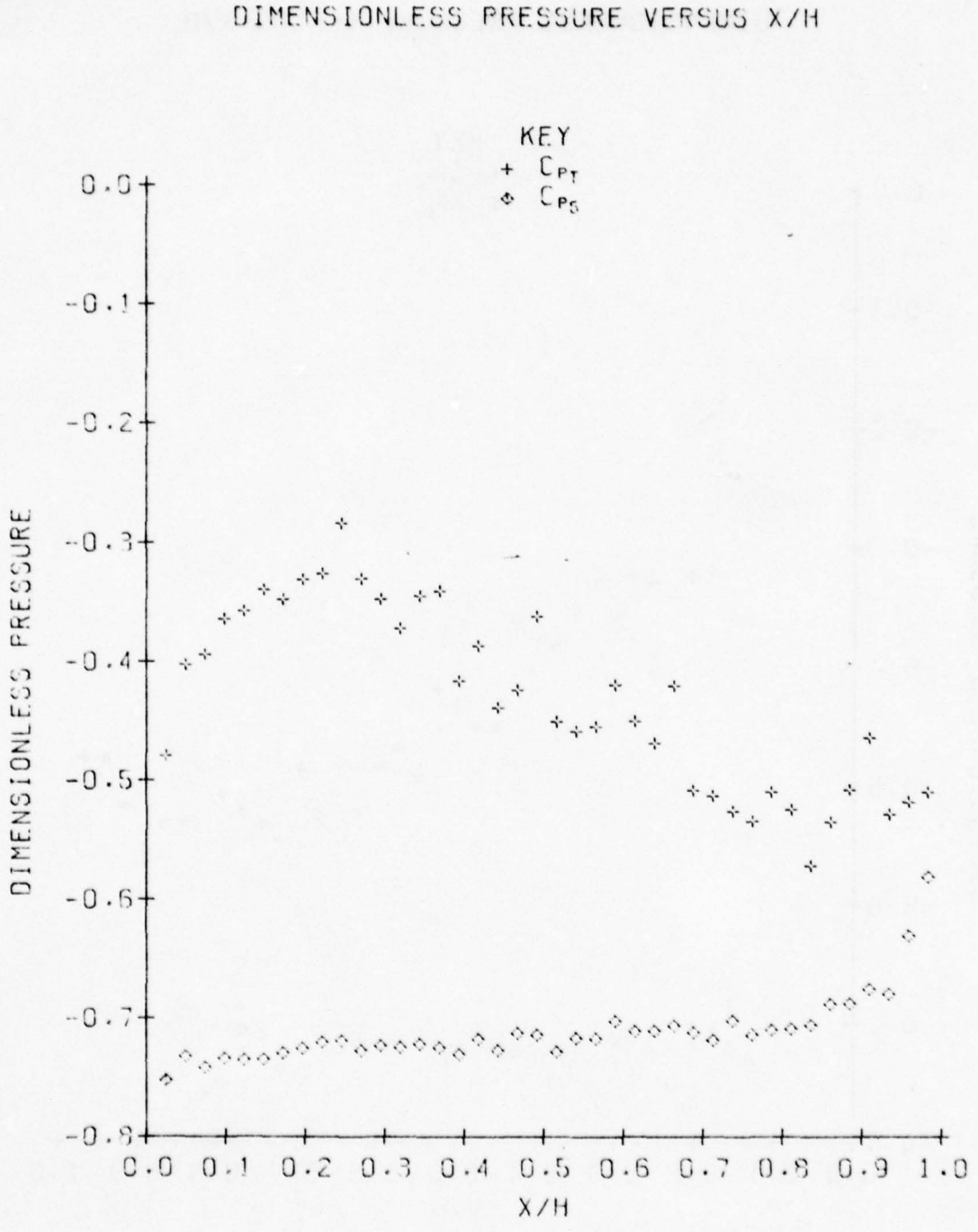

Figure 17 - Pressure Profiles Measured Near the Diffuser Exit With a Three-Hole Probe.

April 4, 1979
AMY:cac

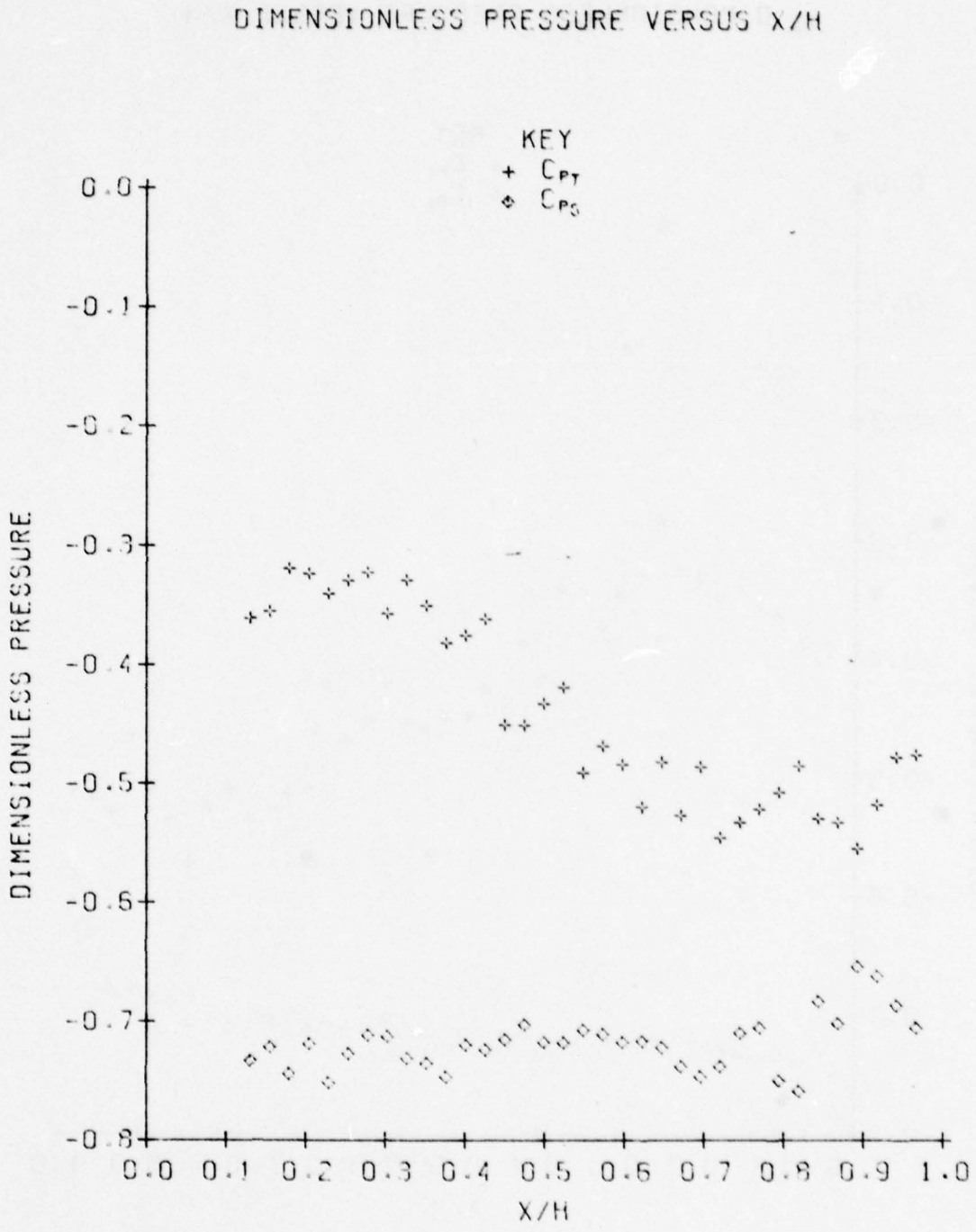

Figure 18 - Pressure Profiles Measured Near the Diffuser Exit With a Five-Hole Probe.

April 4, 1979
AMY:cac

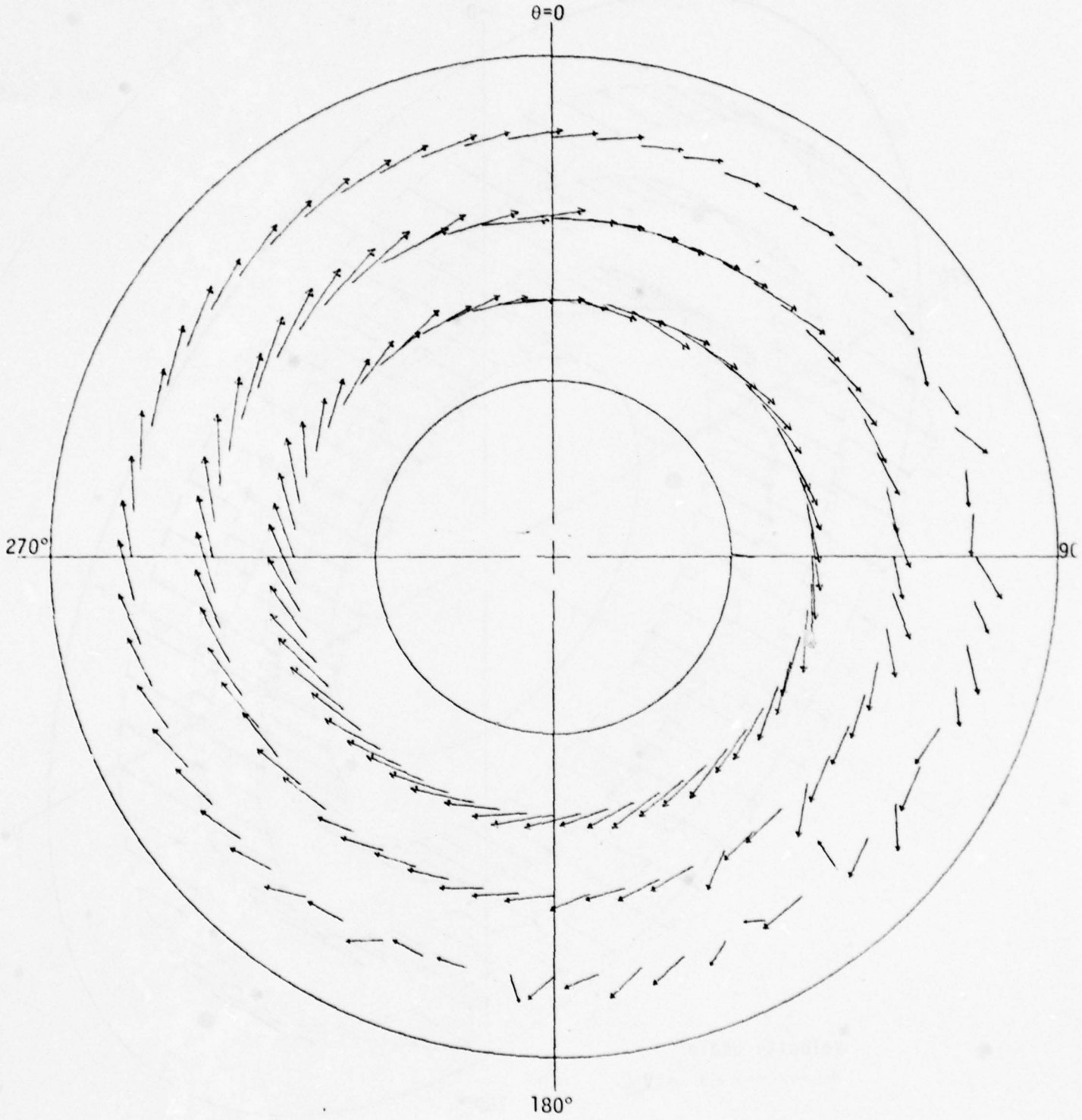

Figure 19 - Velocity Vectors ($V/V_\infty = \sqrt{V_\theta^2/V_\infty^2 + V_R^2/V_\infty^2}$) Measured in a Cross Sectional Plane of the Test Section.

April 4, 1979
AMY:cac

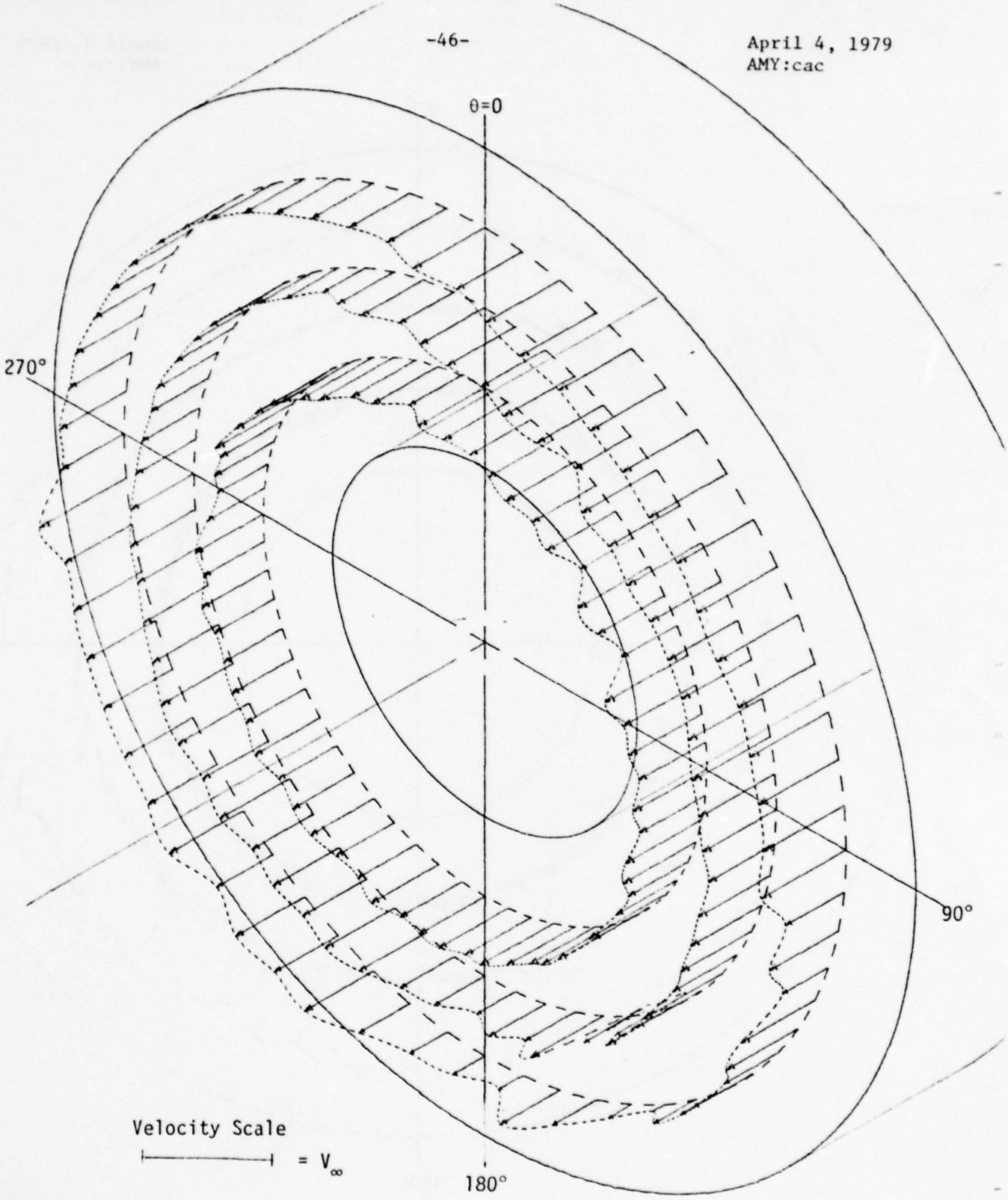

Figure 20 - Pictorial View of the Axial Velocity Vectors in a Cross Section of the Test Section.

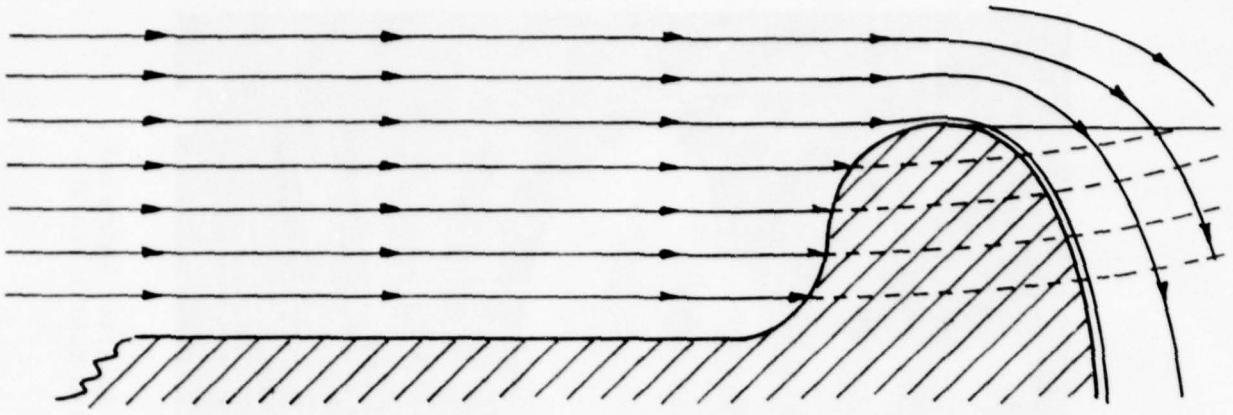

Figure 21a - Cross Section of the Lip of the Inlet at the 90° Circumferential Location Showing the Desired Flow Pattern.

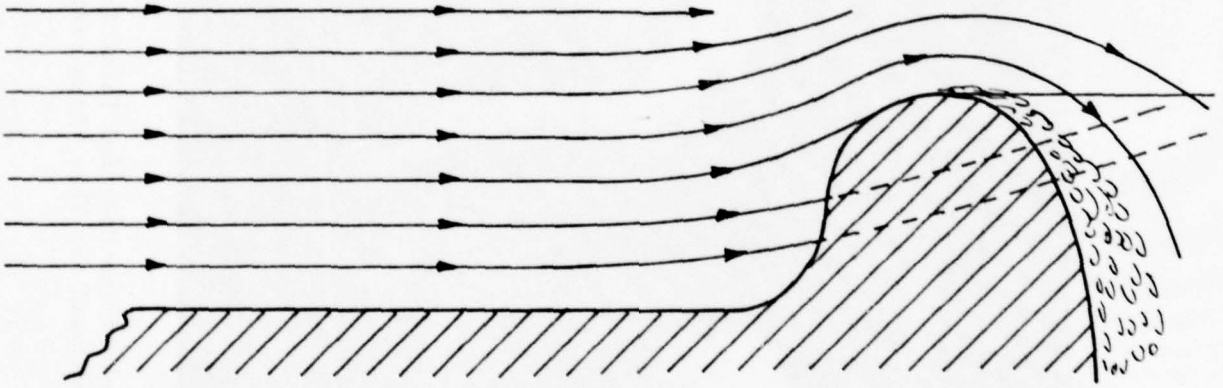

Figure 21b - Cross Section of the Lip of the Inlet at the 90° Circumferential Location Showing the Suspected Flow Pattern.

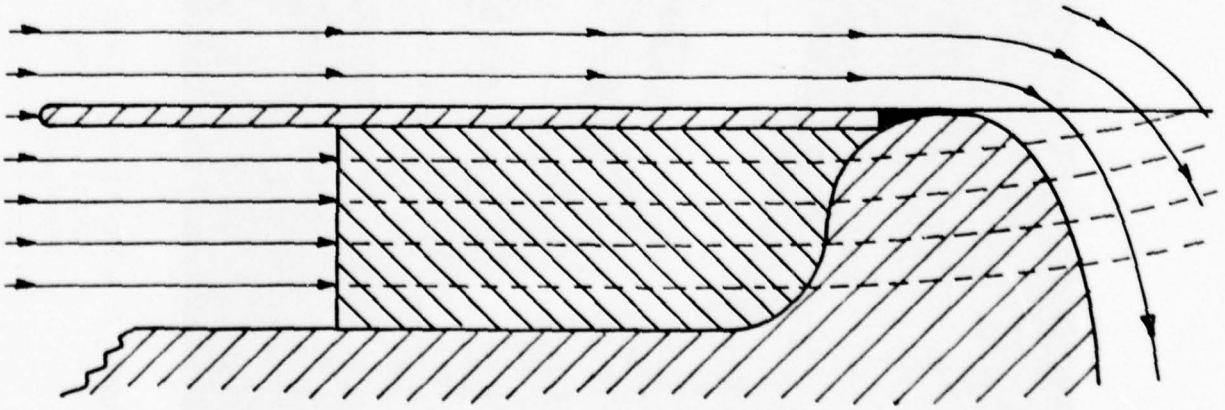

Figure 21c - Cross Section of the Modification Made to the Inlet to Obtain the Desired Flow Pattern.

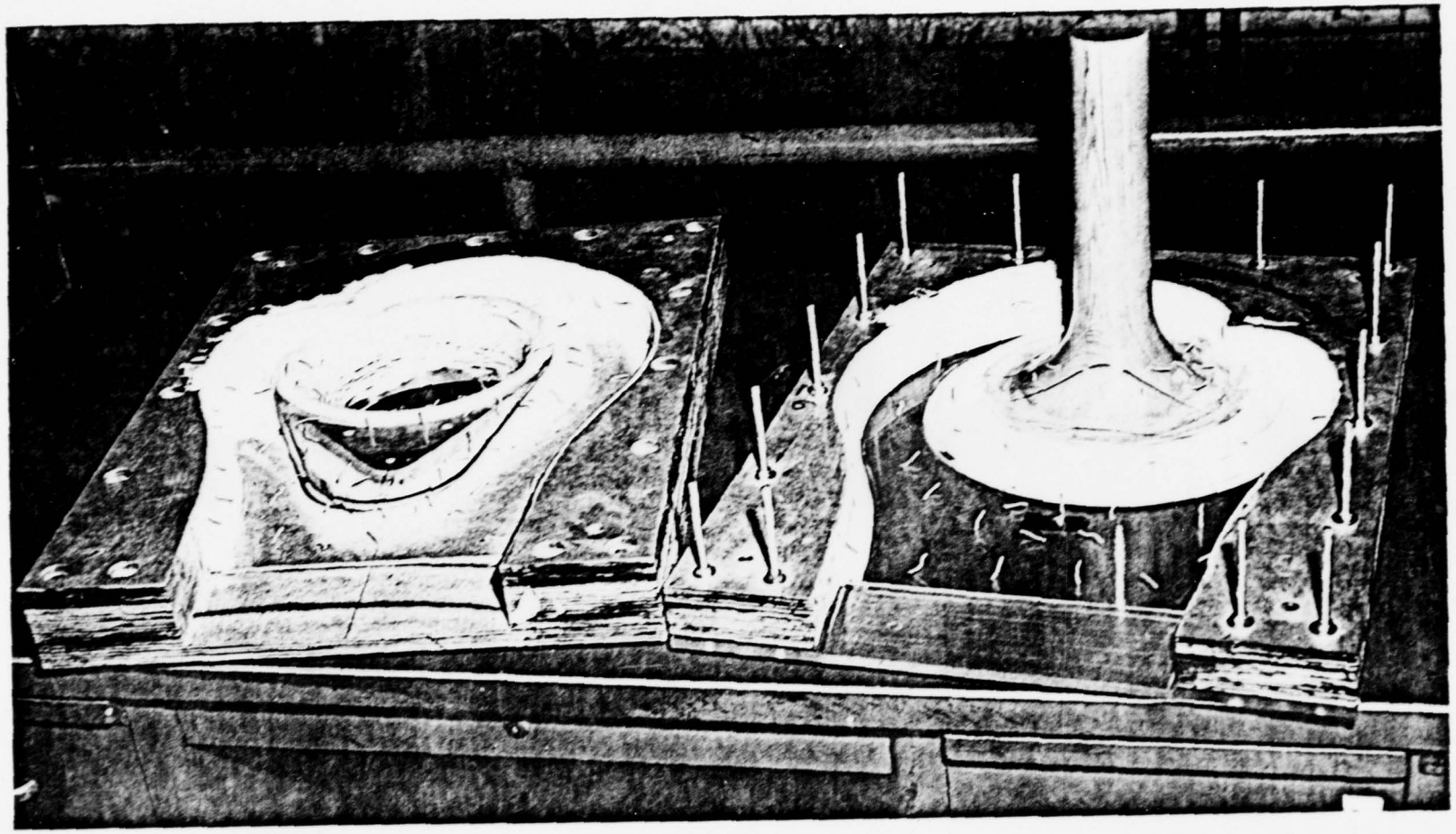

Figure 22 - Photograph of the Two Halves of the Modified Inlet Showing the Splitter Which was Installed. Tufts which were used for Flow Visualization are also Visible in the Photograph.

April 4, 1979
AMY:cac

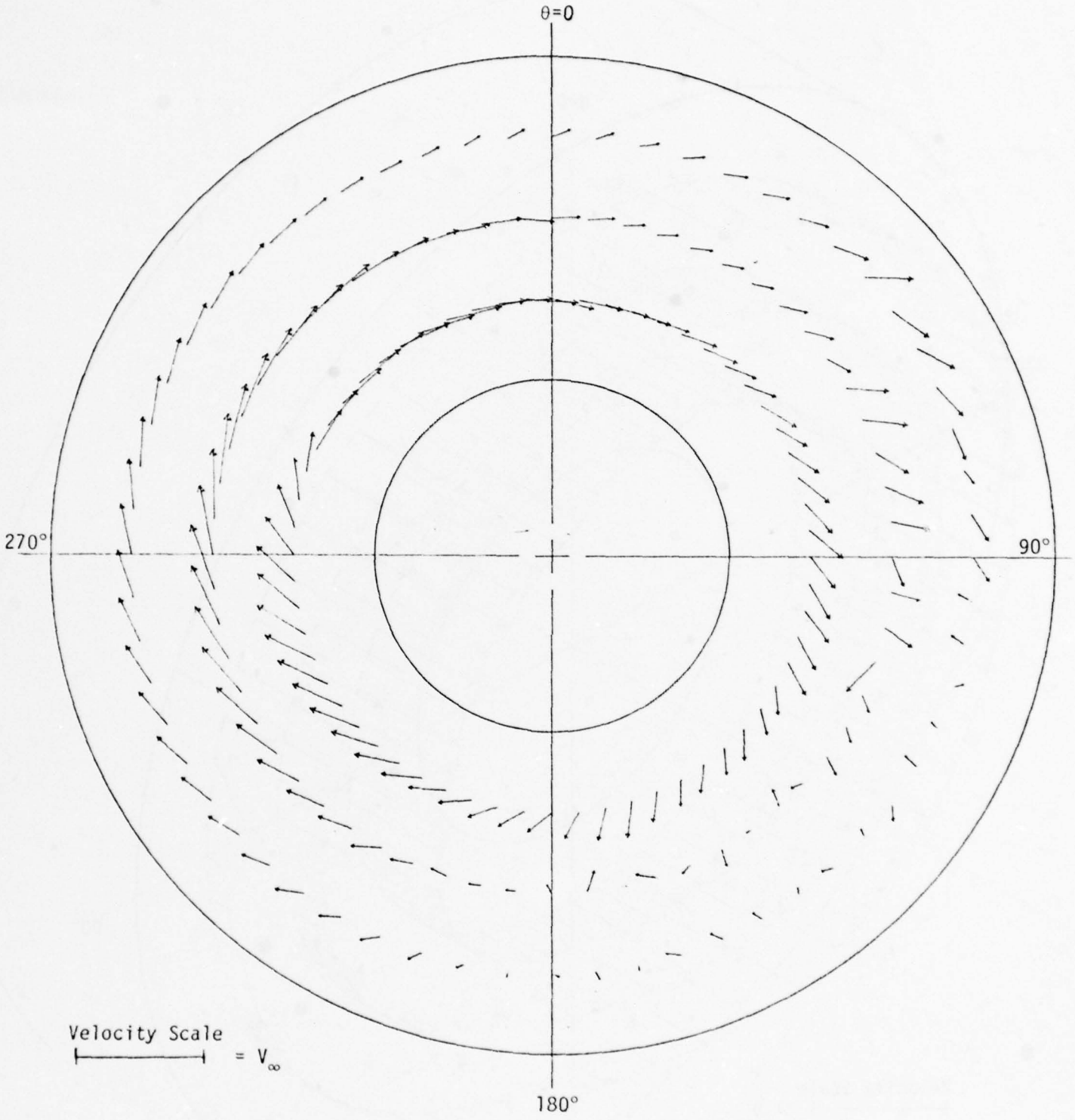

Figure 23 - Velocity Vectors ($V/V_\infty = \sqrt{V_\theta^2/V_\infty^2 + V_R^2/V_\infty^2}$) Measured in a Cross Sectional Plane of the Test Section After the Pump Inlet was Modified.

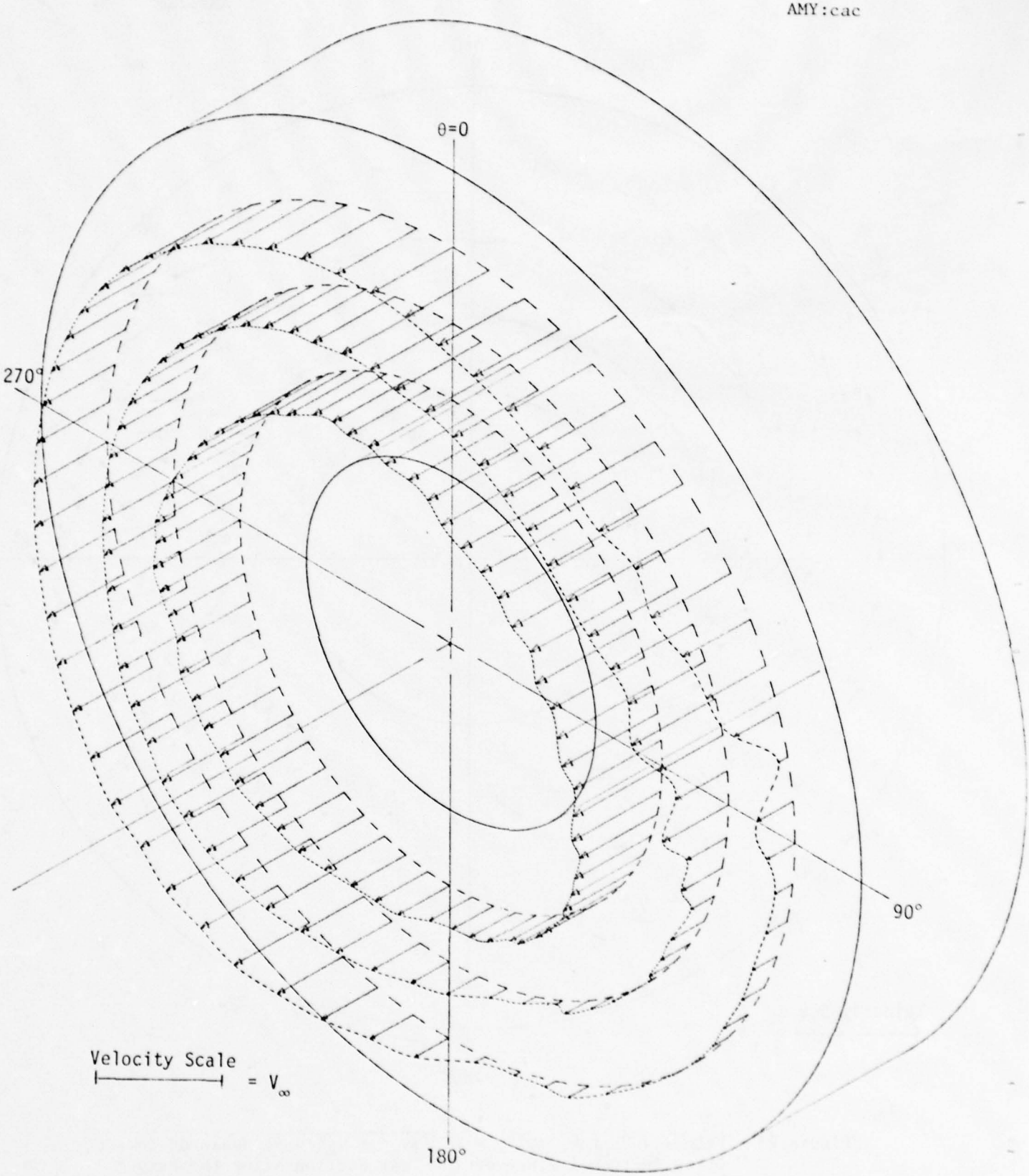

Figure 24 - Pictorial View of the Axial Velocity Vectors in a Cross Section of the Test Section After the Pump Inlet was Modified.

TABLE 1

Average Parameters Calculated for Each Measurement Station

	THROAT	DIFFUSER EXIT 3-hole probe 5-hole probe	TEST SECTION without splitter with splitter
$\left.\frac{V_z}{V_\infty}\right\|_{avg}$	.9388	.5179	.5568
		.5235	.5905
$C_{PT}\|_{\substack{mass \\ avg}}$	-.3241	-.4210	-.6158
		-.4168	-.7159
$\frac{V_{z\ avg}}{V_\infty}\frac{A}{A_1}$	.9388	.9439	.9187
		.9541	.9743

APPENDIX A

Data Measured in the Test Section Before the Splitter was Installed in the Pump Inlet

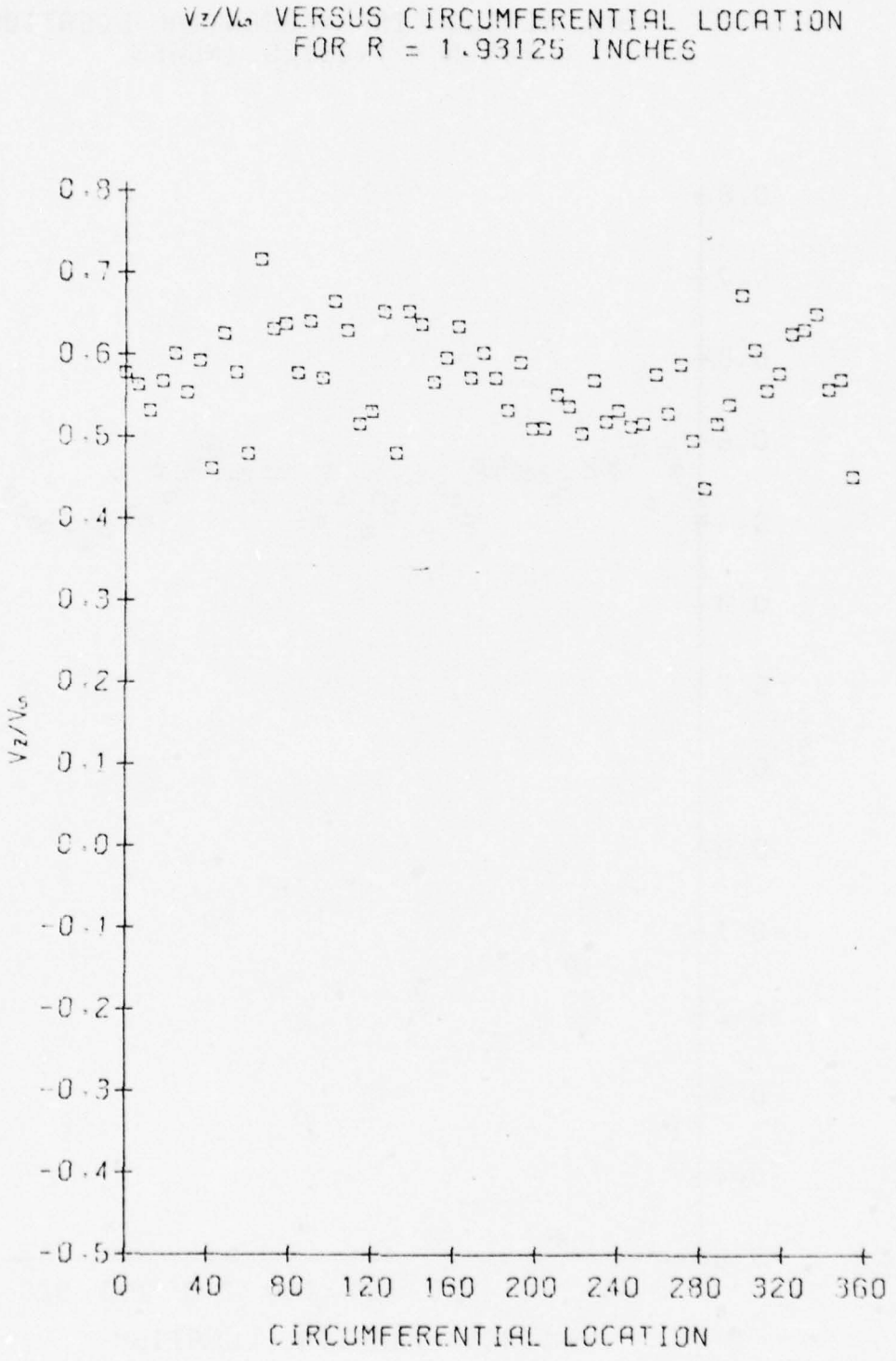
Vz/Vo VERSUS CIRCUMFERENTIAL LOCATION
FOR R = 1.93125 INCHES
0.8
0.7
0.6
0.5
0.4
0.3
0.2
0.1
0.0
-0.1
-0.2
-0.3
-0.4
-0.5
Vz/Vo
0
40
80
120
160
200
240
280
320
360
CIRCUMFERENTIAL LOCATION

Figure A.1

April 4, 1979
AMY:cac

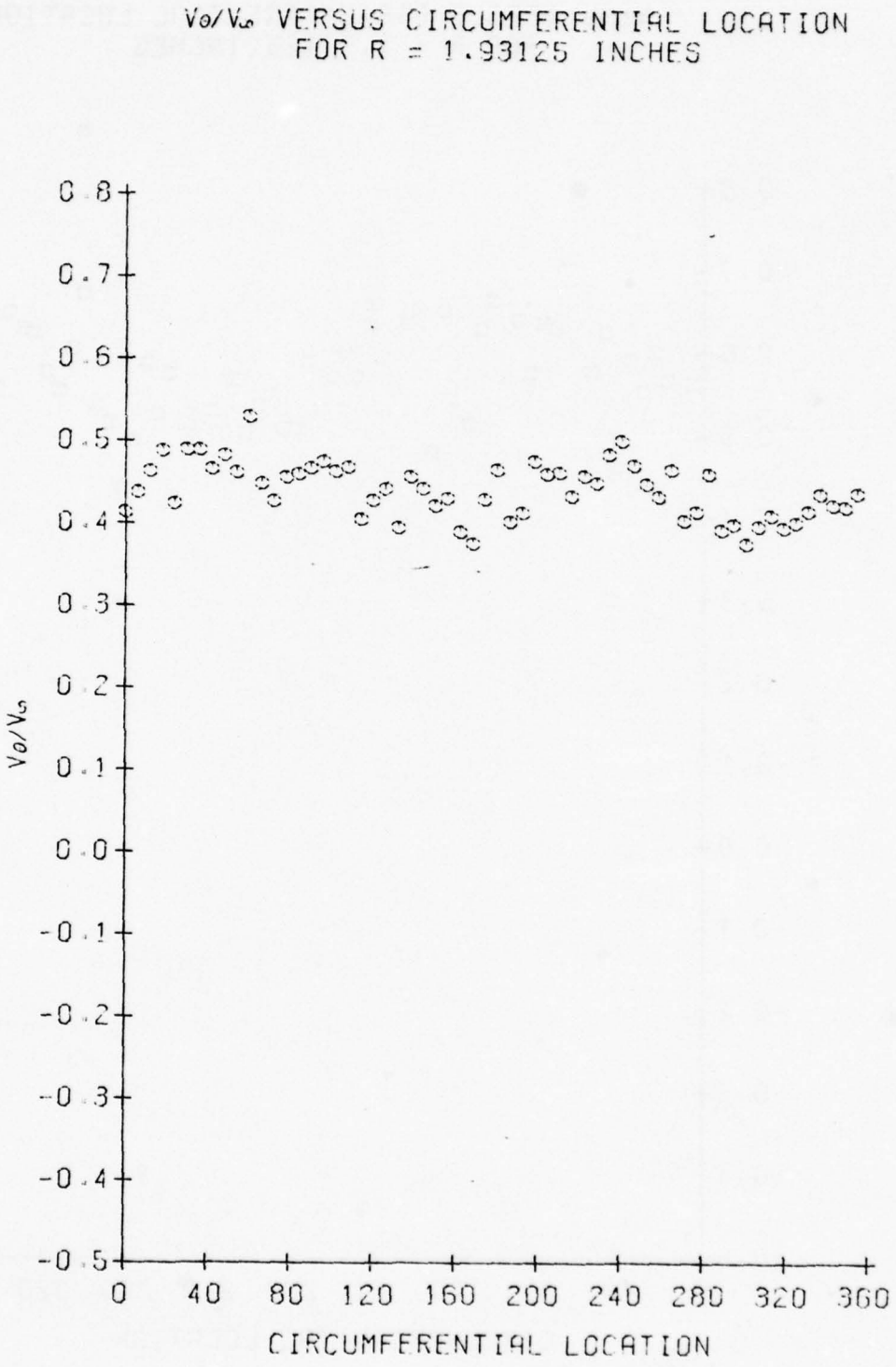

Figure A.2

April 4, 1979
AMY:cac

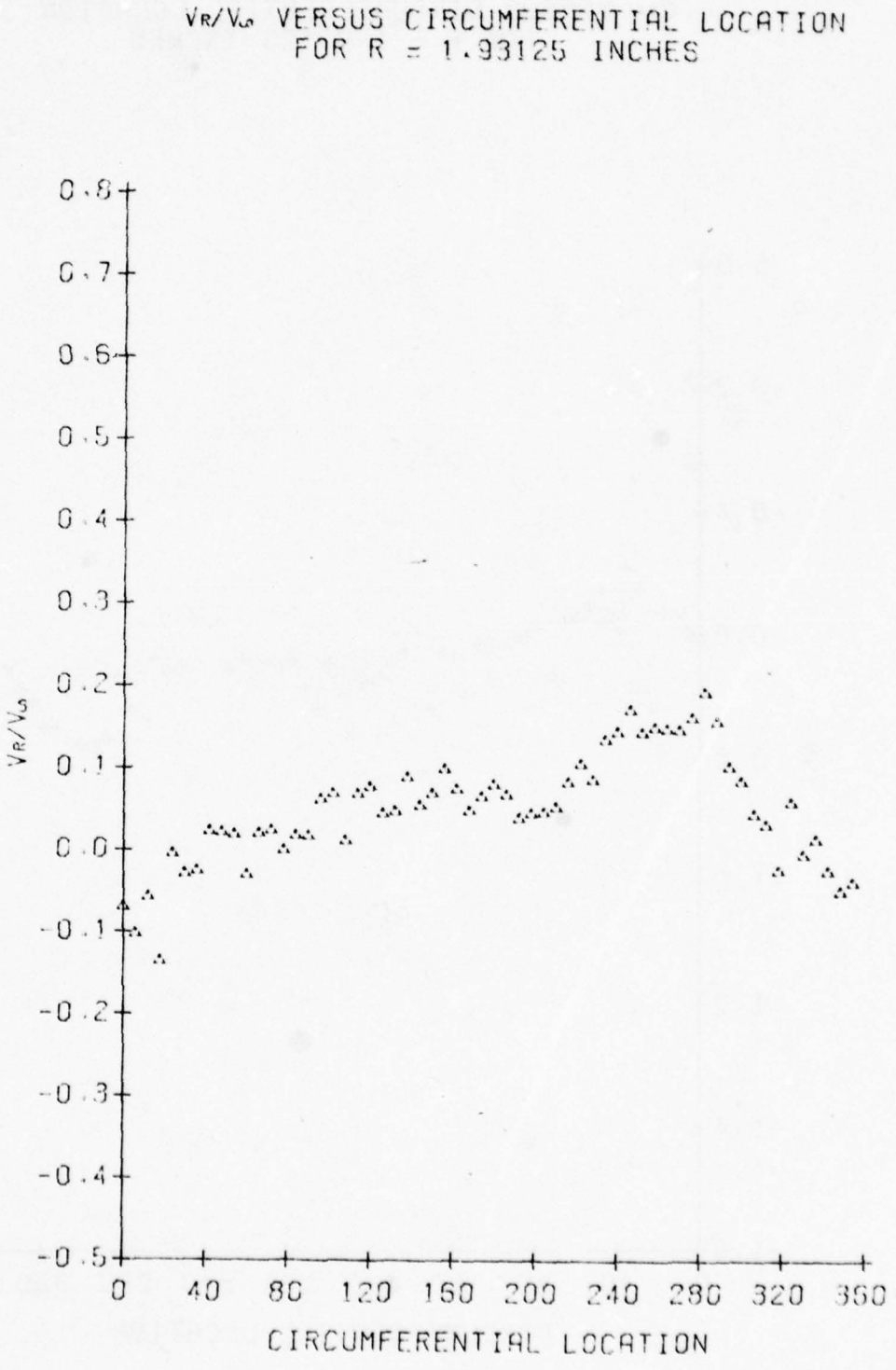

Figure A.3

April 4, 1979
AMY:cac

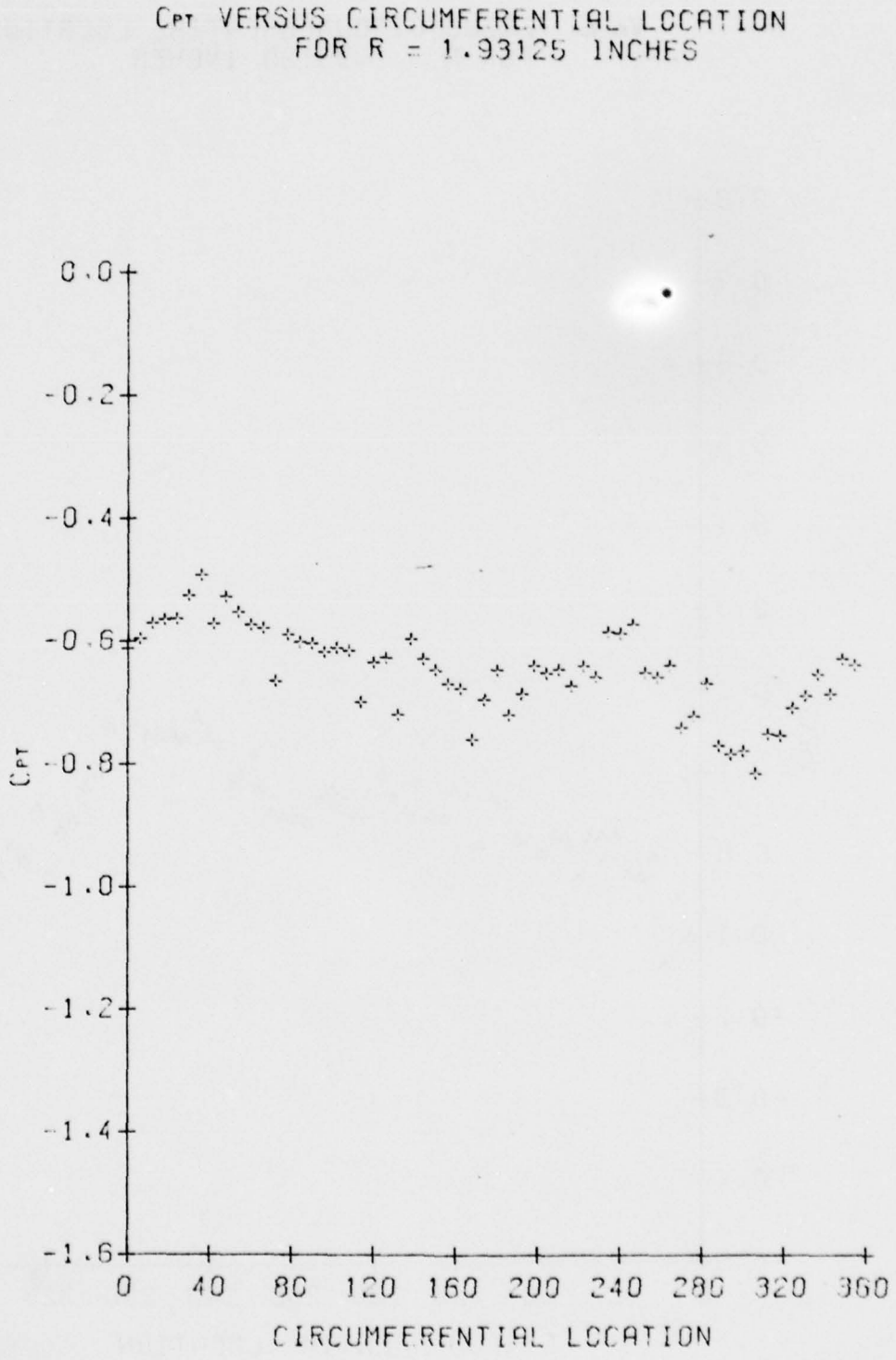

Figure A.4

April 4, 1979
AMY:cac

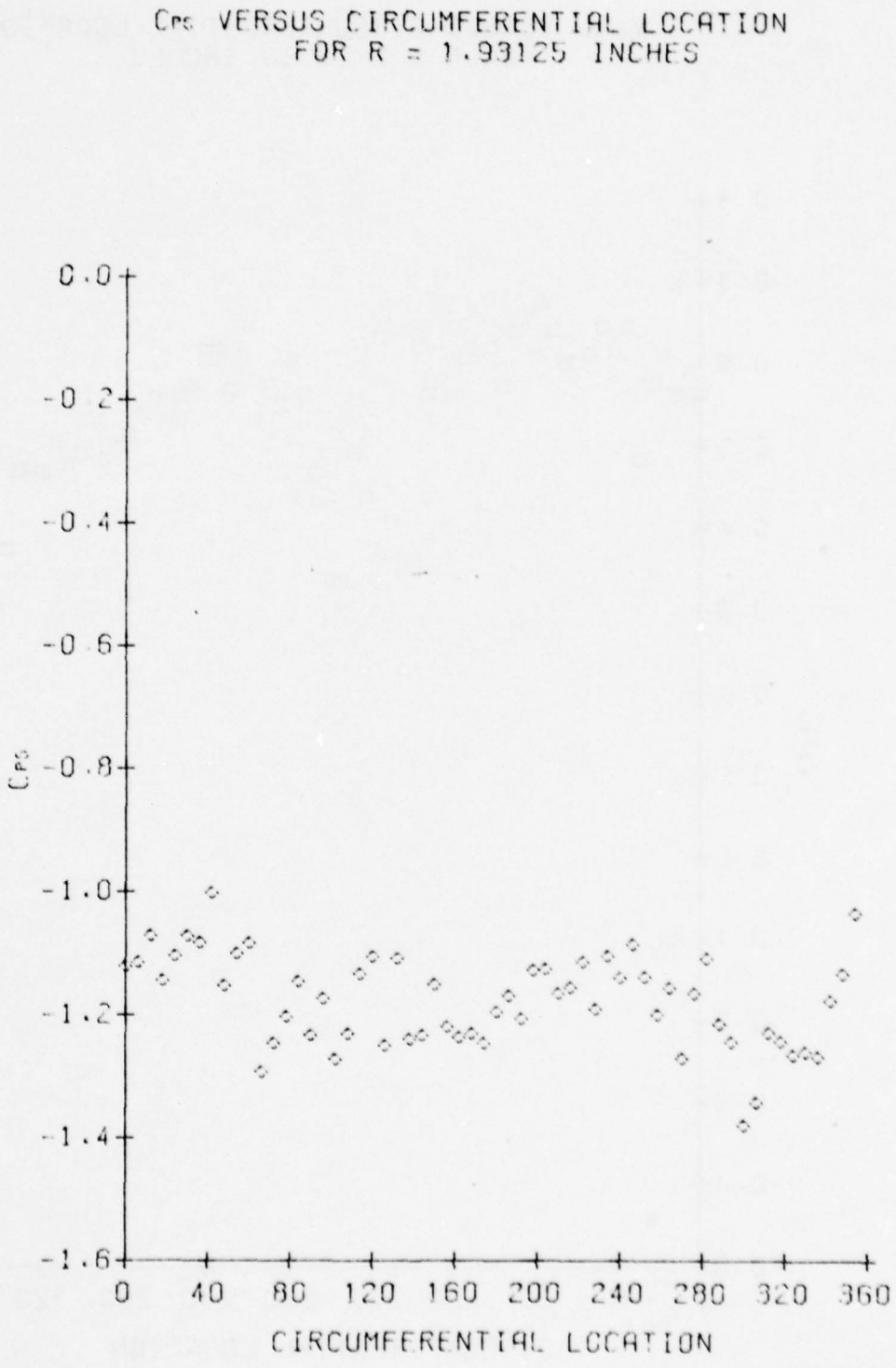

Figure A.5

April 4, 1979
AMY:cac

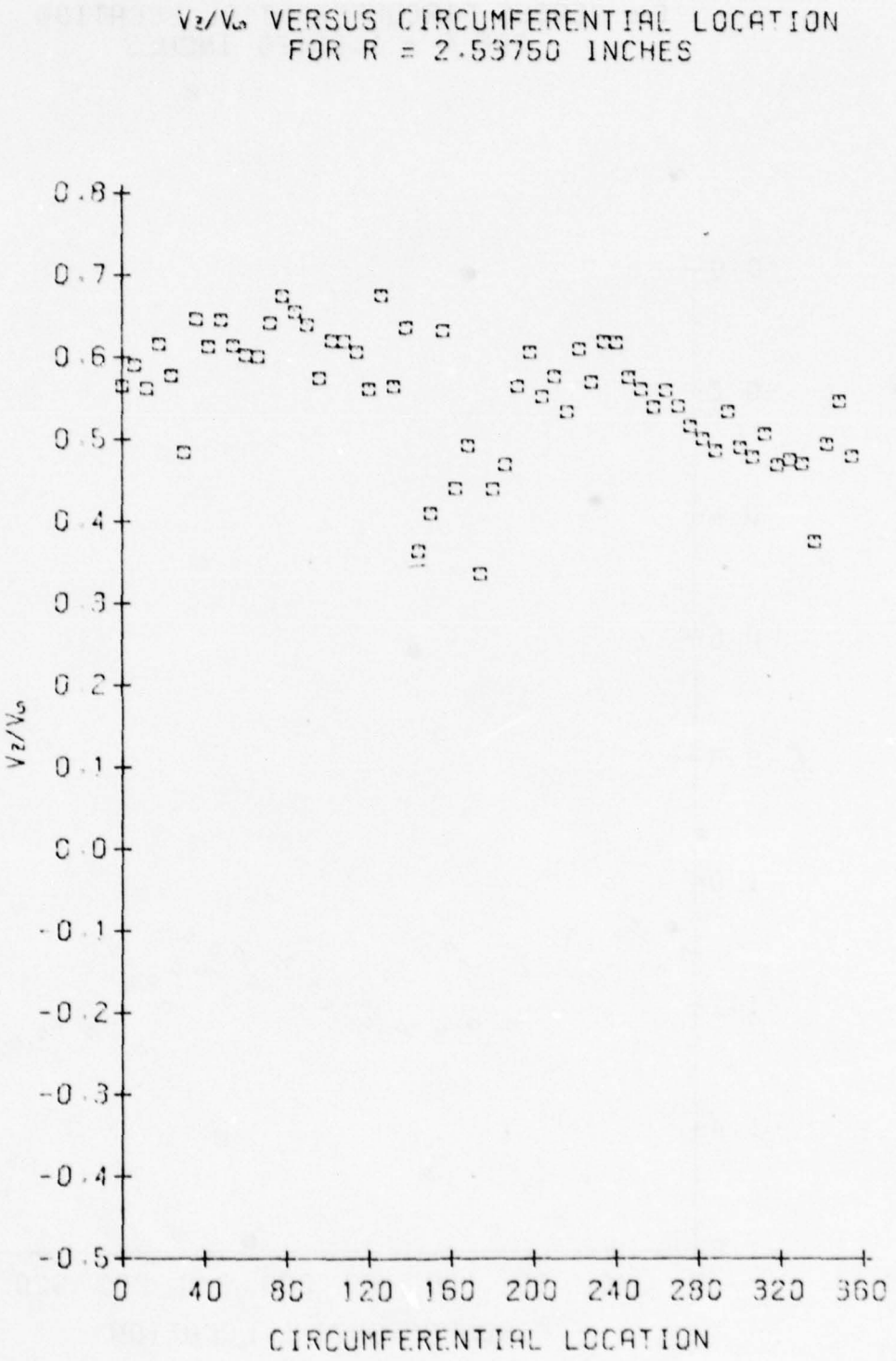

Figure A.6

April 4, 1979
AMY:cac

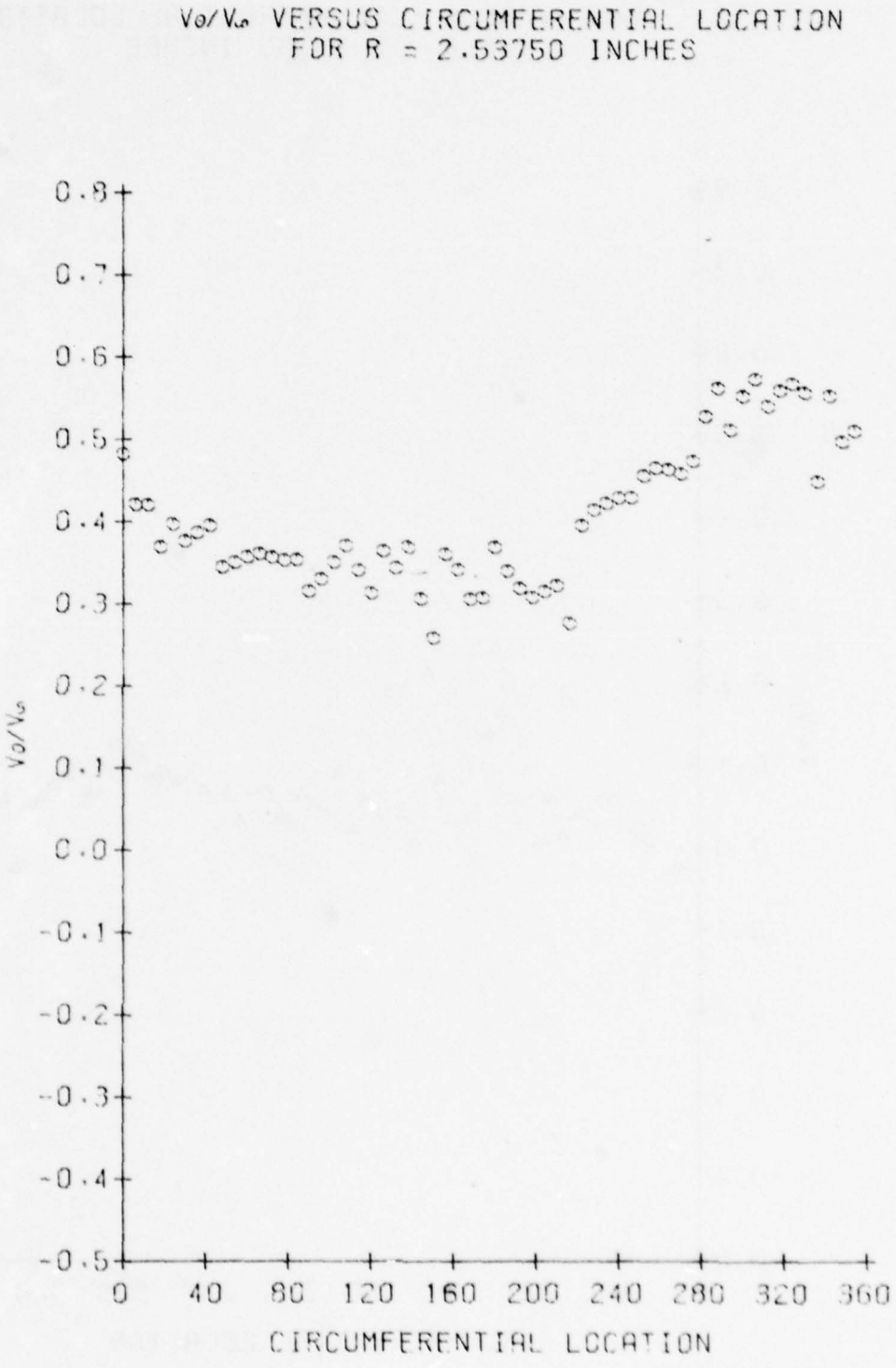

Figure A.7

April 4, 1979
AMY:cac

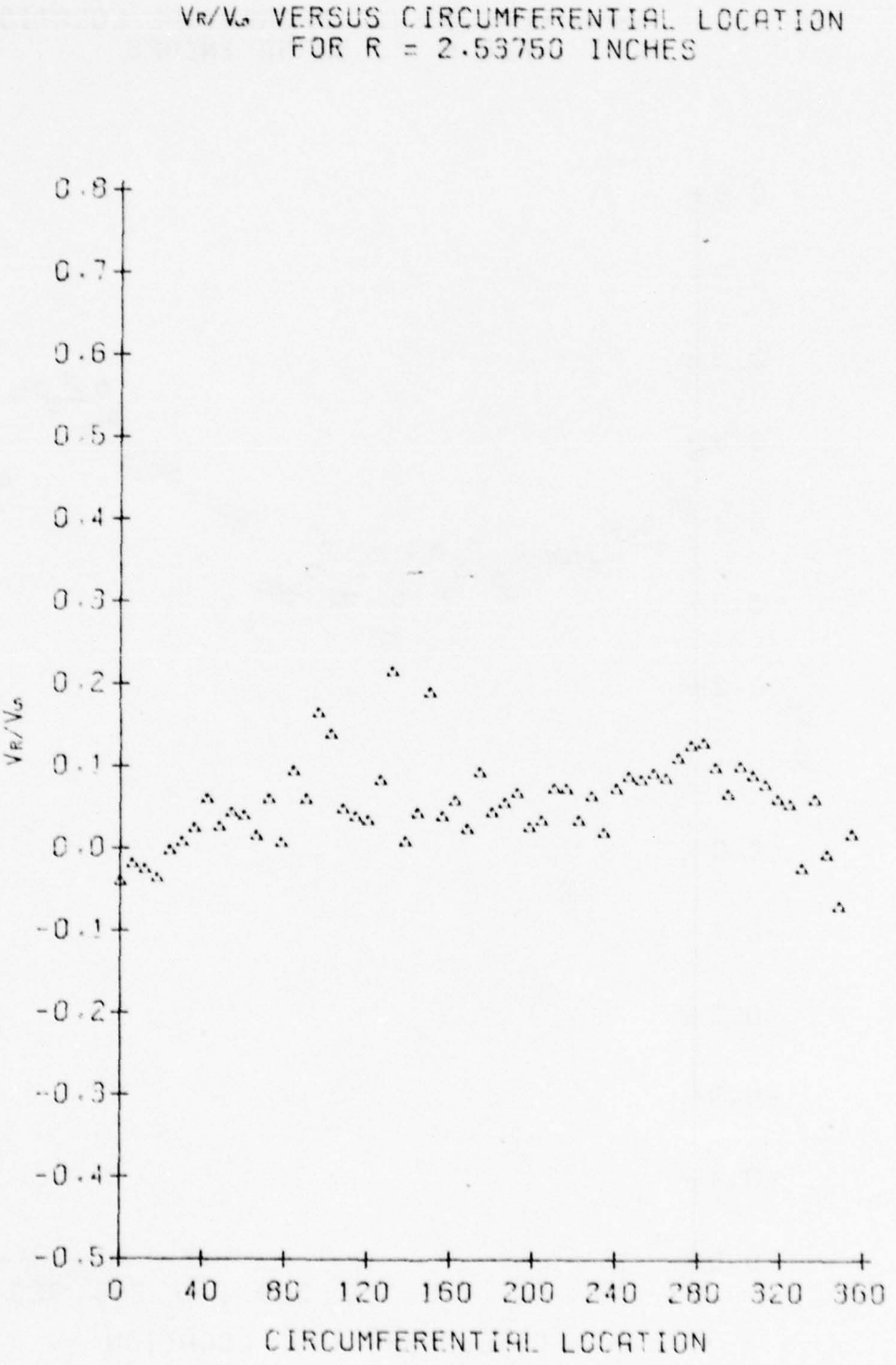

Figure A.8

April 4, 1979
AMY:cac

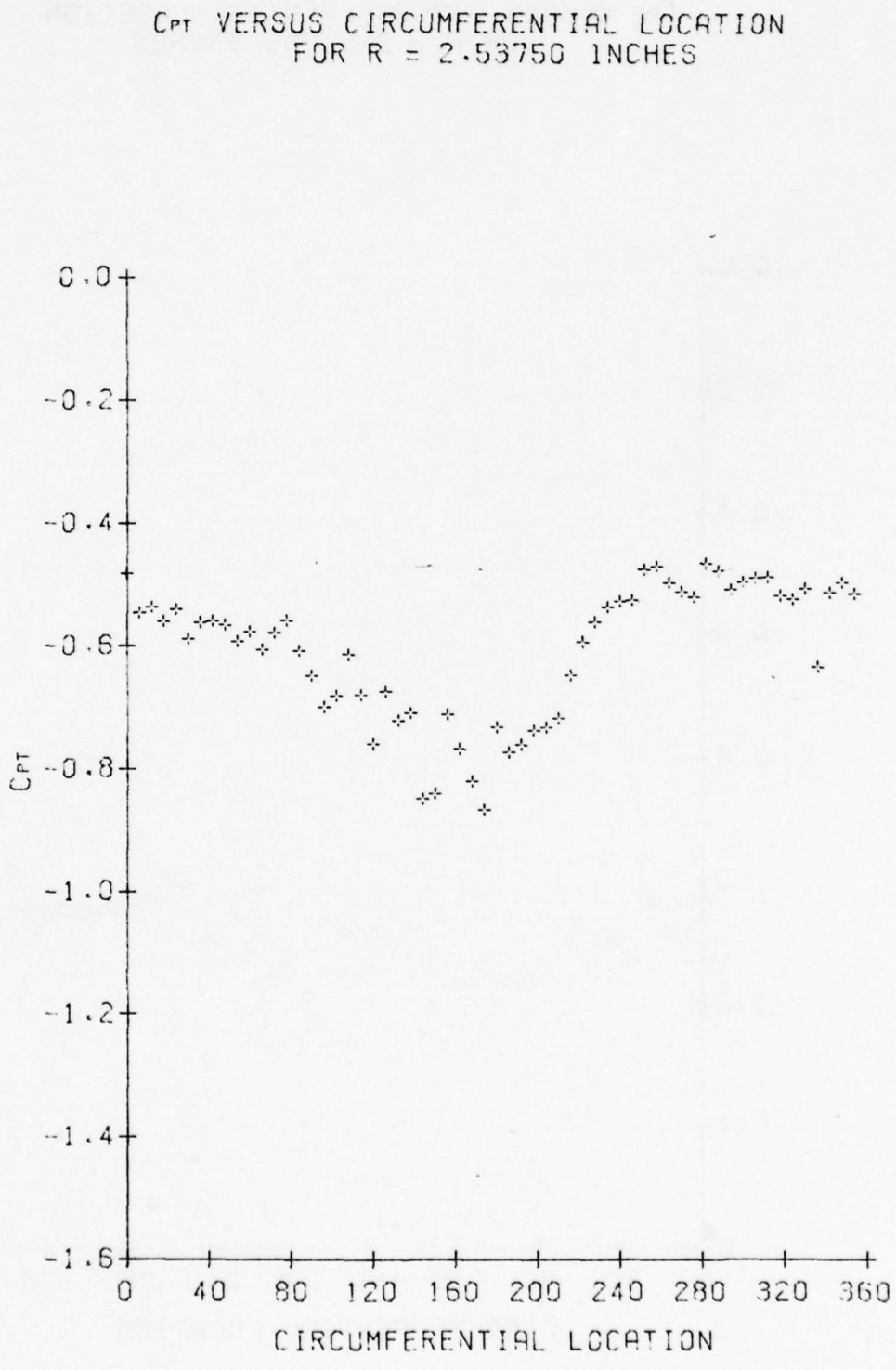

Figure A.9

April 4, 1979
AMY:cac

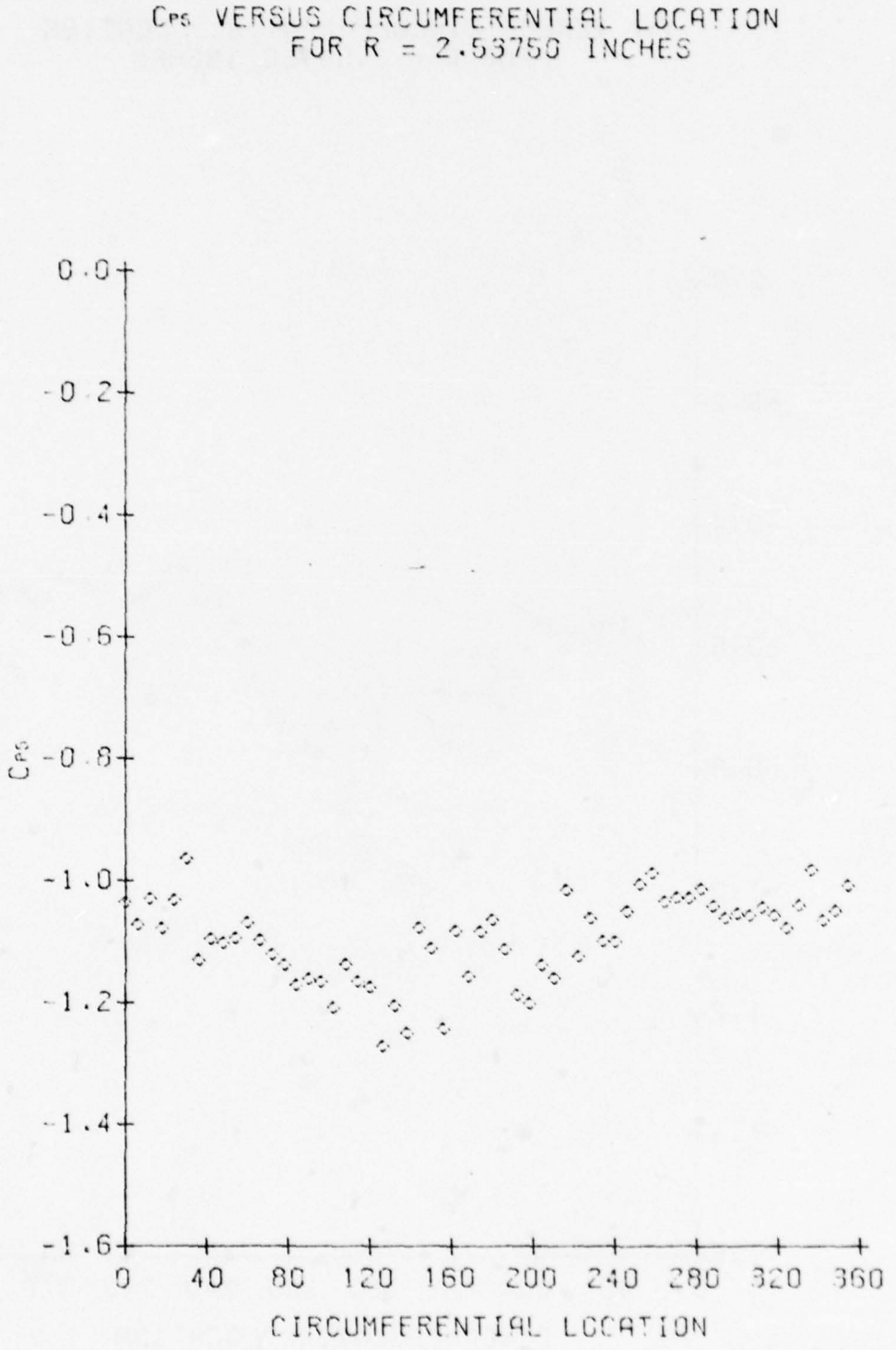

Figure A.10

April 4, 1979
AMY:cac

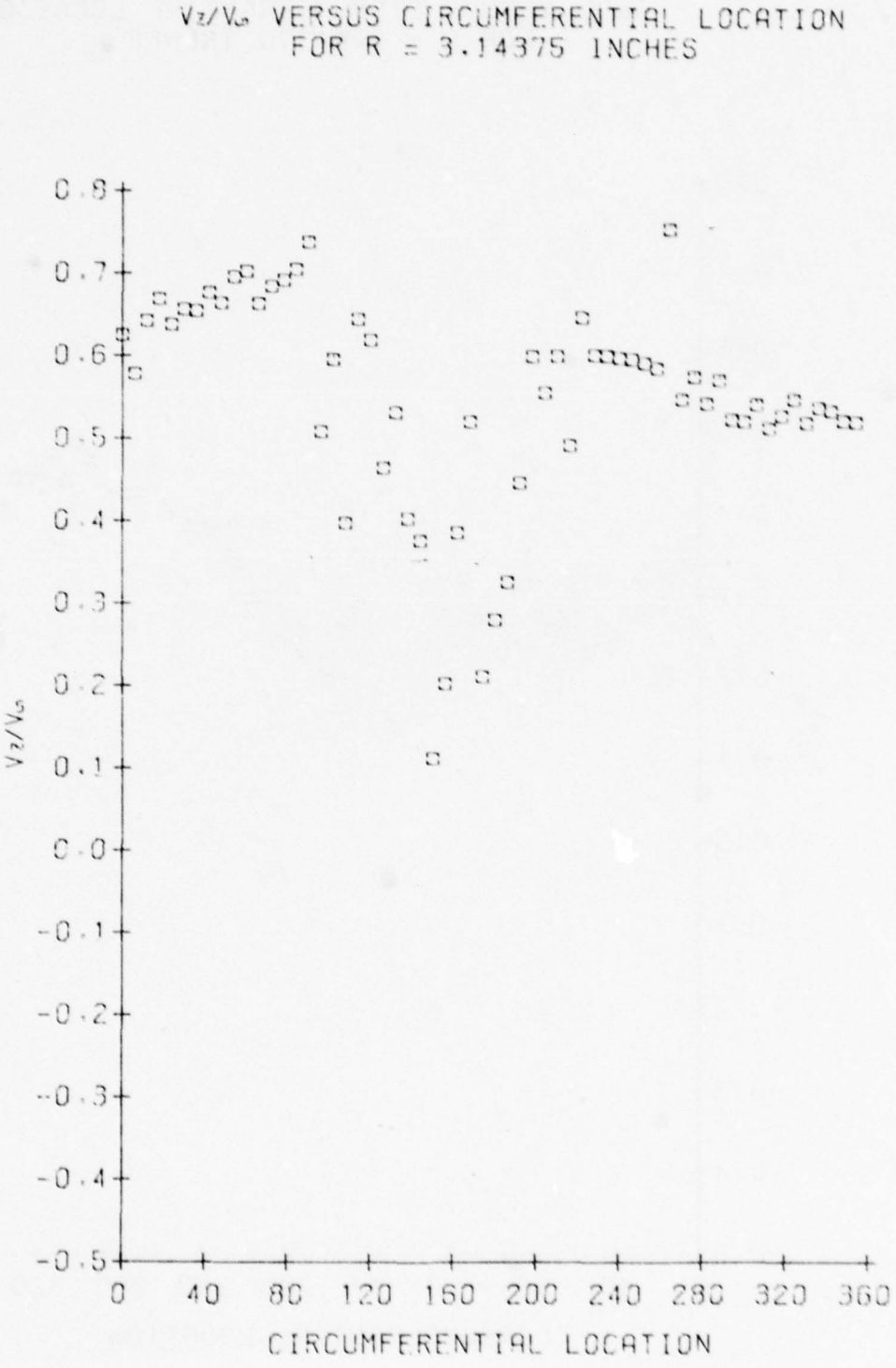

Figure A.11

April 4, 1979
AMY:cac

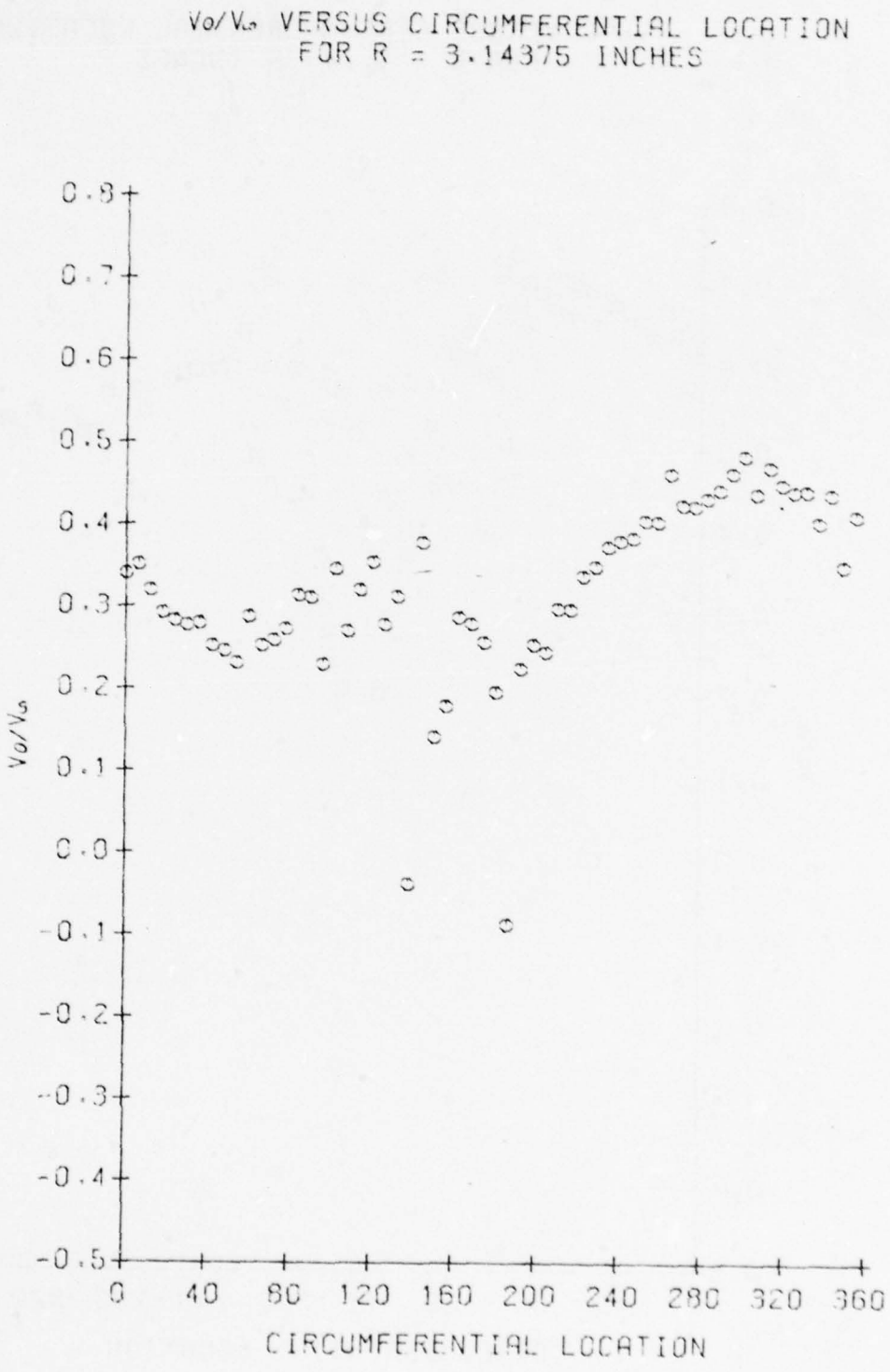

Figure A.12

April 4, 1979
AMY:cac

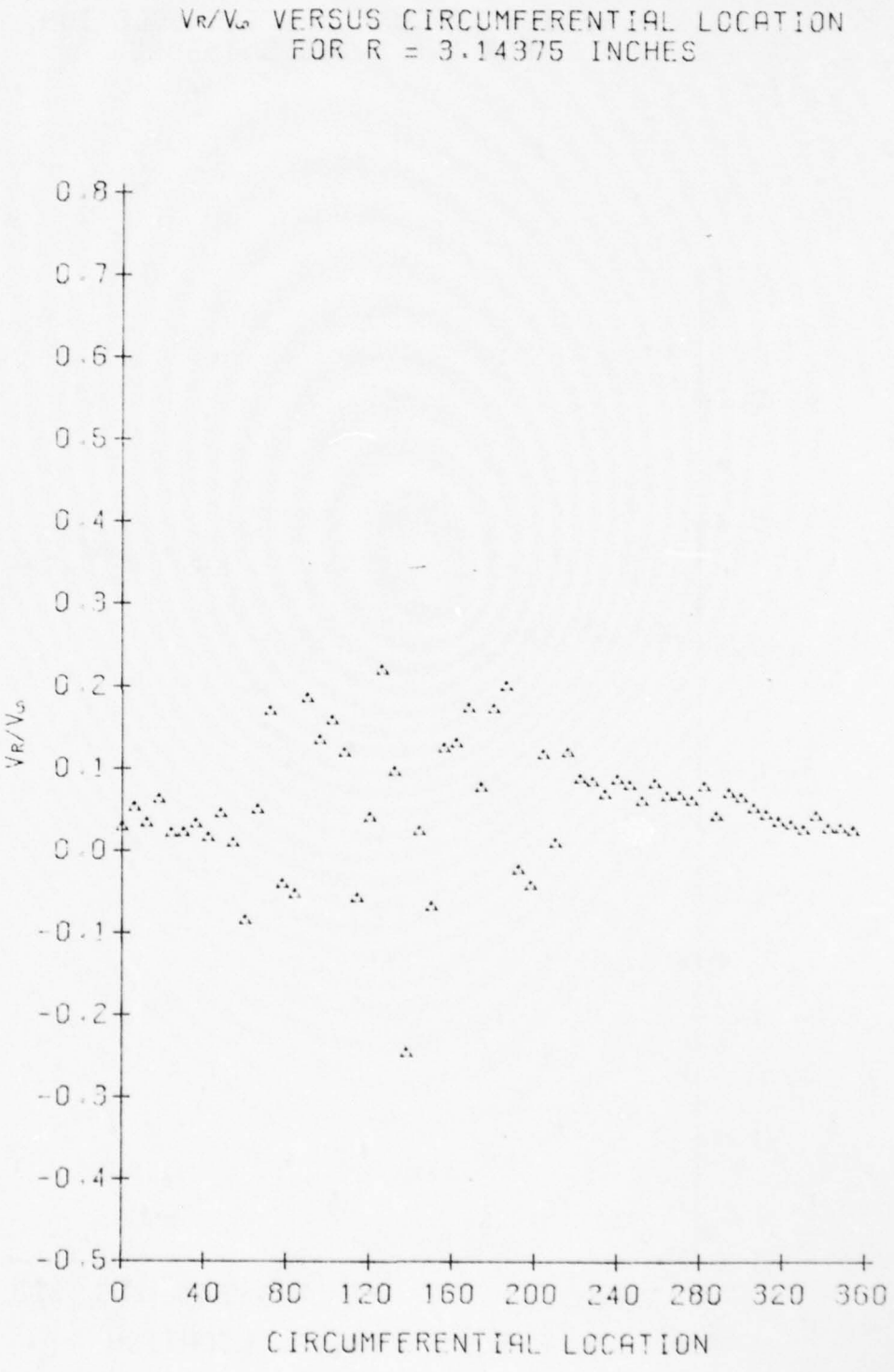

Figure A.13

April 4, 1979
AMY:cac

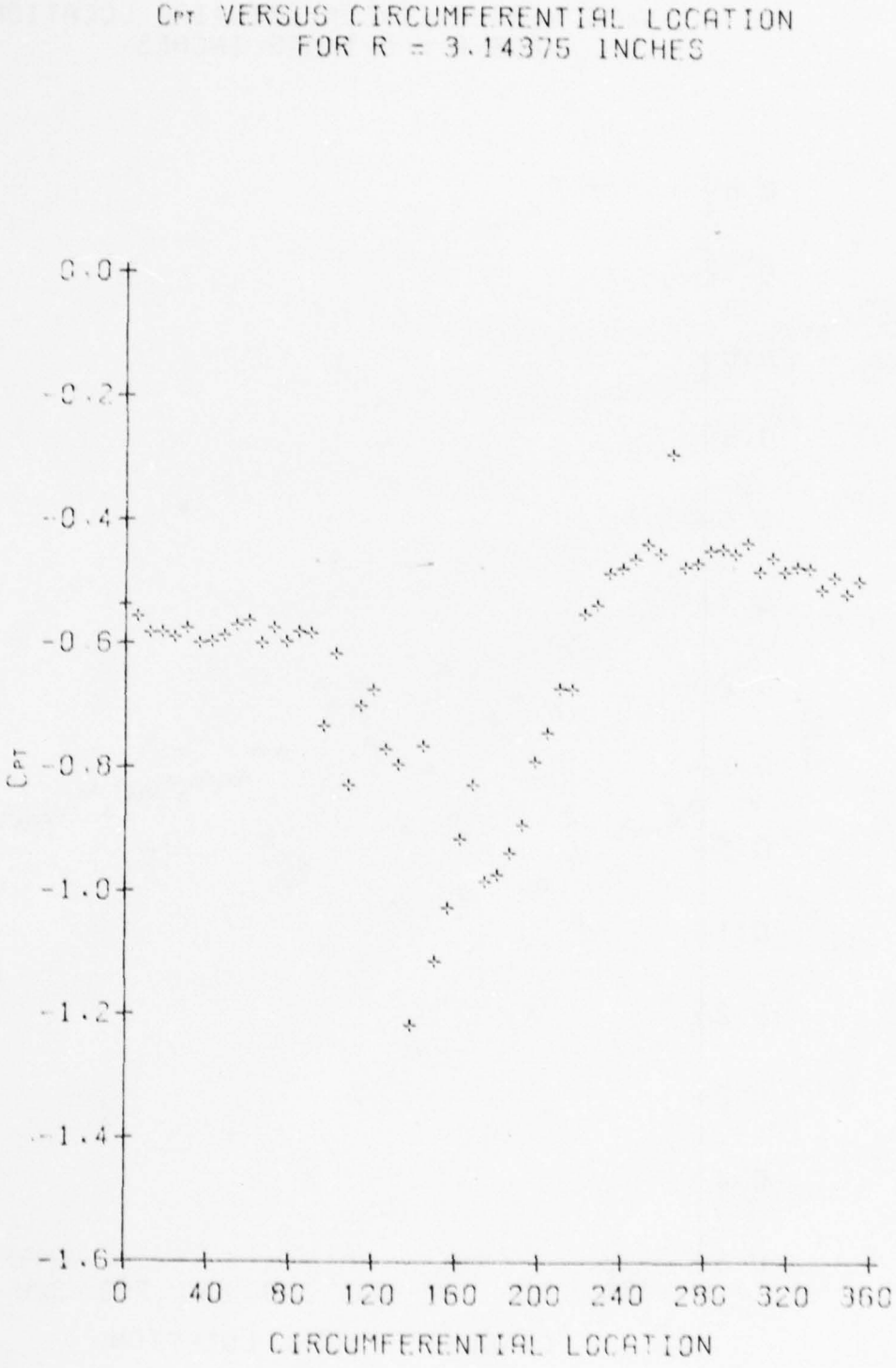

Figure A.14

April 4, 1979
AMY:cac

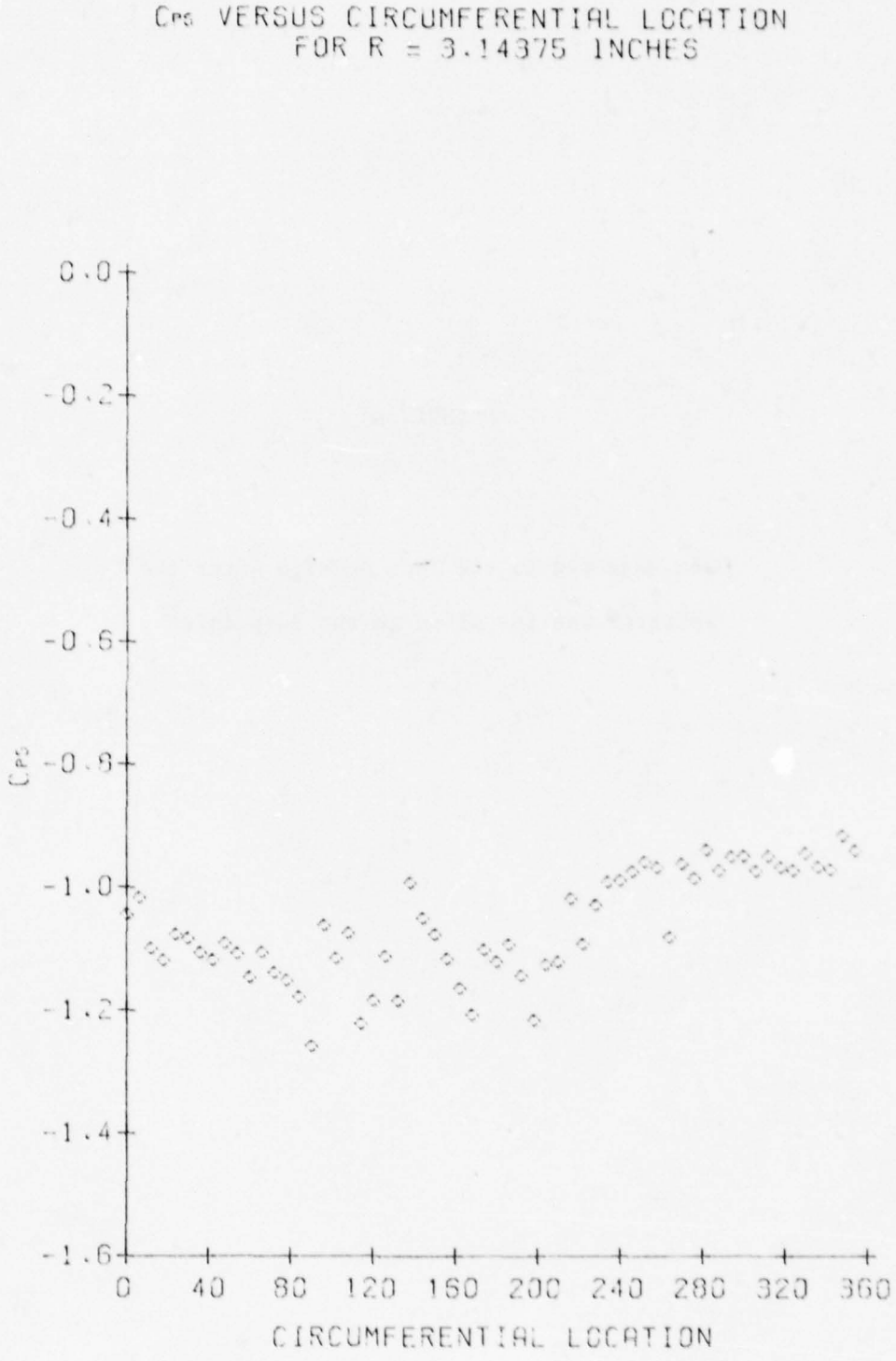

Figure A.15

April 4, 1979
AMY:cac

APPENDIX B

Data Measured in the Test Section After the Splitter was Installed in the Pump Inlet

April 4, 1979
AMY:cac

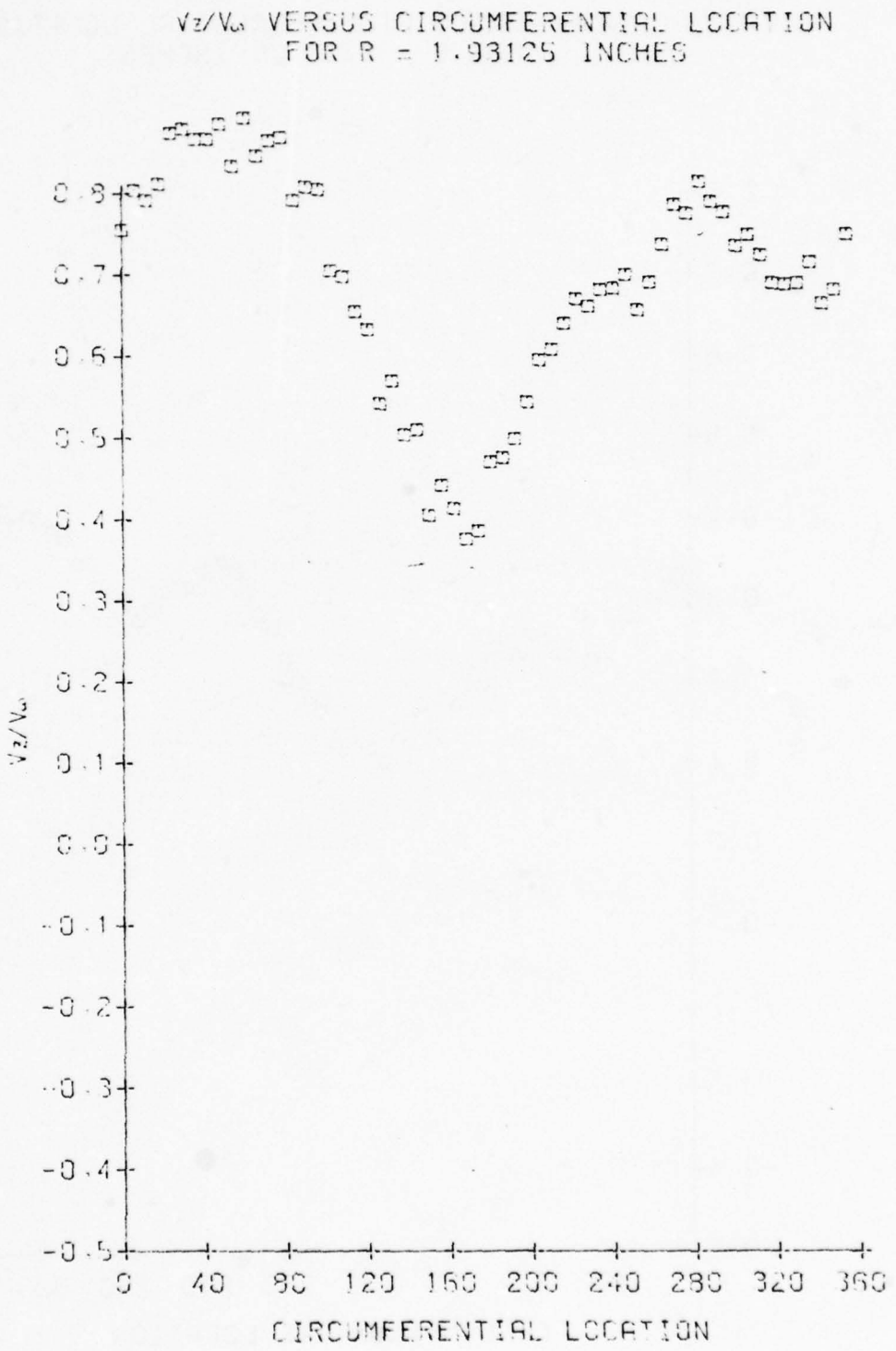

Figure B.1

April 4, 1979
AMY:cac

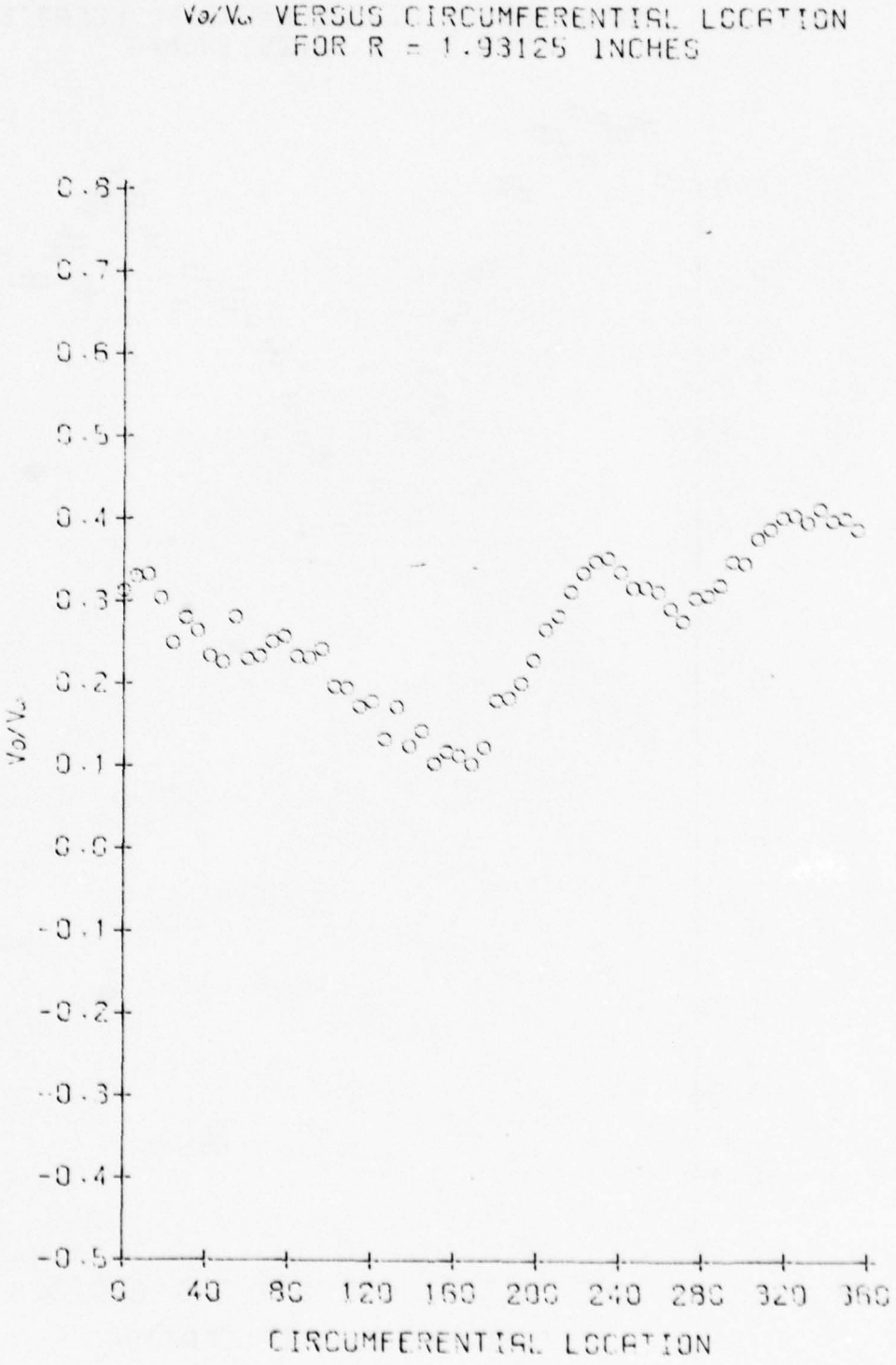

Figure B.2

April 4, 1979
AMY:cac

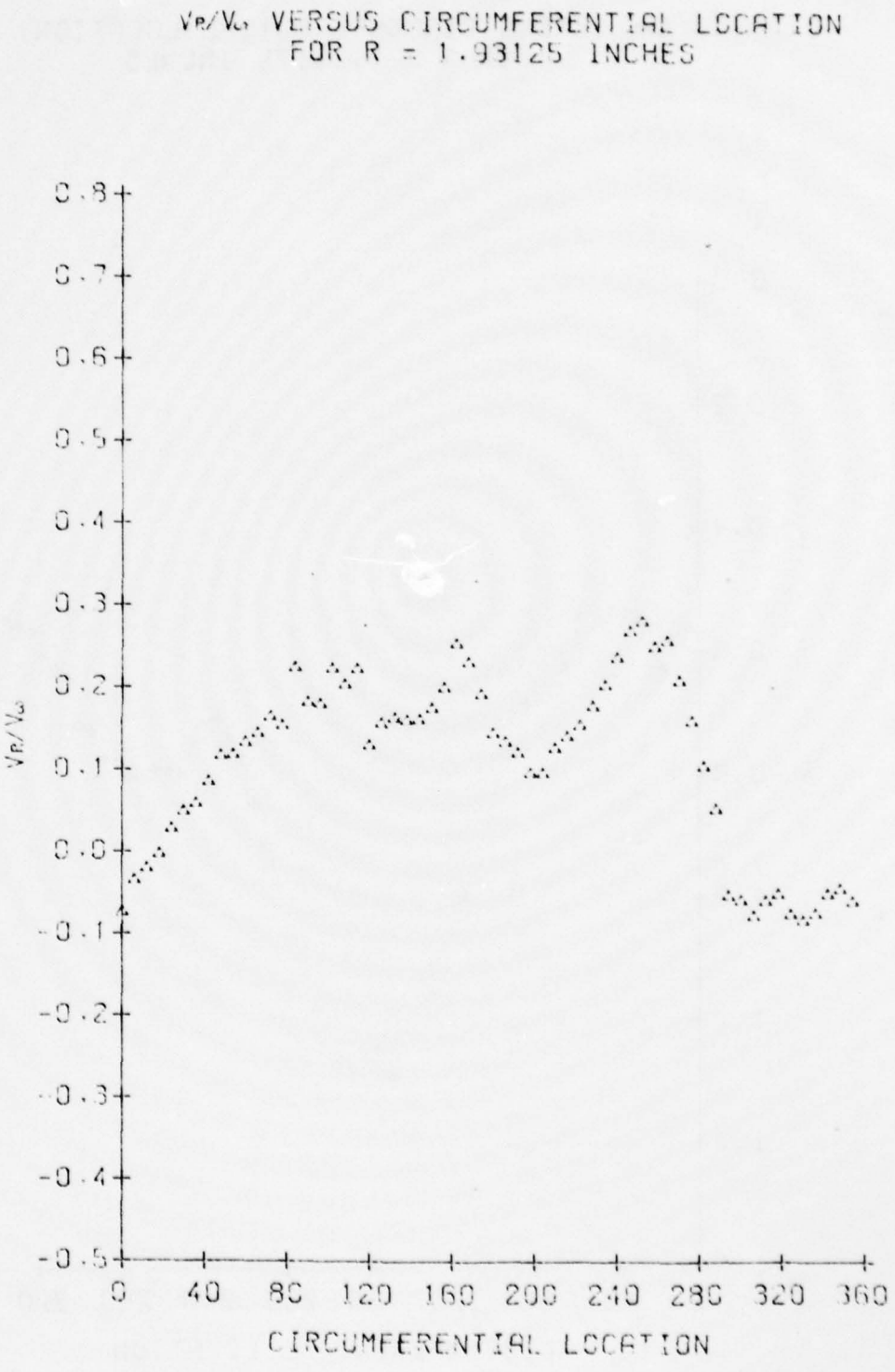

Figure B.3

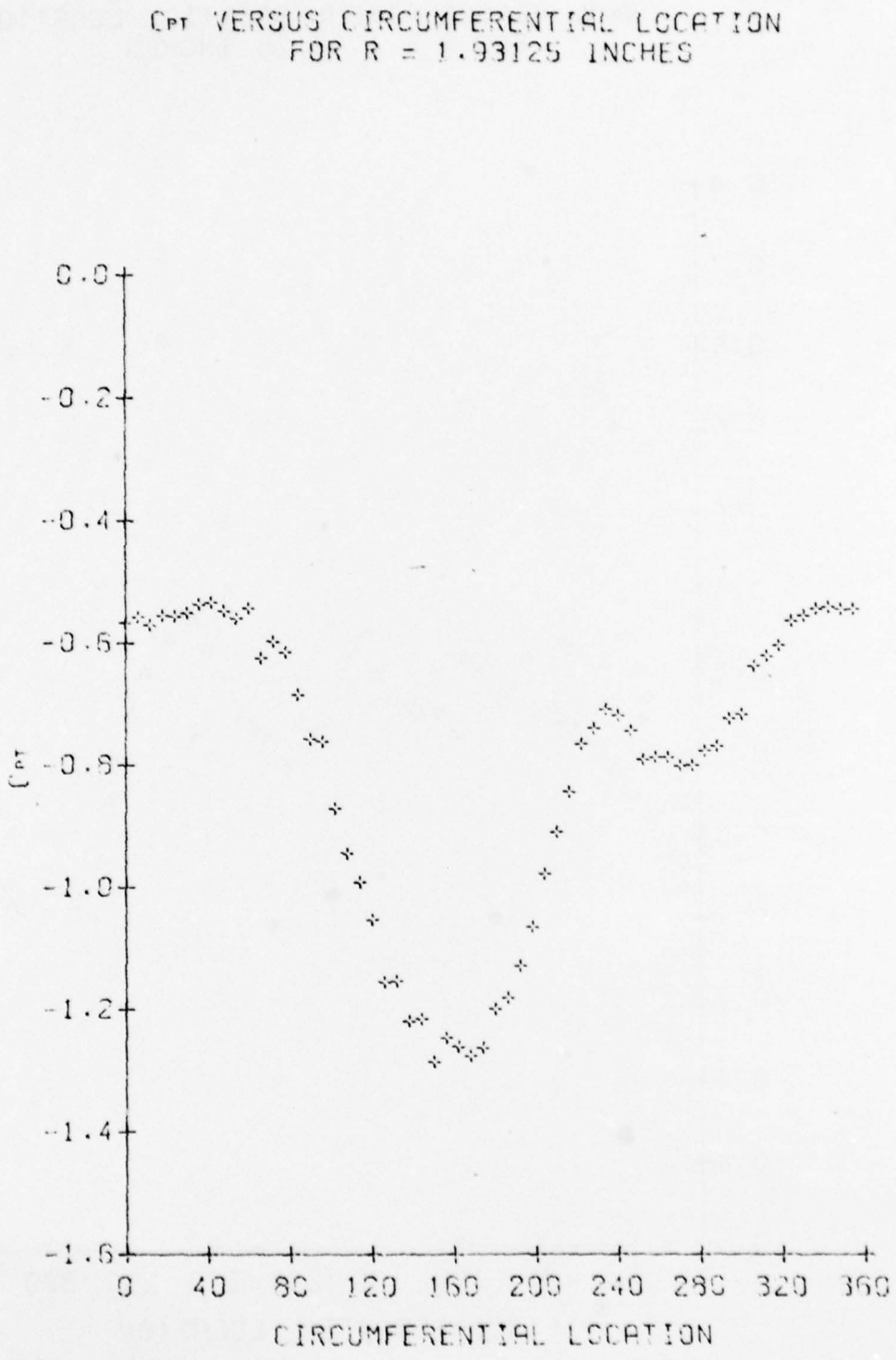
C_{PT} VERSUS CIRCUMFERENTIAL LOCATION
FOR R = 1.93125 INCHES
0.0
-0.2
-0.4
-0.6
-0.8
-1.0
-1.2
-1.4
-1.6
C_{PT}
0
40
80
120
160
200
240
280
320
360
CIRCUMFERENTIAL LOCATION

Figure B.4

April 4, 1979
AMY:cac

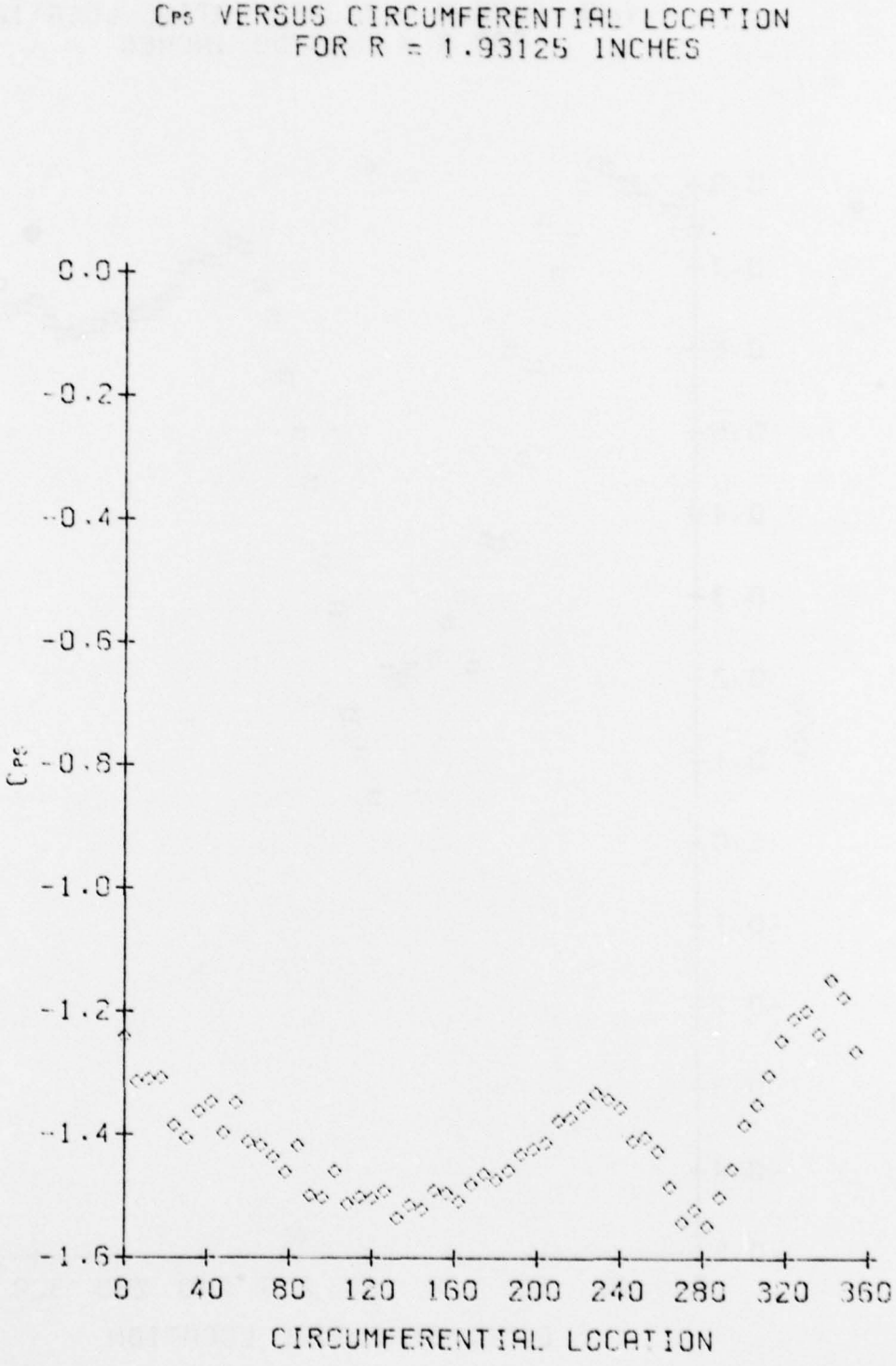

Figure B.5

April 4, 1979
AMY:cac

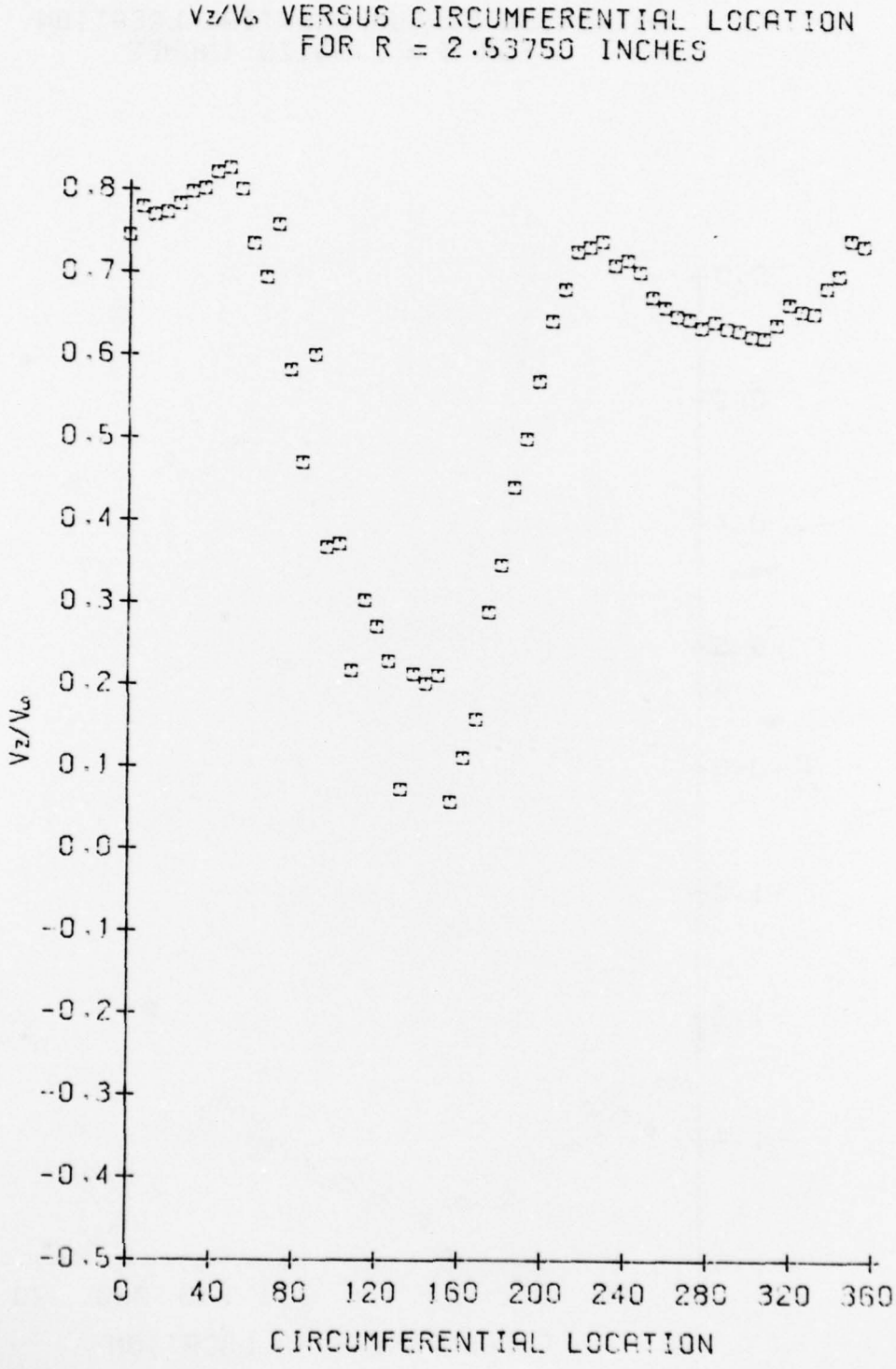

Figure B.6

Figure A.9

April 4, 1979
AMY:cac

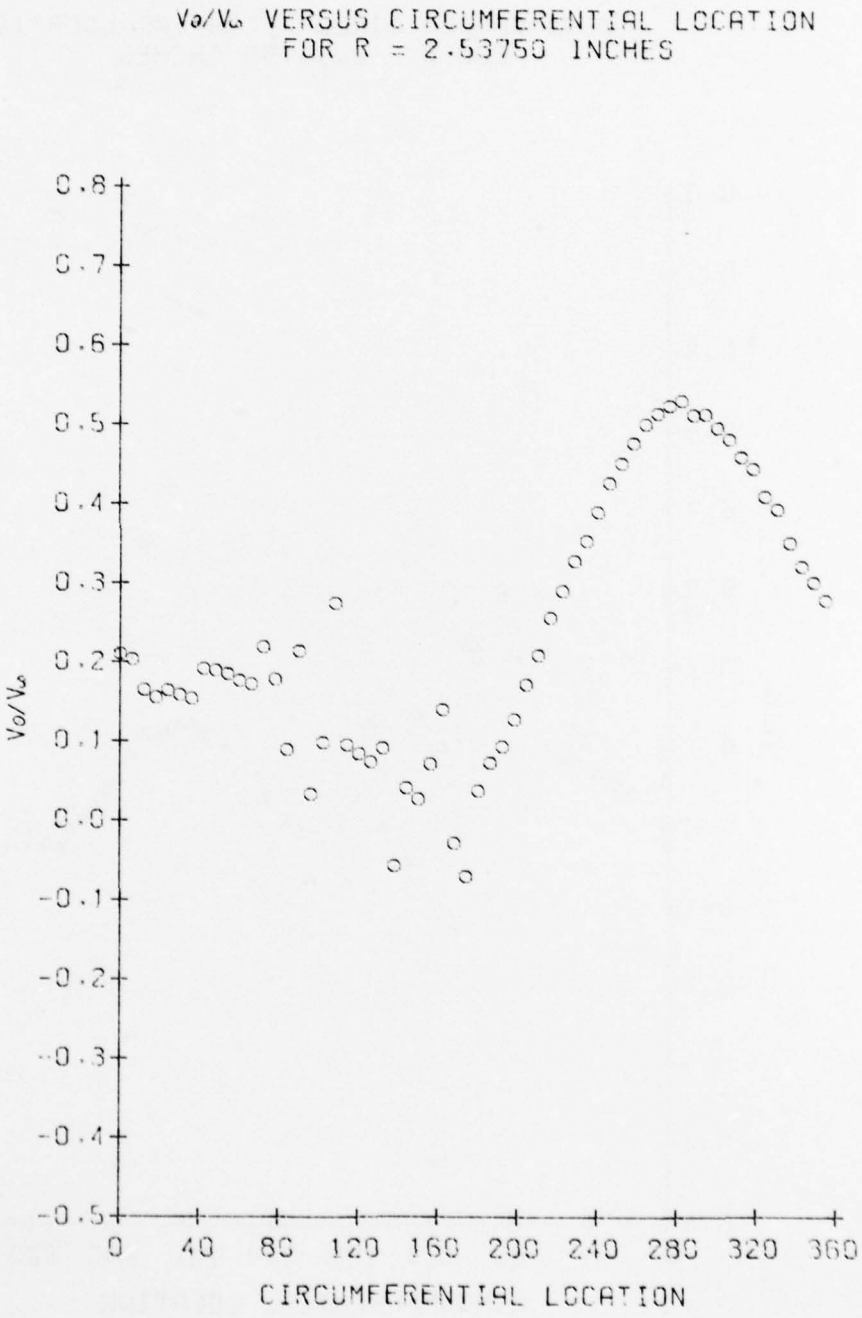

Figure B.7

April 4, 1979
AMY:cac

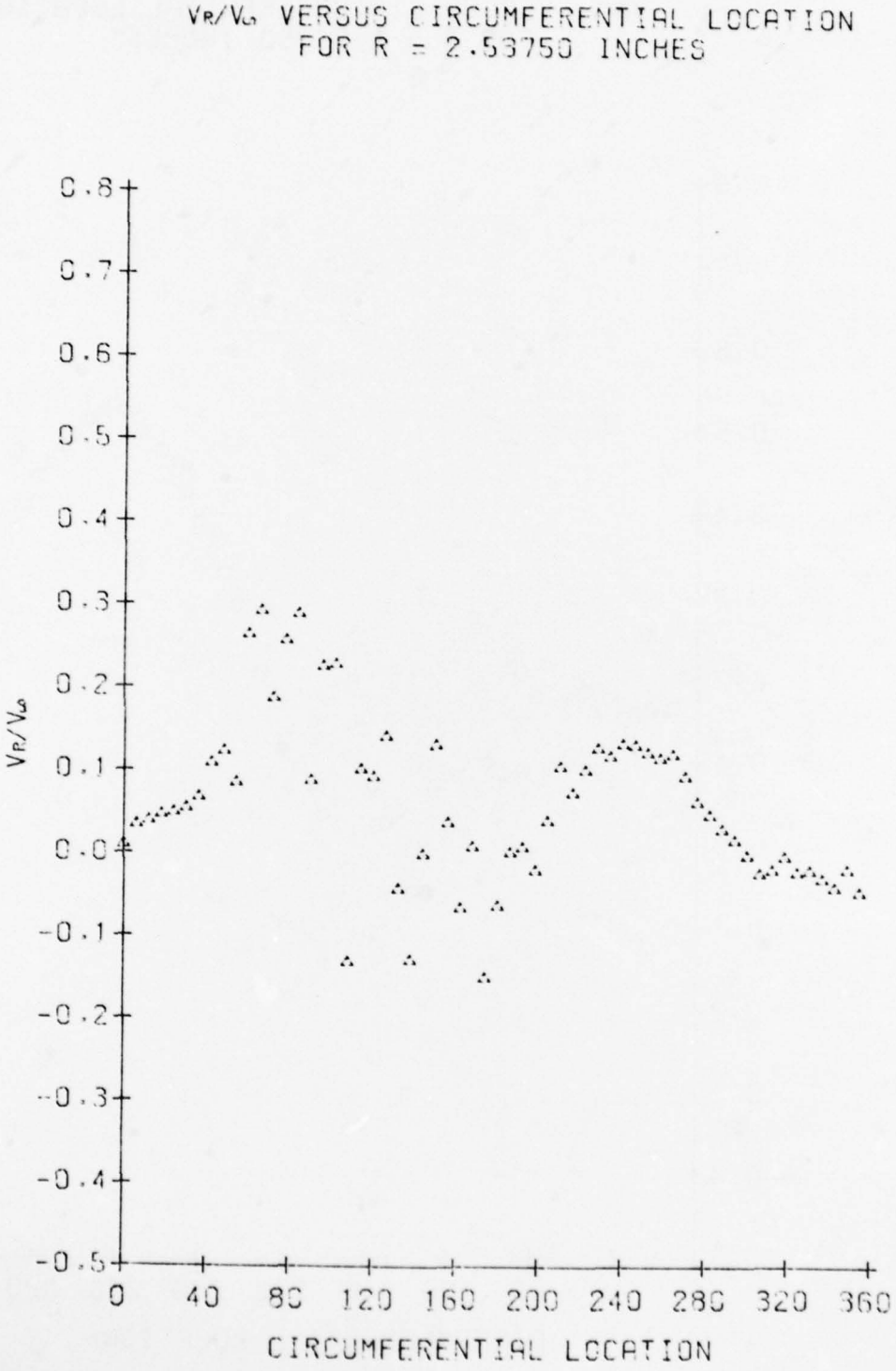

Figure B.8

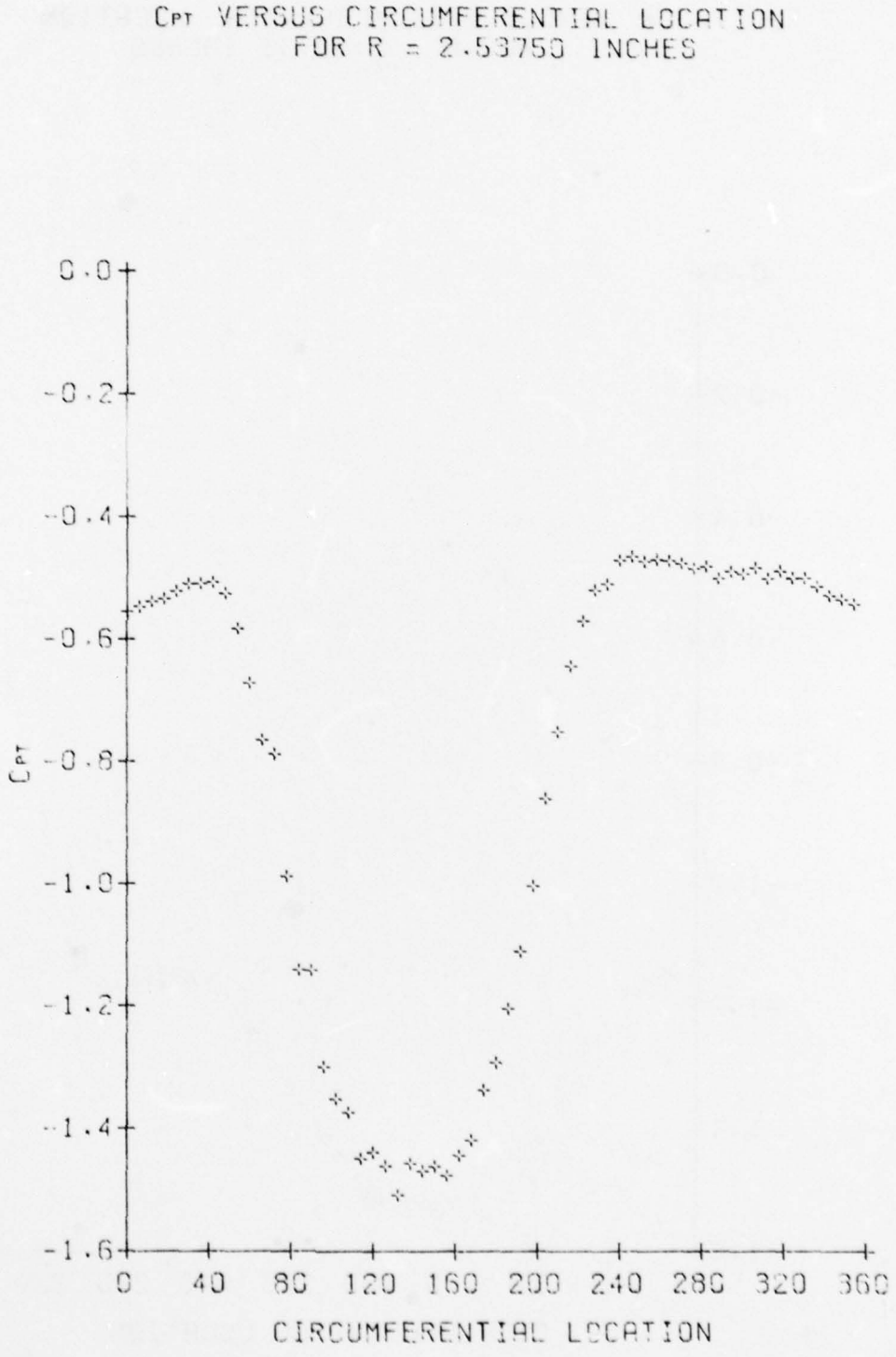
CPT VERSUS CIRCUMFERENTIAL LOCATION
FOR R = 2.53750 INCHES
0.0
-0.2
-0.4
-0.6
-0.8
-1.0
-1.2
-1.4
-1.6
CPT
0
40
80
120
160
200
240
280
320
360
CIRCUMFERENTIAL LOCATION

Figure B.9

April 4, 1979
AMY:cac

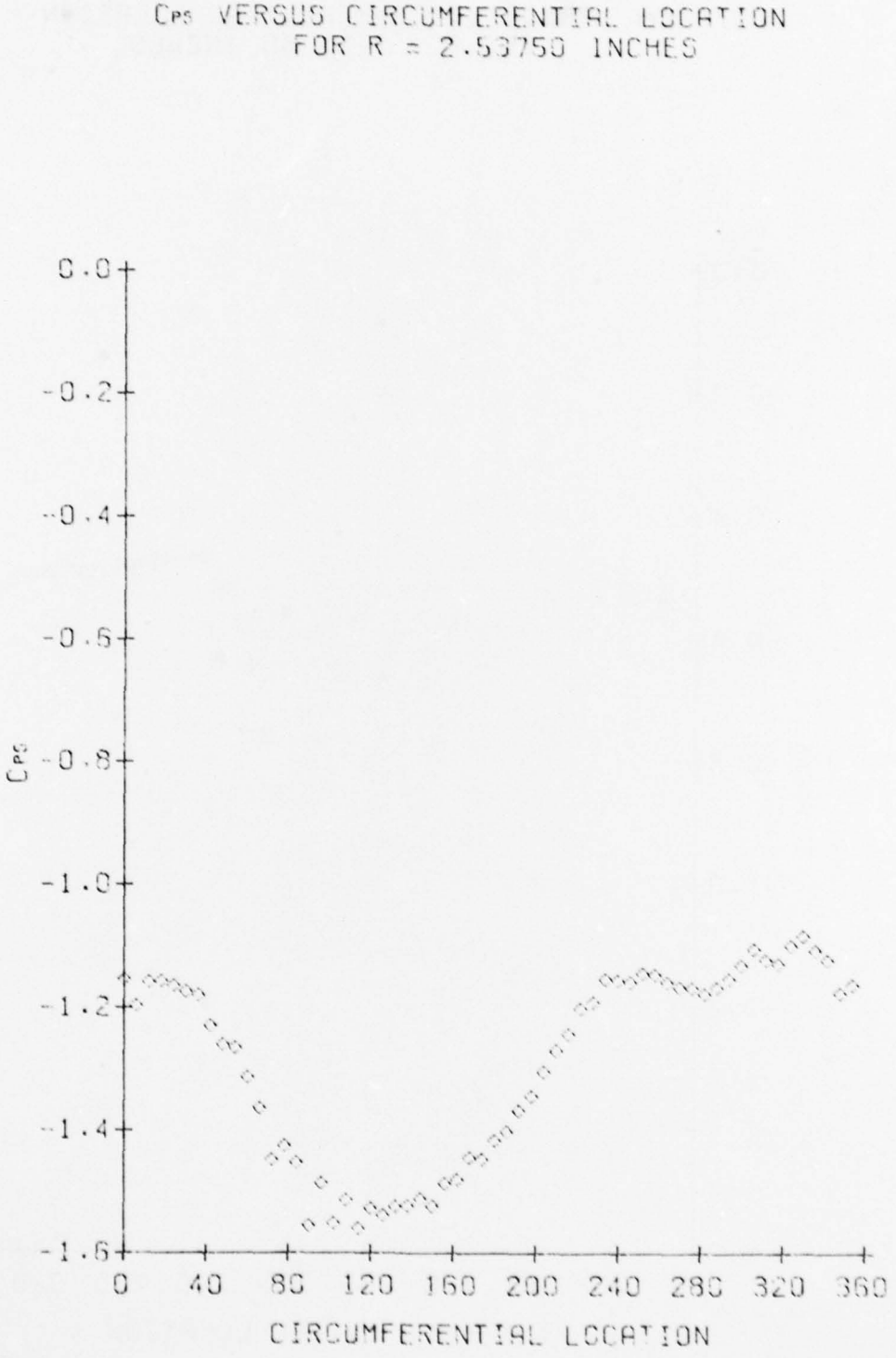

Figure B.10

April 4, 1979
AMY:cac

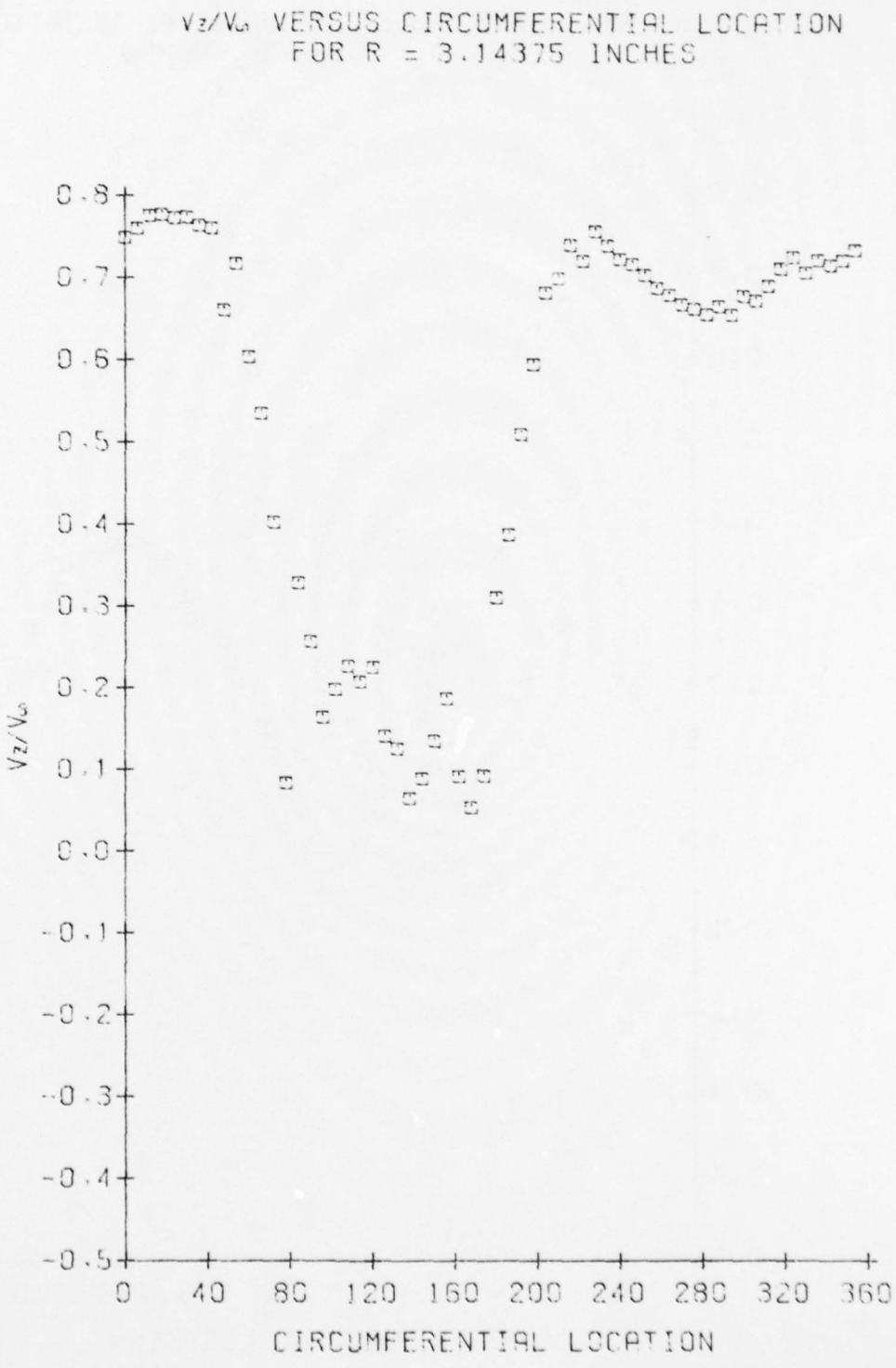

Figure B.11

April 4, 1979
AMY:cac

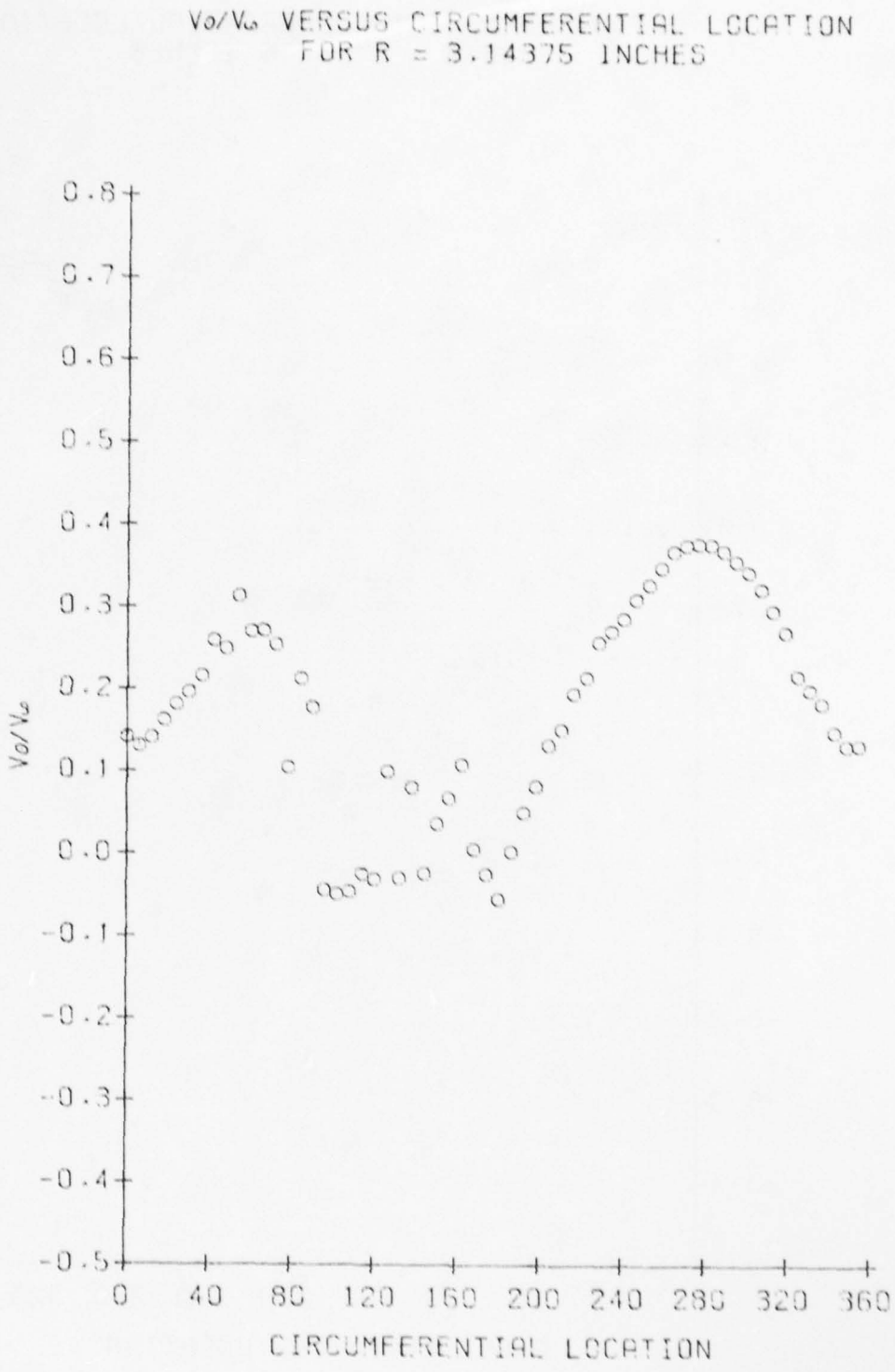

Figure B.12

April 4, 1979
AMY:cac

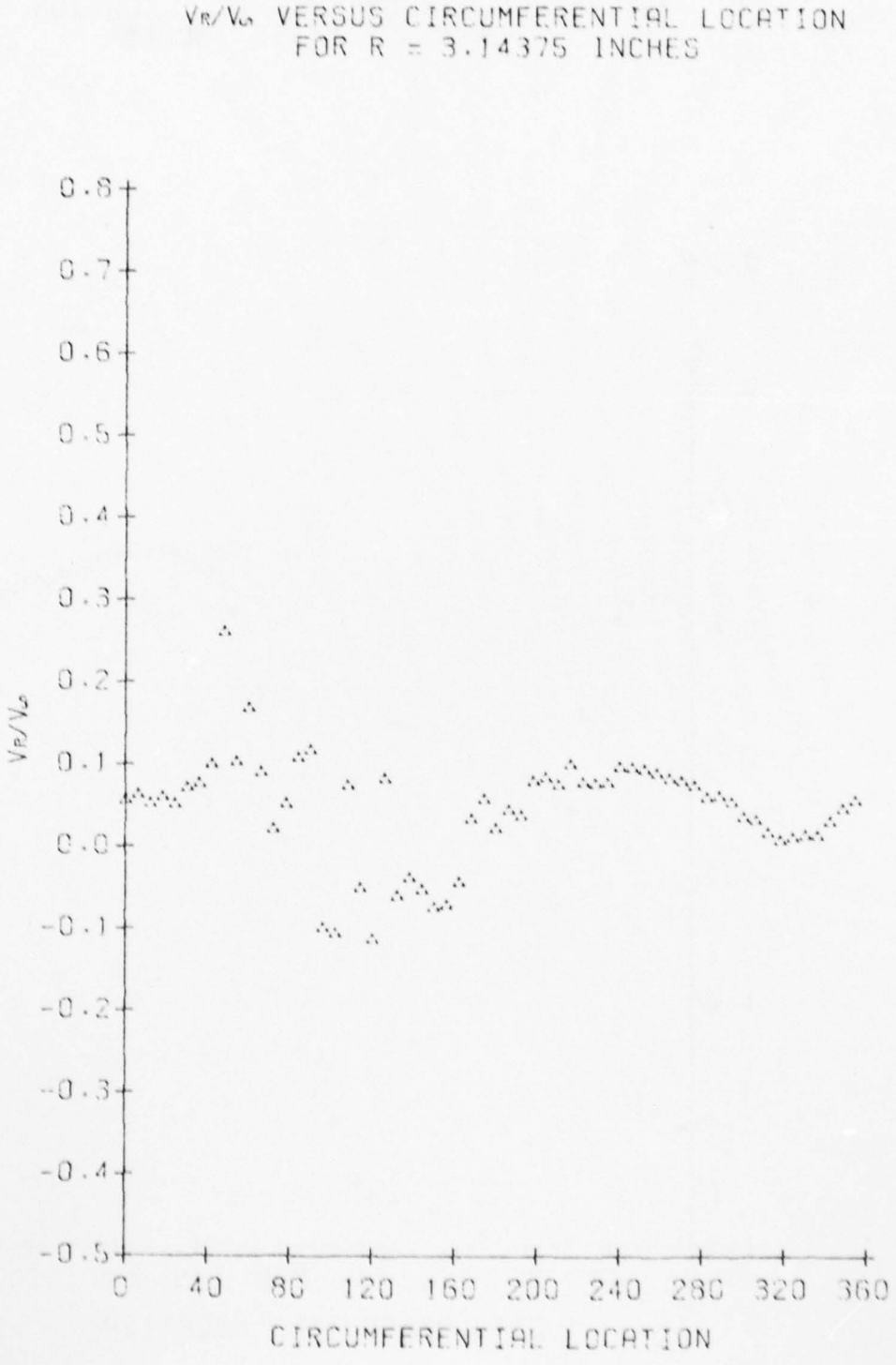

Figure B.13

April 4, 1979
AMY:cac

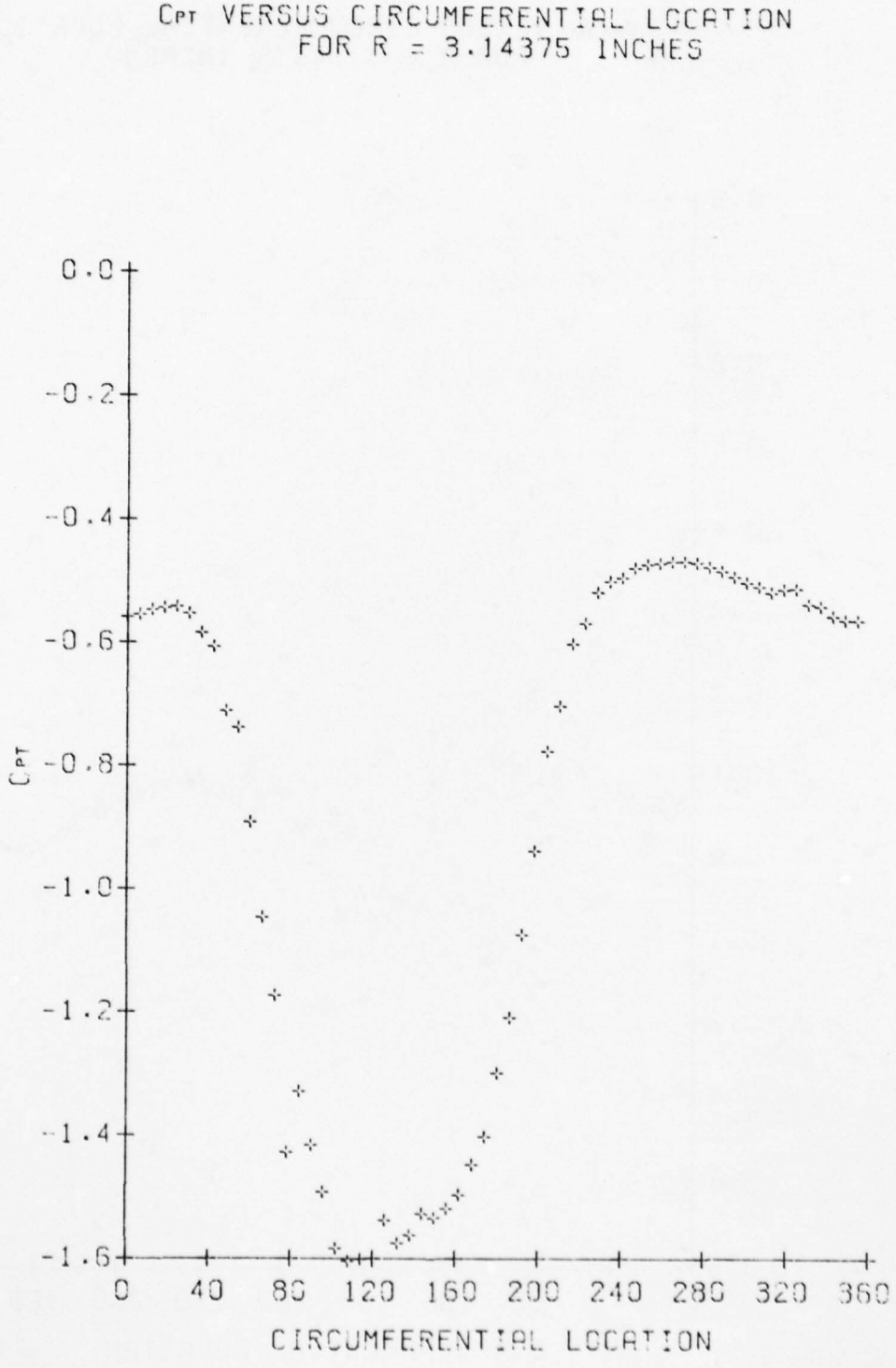

Figure B.14

C_{PS} VERSUS CIRCUMFERENTIAL LOCATION
FOR R = 3.14375 INCHES

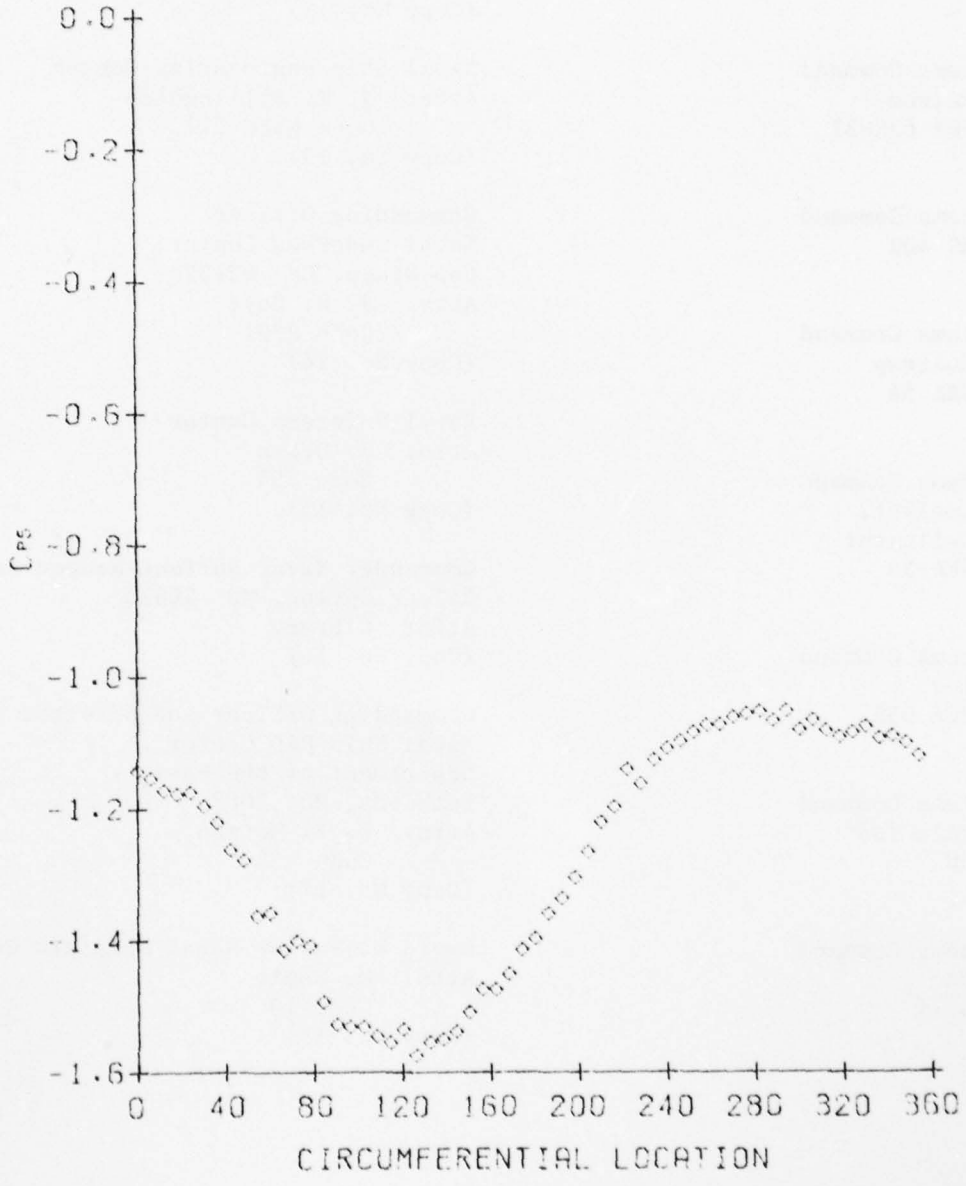

Figure B.15

DISTRIBUTION LIST FOR UNCLASSIFIED TM 79-51, dated 4 April 1979, by A. M. Yocum

Commander
Naval Sea Systems Command
Department of the Navy
Washington, DC 20362
Attn: Library
Code NSEA 09G32
(Copy No. 1 and 2)

Naval Sea Systems Command
Attn: S. R. Marcus
Code ORD 03A
(Copy No. 3)

Naval Sea Systems Command
Attn: T. E. Peirce
Code NSEA 63R-31
(Copy No. 4)

Naval Sea Systems Command
Attn: Code PMS 402
(Copy No. 5)

Naval Sea Systems Command
Attn: G. R. Moltrup
Code NSEA 54
(Copy No. 6)

Naval Sea Systems Command
Attn: Chief Analyst,
J. J. Bellaschi
Code NSEA 54
(Copy No. 7)

Naval Sea Systems Command
Attn: C. Miller
Code NSEA 05R
(Copy No. 8)

Naval Sea Systems Command
Attn: A. R. Paladino
NSEA 05H
(Copy No. 9)

Naval Sea Systems Command
Attn: L. Benen
Code 03411
(Copy No. 10)

Commander
Naval Ship Engineering Center
Department of the Navy
Washington, DC 20360
Attn: W. L. Louis
Code 6136B
(Copy No. 11)

Naval Ship Engineering Center
Attn: R. M. Petros
Code NSEC 6148
(Copy No. 12)

Naval Ship Engineering Center
Attn: J. T. Billingsley
Code NSEC 521
(Copy No. 13)

Commanding Officer
Naval Undersea Center
San Diego, CA 92132
Attn: J. W. Hoyt
Code 2501
(Copy No. 14)

Naval Undersea Center
Attn: J. Green
Code 254
(Copy No. 15)

Commander Naval Surface Weapon Center
Silver Spring, MD 20910
Attn: Library
(Copy No. 16)

Commanding Officer and Director
Naval Ship R&D Center
Department of the Navy
Bethesda, MD 20084
Attn: W. B. Morgan
Code 154
(Copy No. 17)

David W. Taylor Naval Ship R&D Center
Attn: M. Sevik
Code 19
(Copy No. 18)

DISTRIBUTION LIST FOR UNCLASSIFIED TM 79-51, dated 4 April 1979, by A. M. Yocum.

David W. Taylor Naval Ship R&D Center
Annapolis Laboratory
Department of the Navy
Annapolis, MD 21402
Attn: J. G. Stricker
Code 2721
(Copy No. 19-22)

Defense Documentation Center
5010 Duke Street
Cameron Street
Alexandria, VA 22314
(Copy No. 23-34)

Applied Research Laboratory
P. O. Box 30
State College, PA 16801
Attn: Walter S. Gearhart
(Copy No. 35)

Applied Research Laboratory
Attn: R. E. Henderson
(Copy No. 36)

Applied Research Laboratory
Attn: A. M. Yocum
(Copy No. 37)